THE MOMENTS BALANCE METHOD IN ELECTRON TRANSPORT THEORY

- by -

Philip Siu-Yu Cheung

A dissertation submitted to the University of Warwick for admission to the degree of Doctor of Philosophy

[1972]

PAGE

NUMBERING

AS ORIGINAL

MEMORANDUM

This dissertation is submitted to the University of Warwick in support of an application for admission to the degree of Doctor of Philosophy. It contains an account of research undertaken at the School of Physics of the University of Warwick in the period October 1968 to November 1971 under the general supervision of Professor P.N. Butcher and Doctor C.J. Hearn. No part of this dissertation has been previously submitted in a degree thesis to this or any other University. The work described in the thesis is the result of independent research except where specifically acknowledged in the text.

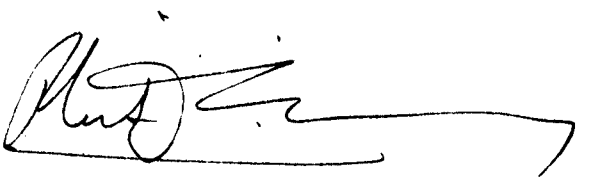

Dec. 1971 P. S. Cheung

ACKNOWLEDGEMENTS

The author is deeply indebted to, and wishes to thank Doctor C.J. Hearn and Professor P.N. Butcher for their generously given guidance, interest and encouragement throughout the course of this work. He would like also to thank Professor A.J. Forty, who has kindly provided the research facilities at the School of Physics, University of Warwick, and all the members of the School, especially the theoreticians, who have helped him to acquire an understanding and appreciation of the diverse aspects of physics through many stimulating discussions.

This research programme has been supported by a C.V.D. contract with the Ministry of Defence. The three-year grant is gratefully acknowledged, as are the invaluable discussions with Dr W. Fawcett of the Royal Radar Establishment who has given this project his continual interest.

Finally, the author wishes to thank Mrs Morrall for her care and patience in typing this thesis.

ABSTRACT

In this thesis an attempt is made to formulate closed sets of transport equations which are applicable to inhomogeneous and time-dependent situations in semiconductor hot electron transport problems. The basis of the formalism is the Boltzmann Transport Equation from which macroscopic, phenomenological transport equations are generated by the Moments Balance Method. The equations describe the behaviour of the electron distribution function in terms of the spatial and time-dependence of its moments. When the behaviour of the electron system is assumed to be typified by that of a finite number of its moments, the components of momentum and energy being the most important members of the set, then closed systems of transport equations are obtained.

In the regime of small and slowly-varying density gradients, a theory of electronic diffusion has been developed. For isotropic, single valleys it is possible to derive a set of generalised Einstein relations which express the diffusion coefficients of the electrons in terms of their mobility, differential mobility and temperature. For many valley, ellipsoidal band structures, the results cannot in general be expressed in terms of simple relations such as the generalised Einstein relations although the theory does provide a semi-analytical framework within which diffusion may be understood in terms of macroscopic quantities. The theory is applied to n-type gallium arsenide and silicon. The effects of anisotropic electron-phonon scattering and electron-electron scattering in silicon have also been examined in some detail and were found to be small in determining the values of the velocity characteristic and diffusion coefficients.

The transport equations derived from the Moment Balance formalism may be modified to form the basic or constituitive equations for the Gunn Effect. These equations are able to give a unified account for the roles of diffusion, intervalley scattering and energy transport in the propagation properties of Gunn Domains, in a manner that is consistent with the Boltzmann Equation. The dynamics of domain propagation are studied by a simulation technique. It is found that heat currents and intervalley scattering have a crucial effect on domain shapes and propagation velocity.

Publications

(1) Energy-Balance Model for Gunn Domains

P. S. Cheung & C. J. Hearn, Electron. Lett 8, 79 (1972)

(2) The Diffusion of Electrons in Semi-conductors in high Electric Fields

P.S. Cheung & C. J. Hearn

(to be published in the Journal of Physics C)

CONTENTS

Chapter 1. The Moments Balance Method

§ 1.1. The Boltzmann Equation and its solution

The Boltzmann Equation approach to hot electron transport theory has in the past been met with considerable success. Its main appeal lies in the simplicity of the underlying physical concepts, and although its basis is very much intuitive and lacking to date a rigorous formulation starting from quantum theory [1, 2, 3], it remains the mainstay of theoretical methods in semiconductor physics. Within the context of this thesis, which concerns non-degenerate electrons in high electric fields, it will be assumed that the Boltzmann Equation is of general validity.

In semiconductors, when details of the band structure and the complexities of the scattering mechanisms have been fully incorporated, the solution of the Boltzmann Equation presents a formidable task. Indeed it is only since about 1968 that exact solutions are possible for a variety of realistic situations [4, 5, 6]. Prior to the advent of these new techniques, it was necessary to employ approximate methods. The moments balance method is one of these approximate schemes developed to evaluate transport coefficients from the Boltzmann Equation.

The various approximate methods are generally built on the philosophy that only the gross features of a distribution function are important in determining the values of the transport coefficients. Since the exact form of the distribution function is not required, the solution, or partial solution of the Boltzmann Equation is greatly facilitated. Briefly, in the moments balance method, the following procedure is adopted for the homogeneous steady state situation: a set of 'moment balance equations' are obtained by integrating some 'moment function' over the Boltzmann Equation (see §§1.2 - 3). If the distribution function is then assumed to have some fixed shape containing a number of adjustable parameters equal to the number of moment balance equations considered, then the parameters may be determined through the condition of self-consistency of the equations. The Boltzmann Equation is then considered solved in

sufficient detail. The moment balance equations considered generally include those corresponding to the conservation of electrons, momentum and energy. Since these represent physically the most important restraints to be imposed on the electron distribution, the resultant distribution function, provided its assumed form is not totally absurd, will yield transport coefficients with some accuracy. By the suitable choice of a general shape for the distribution function and of the moment balance equations, the essential features of a given physical situation can usually be accounted for. Despite the arbitrariness inherent to some extent in this procedure, its application has achieved some notable success (see §1.4). Because the general shape of the distribution function is often assumed to be a displaced Maxwellian, the moments balance method is often known by that name.

The development of exact methods has largely displaced the usefulness of many of the approximate schemes in certain types of calculations. Nevertheless the latter have still much to offer because of their simplicity in application and their ability to allow problems to be formulated and understood in terms of physically significant concepts, such as an electron temperature and its variation. In a later section (§1.4) the relative merits and complementary roles of the exact and approximate methods will be discussed. First we shall describe in greater detail the moments balance method which will be shown to be a particularly convenient framework within which time- and spatially-dependent problems can be formulated. In the next section the moment balance equations are derived and cast into a convenient form. A brief survey of its applications in the past will then be made to provide a background for the later chapters in which a theory of electronic diffusion, and transport equations for the Gunn Effect will be developed.

§1.2. The Moment Balance Equations

Let us consider a semiconductor having N types of non-equivalent valleys in the conduction band which we shall label with an integer $i = 1, 2, \ldots N$. The electron energy/wave-vector relations $E_i(\underline{k})$ for each valley i are typified by effective-mass tensors $\overline{m}_i$ and the electrons are otherwise treated as classical particles which are

capable of both intravalley and intervalley transitions. When there is a constant electric field $\underline{F}$, the distribution functions $f_i(\underline{k};\underline{r},t)$ for the valleys $i = 1, 2, \ldots N$ are determined by the coupled Boltzmann Equations:

$$\frac{\partial}{\partial t} f_i(\underline{k};\underline{r},t) + \underline{v}.\underline{\nabla}_r f_i(\underline{k};\underline{r},t) + \frac{e}{\hbar}\underline{F}.\underline{\nabla}_{\underline{k}} f_i(\underline{k};\underline{r},t) = \sum_j^N \left[\frac{\partial}{\partial t} f_i(\underline{k};\underline{r},t)\right]_j^S \quad (1.1)$$

where $i = 1, 2, \ldots N$, $\underline{\nabla}_r = \left(\frac{\partial}{\partial x}, \frac{\partial}{\partial y}, \frac{\partial}{\partial z}\right)$ and $\underline{\nabla} = \left(\frac{\partial}{\partial k_x}, \frac{\partial}{\partial k_y}, \frac{\partial}{\partial k_z}\right)$. The wave-vector $\underline{k}$ in $f_i(\underline{k};\underline{r},t)$ is measured from the centre of the valley i and $\underline{v}$, the velocity, is equal to $\overline{m_i}^{-1}\hbar\underline{k}$. We have adopted the convention in which the electron carries a positive charge. The right-hand side of (1.1) is the total rate of change of $f_i(\underline{k};\underline{r},t)$ produced by scattering. As is indicated in (1.1), it is convenient to separate in the present context this scattering term into two parts. The first, $\left[\frac{\partial}{\partial t} f_i(\underline{k};\underline{r},t)\right]_i^S$ is defined to be the rate of change of $f_i(\underline{k};\underline{r},t)$ produced by all scattering events for which the initial state is in valley i, irrespective of the location of the final state. Hence

$$\left[\frac{\partial}{\partial t} f_i(\underline{k};\underline{r},t)\right]_i^S = \int f_i(\underline{k}';\underline{r},t)A_{ii}(\underline{k}',\underline{k}) - f_i(\underline{k};\underline{r},t)\left[A_{ii}(\underline{k},\underline{k}') + \sum_{j\neq i}^N B_{ij}(\underline{k},\underline{k}')\right] d\underline{k}' \quad (1.2a)$$

where $A_{ii}(\underline{k},\underline{k}')$ is the intravalley transition rate in valley i and $B_{ij}(\underline{k},\underline{k}')$ is the intervalley transition rate from valley i to valley j for an initial state $\underline{k}$ and a final state $\underline{k}'$. The second part of the right-hand side of (1.1) is $\sum_{j\neq i}^N \left[\frac{\partial}{\partial t} f_i(\underline{k};\underline{r},t)\right]_j^S$, which is defined to be the rate of change of $f_i(\underline{k};\underline{r},t)$ produced by any scattering events for which the initial state lies outside, and the final state inside valley i. Hence

$$\left[\frac{\partial}{\partial t} f_i(\underline{k};\underline{r},t)\right]_j^S = \int f_j(\underline{k};\underline{r},t)B_{ji}(\underline{k}',\underline{k})\, d\underline{k}' \quad (1.2b)$$

where $B_{ji}(\underline{k}',\underline{k})$ is the intervalley transition rate from valley j to valley i for an initial state $\underline{k}'$ and a final state $\underline{k}$. The essential feature of this unusual separation of the scattering integrals is that (1.2a) involves only the distribution function in valley i while (1.2b) involves only the distribution function in valley j.

Before proceeding to derive the moments balance equations it is necessary to define some terms in this connection. The population in valley i per unit volume of the semiconductor is given by:

$$n_i = \int f_i(\underline{k};\underline{r},t)\, d\underline{k} \quad (1.3)$$

and the normalised function in valley i is defined as $n_i^{-1} f_i(\underline{k};\underline{r},t)$. If $\varphi(\underline{k})$ is a homogeneous function of the components of $\underline{k}$, then its average value in valley i is given by:

$$\varphi_i(\underline{r},t) = \langle \varphi(\underline{k}) \rangle_i = n_i^{-1} \int \varphi(\underline{k})\, f_i(\underline{k};\underline{r},t)\, d\underline{k} \quad (1.4)$$

We shall refer to $\varphi(\underline{k})$ as a moment function and to $\varphi_i(\underline{r},t)$ as a moment of the normalised distribution in valley i, or simply a moment in valley i

The moment balance equations are obtained immediately from (1.1) by multiplication with $\varphi(\underline{k})$ and integration over all $\underline{k}$. Thus we obtain

$$\frac{\partial}{\partial t}(n_i \varphi_i) + \underline{\nabla}_r \cdot (n_i \langle \underline{v}\varphi \rangle_i) - \frac{n_i e}{\hbar} \underline{F} \cdot \langle \underline{\nabla}_k \varphi \rangle_i = \sum_j n_j G_{ij}(\varphi) \quad (1.5)$$

where $G_{ij}(\varphi) = n_j^{-1} \int \varphi(\underline{k}) \left[\frac{\partial f_i}{\partial t}\right]_j^s d\underline{k}$ (1.6)

Here and in the remainder of the text we leave the arguments of the functions understood for the sake of brevity. Since $\underline{v}$ is a homogeneous function of the components of $\underline{k}$, the terms $\langle \underline{v}\varphi \rangle_i$ and $\langle \underline{\nabla}_k \varphi \rangle_i$ are also moments of valley i. The physical interpretation of $G_{ij}(\varphi)$ is clear by inspection of (1.5) and (1.6): it is the generation rate of the moment density $n_i \varphi_i$ in valley i due to all scattering events originating in valley j per electron therein. Consequently, $G_{ij}(\varphi)$ is a functional of the normalised distribution function $n_j^{-1} f_j$ in valley j; it may therefore be regarded as a function of all the moments in valley j, and is completely independent of the moments in the other valley. The moment balance equations relate thus the moments in the various valleys without explicit reference to the distribution functions.

In dealing with diffusion we consider the effect on the system of a spatial gradient in the total electron concentration $n = \sum_j n_j$. It is useful therefore to introduce n explicitly into (1.5) by writing

$$n_i = p_i\, n \quad (1.7)$$

where p_i is the fractional population of valley i. The resulting equation

involves both $\partial n/\partial t$ as well as $\underline{\nabla}_r n$. However, $\partial n/\partial t$ may be eliminated with the aid of the continuity equation

$$\frac{\partial n}{\partial t} = -\underline{\nabla}_r (n \bar{\underline{v}}) \qquad (1.8)$$

which follows immediately from (1.5) on setting $\varphi = 1$. In (1.8), $\bar{\underline{v}} = \sum_j p_j \underline{v}_j$ is the overall electron velocity. By proceeding in this manner we obtain the moment balance equations in their final form:

$$\frac{\partial}{\partial t}(p_i \varphi_i) + \underline{\nabla}_r \cdot (p_i \langle \underline{v} \varphi \rangle_i) - \frac{e}{\hbar} p_i \underline{F} \cdot \langle \underline{\nabla}_k \varphi \rangle_i$$

$$= \sum_j p_j G_{ij}(\varphi) + p_i \varphi_i \underline{\nabla}_r \cdot \bar{\underline{v}} + p_i \underline{\Gamma}_i(\varphi) \cdot \underline{w} \qquad (1.9)$$

where

$$\underline{\Gamma}_i(\varphi) = (\langle \underline{v} \varphi \rangle_i - \varphi_i \bar{\underline{v}}) \qquad (1.10)$$

and

$$\underline{w} = -n^{-1} \underline{\nabla}_r n \qquad (1.11)$$

which we refer to as the diffusion driving force.

§ 1.3. The Homogenous Steady State

The moment balance equations for the homogenous steady state are obtained on setting all spatial and time derivatives to zero in (1.9), giving:

$$\sum_j p_j G_{ij}(\varphi) + \frac{e}{\hbar} p_i \underline{F} \cdot \langle \underline{\nabla}_k \varphi \rangle_i = 0 \qquad (1.12)$$

When $G_{ij}(\varphi)$ can be expressed as a function of the moments in valley j, the steady state values of the fractional population p_i and moments φ_i may be determined, in principle at least, by inserting all possible moment functions

into (1.12) [see Appendix I]. In practice, one adopts some approximation scheme whereby the infinite set of equations, starting from moment functions of the lowest order in $\underline{k}$, is truncated after a conveniently small number of equations have been considered. One way of doing this is to assume that the distribution function has some fixed shape, a displaced Maxwellian, say, i.e.

$$f_1(\underline{k}) = \frac{n\, p_1 \hbar^3}{(2\pi m^* k_B T)^{3/2}} \exp - \frac{\hbar^2(\underline{k} - \underline{k}_1)^2}{2m^* k_B T_1} \qquad (1.13)$$

where for simplicity, we have chosen the case of a constant scalar effective mass m^*. Then, because (1.13) contains five adjustable parameters in p_1, the components of $\underline{k}_1$ and T_1, we need consider only five moment balance equations to determine the distribution function. Starting from the lowest order in $\underline{k}$, the first five equations are those for $\varphi = 1$, k_x, k_y, k_z and k^2, corresponding respectively to the number, the average momentum in the $\hat{x}$-, $\hat{y}$- and $\hat{z}$- directions, and the energy of the electron distribution. The solution of the truncated set of equations is usually straightforward. The moment generation functions $G_{ij}(\varphi)$ must be evaluated for the relevant scattering mechanisms and for the assumed shape of the distribution function. For a displaced Maxwellian, $G_{ij}(\varphi)$ for $\varphi = 1$, $\underline{k}$ and k^2 are well-known for a large variety of scattering mechanisms (Butcher & Fawcett [8]) Some additional $G_{ij}(\varphi)$ for other moments and distribution shapes are derived and listed in Appendix II.

§1.4. Applications and critique

The moments balance method as outlined in §1.3 has been employed to calculate the distribution function in gallium arsenide by Butcher & Fawcett [9] and Heinle [10], in n-type silicon by Costato & Reggiani [11] and in indium antimonide by Hillbrand & Kranzer [12]. In the first three works, displaced Maxwellians were used and in the fourth, a hybrid displaced Maxwellian containing two electron temperatures, normal and parallel to the electric field, was used. (In addition to $\varphi = 1$, k_x, k_y, k_z and k^2, the balance of the moment function $\varphi = k_{11}^2$, where k_{11} is the component of $\underline{k}$ parallel to

the applied field, was included in the calculation).

Although in all cases, reasonably good velocity characteristics were predicted in comparison with experiment, the accuracy of the calculations was by not means always proven as a result, since the material parameters used such as deformation potentials and effective masses were often uncertain, and a fortuitous choice of these may conceal the inherent inaccuracy of a given calculation. Whether a calculation of this kind is accurate depends ultimately on how well the chosen form of the distribution function approximates to the true distribution function. When electron-electron scattering is the dominant process governing the exchange of energy and momentum of an electron then the displaced-Maxwellian is a good approximation to the true distribution function. For n-type silicon, the approximation appears to be good for electron concentrations of the order $10^{16}cm^{-3}$. The velocity characteristics predicted over a large range of lattice temperatures ($77^{o}K$ - $300^{o}K$) and electric fields (1 - $10^{4}V/cm$), and for different orientations of the electric field, are in good agreement with experiment [11].

For gallium arsenide a detailed Monte Carlo calculation of the distribution function has been made [4] and the displaced Maxwellian was shown to be an inadequate approximation to the true distribution function. Fawcett [13] has discussed in some detail the errors contained in the approximate solutions of the Boltzmann Equation in comparison with the exact methods. In general, the displaced Maxwellian tends to underestimate the number of high energy electrons. In gallium arsenide, this error is of crucial importance since only electrons with energy above $\sim$.36 eV can make transitions from the central to the satellite minima. Agreement with experiment in the displaced Maxwellian calculations was possible only as a result of a fortunate choice of material parameters. In silicon and germanium, such a situation does not arise although there are energy thresholds for processes such as optical phonon emission. These, however, are usually of the order of hundredths of an electron volt. Persky and Bartelink [14, 15] have developed a variation of the moments balance method in which only the shape of the spherically symmetric part of the distribution function is postulated, and the anisotropic part is completely

unspecified. For the former part they used a two-temperature Maxwellian joined at the energy threshold for optical phonon emission (non-polar optical phonon for p-germanium and polar for indium antimonide). Comparison with Monte Carlo results [7, 13] shows however, errors comparable with straightforward displaced Maxwellian calculations for indium antimonide.

Notwithstanding the frequent inadequacies of the moments balance method, we shall proceed on the basis that a semi-analytical theory for spatially and time-dependent problems is still a worthwhile proposition, even though it may not in all cases give quantitative results. As far as calculations for the homogenous steady state are concerned, several channels are still to be investigated fully, such as the use of other distribution functions than, and variations on, the displaced Maxwellian. In later chapters some results in this direction of investigation will be discussed (see § 2.6). It is also possible ~~for~~ to formulate time- and spatially-dependent problems within the framework of the moments balance method, but use data for the homogenous steady state from results derived by exact calculations, as will be shown in the next chapter.

In the problem of Gunn Domain Dynamics, where the electric field is strongly dependent on space and time, no exact solution of the Boltzmann Equation appears probable in the near future. It is therefore necessary to continue with approximate methods. In the work to date on this subject, one relies very heavily on physical concepts, such as energy and momentum relaxation, and the effects of a finite intervalley relaxation time. These arise quite naturally out of the moments balance method, generalised to encompass time - and spatially-dependent effects. As a last section to this chapter we shall describe the basic postulates in the extension of the moments balance method to deal with these situations.

§ 1.5. Formulation of time- and spatially-dependent problems

The time- and spatially-dependent behaviour of the moments φ_i, hence of the distribution function $f_i(\underline{k};\underline{r},t)$, is described fully by the infinite set of moments balance equations (1.9). As with the case

of the homogeneous steady state, one needs a truncation scheme to reduce the set to a manageable number. We may again adopt the approximation of assuming some fixed shape for the distribution function; the adjustable parameters contained therein are now to be treated as functions of time and position. However, even in the simple case when the distribution functions are assumed to be displaced Maxwellians, the truncated equations are not easily solvable for arbitrary variations of external parameters, such as the applied field, with respect to space and time. (Butcher and Hearn [16] have considered the case of a uniform field varying sinusoidally with time, as an approximation of the l.s.a. mode in gallium arsenide, assuming displaced Maxwellians.) To make any progress one must either simplify further the truncated system of equations, as will be shown in the chapter concerning the Gunn effect, or restrict oneself to the case where the system is only slightly perturbed about its steady state, i.e. deal with the linearised equations.

For the case of small perturbations about the steady state, it is convenient to start from the infinite set of moments balance equations. Suppose the system is perturbed from the steady state by fluctuations in the electric field or electron density; it will tend to relax back into a homogeneous steady state against the perturbing force. The perturbed distribution function can be represented by independent perturbations on the fractional populations p_i and the moments φ_i. i.e. $p_i \to p_i + \delta p_i$, $\varphi_i \to \varphi_i + \delta\varphi_i$ where $|\delta p_i| \ll p_i$, $|\delta\varphi_i| \ll \varphi_i$. In general δp_i and $\delta\varphi_i$ are functions of time and position, and are related to the perturbing force. To derive the essential features of the relaxation mechanisms we shall consider the simple case where the perturbing force is spatially homogeneous and 'switched-off' at some instant of time. The perturbations are then functions of time only and after the perturbing force is switched off, their behaviour is governed by the set of equations derived from (1.9) on linearising in terms of the perturbations, and setting all the space derivatives to zero, i.e.

$$\varphi = 1, \quad \frac{d}{dt}\delta p_i = \sum_j^N G_{ij}(1)\,\delta p_j + \sum_{\Psi_i} \sum_j^N \frac{\partial G_{ij}(1)^*}{\partial \Psi_j}\,\delta \Psi_j \qquad (1.14a)$$

$$\varphi \neq 1, \quad p_i \frac{d}{dt}\,\delta\varphi_i + \varphi_i \frac{d}{dt}\,\delta p_i =$$

$$\frac{e p_i}{\hbar}\,\underline{F}.\underline{\delta}\,(<\underline{\nabla}_k \varphi>) + p_i^{-1} \sum_{j\neq i}^N G_{ij}(\varphi)\,(p_i \delta p_j - p_j \delta p_i) + \sum_{\Psi} \sum_j^N p_j \frac{\partial G_{ij}(\varphi)}{\partial \Psi_j}\,\delta\Psi_j \qquad (1.14b)$$

subject to the conditions

$$\sum_j^N \delta p_j = 0, \quad \sum_j^N p_j = 1$$

where in (14a) and 14b) Ψ_j is a moment of valley j and Ψ is summed over all moment functions. The coefficients of the perturbations are understood to have their steady state values and the steady state equations (1.12) have been used to simplify the coefficient of δp_i on the right-hand side of (14b).

The coefficients of (1.14a) and (1.14b) are all constants so the equations describe a multiple exponential relaxation back to the steady state. The relaxation process is controlled by the steady state values of the quantities $G_{ij}(\varphi)$ and $\partial G_{ij}(\varphi)/\partial \Psi_j$ and we therefore refer to the infinite two-dimensional array of these quantities as the relaxation matrix. It is clear that the reciprocals of the diagonal matrix elements $G_{ii}(1)$ and $\partial G_{ii}(\varphi)/\partial \Psi_i$ have the dimensions of time; they are referred to as the principal relaxation times

---

* $G_{ij}(\varphi)$ is a function of the parameters φ_j contained in the distribution function f_i. In general φ_j may be expressed as a function of the moments Ψ_j of the distribution function. The derivatives of $G_{ij}(\varphi)$ w.r.t. Ψ_j is then defined by:

$$\frac{\partial G_{ij}(\varphi)}{\partial \Psi_i} = \sum_{\varphi_j} \frac{\partial G_{ij}(\varphi)}{\partial \varphi_j}\,\frac{\partial \varphi_j}{\partial \Psi_i}$$

of p_i and φ_i respectively in the remainder of the text.

When $\varphi(\underline{k}) = \underline{k}$, $E(\underline{k})$ where $E(\underline{k})$ is the energy of an electron with wave-vector $\underline{k}$ and is a homogeneous function of the components of $\underline{k}$, then $\partial G_{ii}(\varphi)/\partial \varphi_i$ is respectively the principal momentum and energy relaxation time. We observe that in general, the processes of relaxation of the fractional population, momentum and energy are coupled with the relaxation of all the other moments and we can speak of intervalley, momentum and energy relaxation as independent processes only if the conditions

$$|\varphi_i| \frac{\partial G_{ii}(\varphi)}{\partial \varphi_i} \gg \left| \frac{\partial G_{ij}(\varphi)}{\partial \Psi_j} \Psi_j \right| ; \quad G_{ij}(i) \gg \frac{\partial G_{ij}(1)}{\partial \Psi_j} |\Psi_j| \qquad (1.16)$$

are valid for $\varphi = \underline{k}$, E and for all j and Ψ_j. $(\Psi_j \neq \varphi_i)$ i.e. when the off-diagonal elements of the scattering matrix are negligible in comparison with the diagonal ones. Under these circumstances, the principal relaxation times for fractional population, momentum and energy reduce to what is ordinarily known as the intervalley, momentum and energy relaxation times.

The relaxation matrix as defined describes the transient response of the system after a perturbing force is switched-off. When we examine the problem of diffusion we shall deal with the response of the system to a perturbing force which is the diffusion driving force $\underline{w}$ as defined in (1.11). To carry out a numerical calculation the infinite set of equations such as (1.14), each member of which contains an infinite number of terms from the summation over ψ, must be truncated suitably. By assuming that the distribution function retains a constant shape, as with the case of the homogeneous steady state, both the number of the equations and of the terms contained therein become finite. The latter follows from the fact that the variations of a finite number of parameters in the distribution function f_i can be represented exactly by the dependence of the moment generation function $G_{ij}(\varphi)$ in an equal number of moments Ψ_j. An alternative approach to truncation is described in the next chapter (§ 2.2) whereby steady state distribution functions derived from exact calculations may be adapted for use in conjunction with the relaxation equations.

To complete the chapter, we reiterate the two principal

approximations in the present formulation of time- and spatially-dependent problems in the framework of the moments balance method:

I. The truncation of the infinite set of mements balance equations by assuming the distribution to have some fixed shape.

II. Further simplification of the truncated equations such as through linearisation.

The consequences of I are partly discussed in relation to the homogeneous steady state. By insisting that the distribution function retain its assumed shape during time- and spatially-dependent perturbations, we would incur no further error only if the time scale involved in the perturbations are much larger than the relaxation times so that the system is always in a quasi-'homogeneous steady state'. This is automatically implied if linearisation of the equations is justified. The consequences of II are best discussed in the context of the physical situation to which the equations are to be applied.

Chapter 2 A theory of diffusion and its application to gallium arsenide

§ 2.1 Introduction

In this chapter we shall develope a theory of diffusion for semiconductors with isotropic effective mass along the lines indicated in chapter 1. The theory is essentially a linear response theory for the perturbations on the steady state distribution function produced by an electron density gradient. The 'diffusion equations' are derived in § 2.2 by linearising the moment balance equations (1.9). By adopting a truncation scheme in which moments of order higher than the second are neglected, some general results are derived for the 'diffusion coefficients', and in particular, the velocity diffusion tensor. It is seen that diffusion effects can be attributed to thermal and multivalley origins; and under the appropriate circumstances, the two contributions can be separated and reduced to simple forms. Thermal effects lead to the generalised Einstein relations (§ 2.3) and intervalley scattering effects to results that provide a continuity to a previously established expression (§ 2.4).

The theory of diffusion is applied to gallium arsenide where the conduction band can be typified by two sets of equivalent minima of isotropic mass (§ 2.5). Calculations of the diffusion coefficients are made for various assumptions concerning the steady state. (§ 2.6). The results are compared with the Monte Carlo calculation of Fawcett and Rees [17]. Qualitative agreement is not expected because it has proved impossible to find a simple parameterised distribution that would approximate the distribution function in the central valley satisfactorily. However, the behaviour of the diffusion coefficients as derived by the Monte Carlo calculation is qualitatively explicable in terms of the concepts developed in the theory of diffusion. Comprison with experiment is limited by the scarcity of experimental date.

§ 2.2 The diffusion equations - truncation to second order

We shall consider an approximate solution to the infinite set of moments balance equations

$$\frac{\partial}{\partial t}(p_i\varphi_i) + \underline{\nabla}_r(p_i\langle \underline{v}\,\varphi\rangle_i) - \frac{ep_i}{m}\underline{F}.\langle\underline{\nabla}_k\varphi\rangle_i = \sum_j p_j\, G_{ij}(\varphi) + p_i\varphi_i\underline{\nabla}_r.\underline{\bar{v}} + p_i\underline{\Gamma}_i(\varphi).\underline{w} \tag{1.9}$$

when the total electron density n, which enters the equations through the diffusion driving force $\underline{w} = -n^{-1}\nabla_r n$, is a slowly-varying function of space and time. If no appreciable space-charge accumulation or depletion occurs, then the electron field $\underline{F}$ may be assumed to be a constant throughout. This neglect of space-charge effects is necessary at the first instance in order that purely diffusion effects may be analysed systematically. For small electron density fluctuations, a simple correction for space-charge effects can be made subsequently as detailed in §2.7.

To obtain a zeroth order solution to the equations (1.9) we neglect all space and time derivatives and obtain in effect the steady state equations (1.12) in which $n(\underline{r}, t)$ does not appear. The zeroth order approximation to p_i and φ_i are therefore just the steady state values in the constant electric field $\underline{F}$, and are independent of both $\underline{r}$ and t. If we denote the first order perturbations to the steady state values by δp_i and $\delta\varphi_i$, where these are functions of $\underline{r}$ and t, then equations for the perturbations are obtained by linearising (1.9) in terms of first order quantities, namely, the perturbations themselves and the diffusion driving force $\underline{w}$. The derivatives of the perturbations are of an order smaller than the perturbations themselves since all space and time variations are assumed to be small. Then because the steady state values are constants the resultant equations take the form, after simplification with the help of (1.12),

$$\sum_\Psi\sum_j p_j\frac{\partial G_{ij}(1)}{\partial\psi_j}\,\delta\psi_j + \sum_j G_{ij}(1)\,\delta p_j = -p_i\underline{\Gamma}_i(1).\underline{w} \tag{2.1a}$$

$$\sum_\Psi\sum_j p_i\frac{\partial G_{ij}(\varphi)}{\partial\psi_j}\,\delta\psi_j + p_i^{-1}\sum_j G_{ij}(\varphi)\,[p_i\delta p_j - p_j\delta p_i] + \frac{ep_i}{m}\sum_\alpha F_\alpha\,\delta\Big(\Big\langle\frac{\partial\varphi}{\partial k_\alpha}\Big\rangle_i\Big) = -p_i\underline{\Gamma}_i(1).\underline{w} \text{ for } \varphi\neq 1 \tag{2.1b}$$

where $\sum_{\alpha}$ signifies the summation over the components of a vector in a Cartesian coordinate system. We observe that the equations (2.1a) and (2.1b) are a set of inhomogeneous linear algebraic equations for the perturbations in which the inhomogeneous term is $-p_i \underline{\Gamma}_i(\phi).\underline{w}$. We may therefore introduce three-component diffusion coefficients for p_i and ϕ_i by writing

$$\delta p_i = \underline{D}(p_i).\underline{w} \tag{2.2a}$$

$$\delta \phi_i = \underline{D}(\phi_i).\underline{w} \tag{2.2b}$$

where the scalar produce notation has the usual interpretation in any Cartesian coordinate system, and obtain finally the diffusion equations:

$$\sum_{\psi} \sum_{j}^{N} p_j \frac{\partial G_{ij}(1)}{\partial \psi_j} \underline{D}(\psi_j) + \sum_{j}^{N} G_{ij}(1) \underline{D}(p_j) = -p_i \underline{\Gamma}_i(1) \tag{2.3a}$$

$$\sum_{\psi} \sum_{j}^{N} p_j \frac{\partial G_{ij}(\phi)}{\partial \psi_j} \underline{D}(\psi_j) + p_i^{-1} \sum_{j}^{N} G_{ij}(\phi) \left[p_i \underline{D}(p_j) - p_j \underline{D}(p_i) \right]$$

$$+ \frac{e p_i}{k} \sum_{\alpha} F_{\alpha} \underline{D} \left(\left\langle \frac{\partial \phi}{\partial k d} \right\rangle_i \right) = -p_i \underline{\Gamma}_i(\phi)$$

$$\phi \neq 1. \tag{2.3b}$$

where every quantity, apart from the diffusion coefficients, is understood to have its steady state value. We see by inspection that the matrix which appears in the diffusion equations (2.3) is precisely the relaxation matrix which appears in the relaxation equations (1.14). Since $\sum_i \delta p_i = 0$ by definition, we have from (2.2a) a useful result: $\sum_i \underline{D}(p_i) = 0$.

To discuss further the evaluation of the diffusion coefficients from the equations (2.3a) and (2.3b) it is convenient at this stage to make explicit the truncation scheme we shall adopt to reduce the infinite set of equations to a closed form. Some useful general results can be obtained when moments of higher order than the second are ignored. Accordingly, we shall assume that the dependence of the moment generating functions $G_{ij}(\varphi)$ on the moment ψ_j is negligible when ψ_j is of an order higher than the second. In the summation over ψ_j in (2.3) we shall therefore set ψ_j equal to the nine independent moments $k_{\alpha j}$ and $<k_\alpha k_\beta>_j$ only, where the Greek subscripts label the coordinate axes as before. The ten equations for the moment functions $\varphi = 1$, k_α, $k_\alpha k_\beta$ for each of the N valleys form then a closed set for the ten diffusion coefficients $\underline{D}(p_i)$, $\underline{D}(k_{\alpha i})$ and $\underline{D}(<k_\alpha k_\beta>_i)$, where $i = 1, 2 \ldots N$. Since the equations and diffusion coefficients contain three components each, we have thus 30 x N equations for 30 x N unknowns. Fortunately, the number of unknowns can usually be reduced when the symmetry properties of the diffusion coefficients are taken into account. This will be discussed in detail when the equations are applied to specific situations in chapter 3 and for the case of isotropic valleys in § 2.3.

The truncation scheme described above is not exactly the same as that outlined in the previous chapter (§ 1.5). So far, no restriction has been placed on the steady state distribution function beyond the implicit one that the dependence of $G_{ij}(\varphi)$ on the higher moments is negligible. To carry out a numerical calculation one can therefore evaluate $G_{ij}(\varphi)$ and its derivatives with respect to the moments using steady state distribution functions derived by the

moments balance method, or by one of the exact methods, as long as a means of parameterising the distribution function can be found for the latter case, to give the derivatives of $G_{ij}(\varphi)$ an operational meaning (see footnote to equation (1.14)). When the number of parameters for either case is less than 10, the number of equations contained in the truncation scheme to second order, then some of the equations reduce automatically to trivial identities, leaving as many non-trivial equations as there are independent parameters, and consequnetly, independent moments and corresponding diffusion coefficients. In such a case, the truncation scheme becomes identical to the one in which one starts off with a fixed distribution function and considers as many diffusion equations as there are parameters in the distribution function, as outlined in (§ 1.5). In practice the number of parameters contained in the steady state distribution functions are never greater than 10.

The results of the remainder of the chapter will be independent of the procedure to obtain the steady state, and it is to be understood hereafter that the summation over the moments will be restricted to those up to the second order.

§ 2.3 Thermal Diffusion and the generalised Einstein Relations

We see from the diffusion equations (2.3a) and (2.3b) that the diffusion coefficients are closely related to the inhomogeneous term $-p_i \underline{\Gamma}_i(\varphi)$. The analysis of diffusion effects is greatly facilitated if one recognises that $\underline{\Gamma}_i(\varphi)$ is composed of two parts which have distinct physical origins. Since $\overline{\underline{v}} = \sum_j^N p_j \underline{v}_j$ and $\sum_j p_j = 1$, we see from the definition of $\underline{\Gamma}_i(\varphi)$ (1.10) that

$$\underline{\Gamma}_i(\varphi) = \underline{\Gamma}_i^{th}(\varphi) + \sum_{j \neq i}^N \underline{\Gamma}_i^{ij}(\varphi) \qquad (2.5)$$

where

$$\underline{\Gamma}_i^{th}(\varphi) = \langle (\underline{v} - \underline{v}_i)\,\varphi \rangle_i \qquad (2.6a)$$

and

$$\underline{\Gamma}_i^{ij}(\varphi) = \varphi_i p_j (\underline{v}_i - \underline{v}_j). \qquad (2.6b)$$

We shall refer to $\underline{\Gamma}_i^{th}(\varphi)$ as the thermal part of $\underline{\Gamma}_i(\varphi)$ and $\underline{\Gamma}_i^{ij}(\varphi)$ as the intervalley part arising from transfer of electrons to and from valley j. This nomenclature is obvious from the structure of (2.5) and (2.6). $\underline{\Gamma}_i^{th}(\varphi)$ clearly relates the contribution to diffusion effects arising from the spread of the velocity distribution in valley i and is dependent on the distribution in valley i only. $\underline{\Gamma}_i^{ij}(\varphi)$ on the other hand, relates the contribution of intervalley scattering between valleys i and j to diffusion effects in valley i. The summation over j in (2.5) is analogous to the averaging in (2.6a), so explicit intervalley diffusion effects may be seen to arise from the spread of the average velocities in the various valleys, just as thermal diffusion within a single valley is a result of the thermal spread of velocities within the single valley. We have qualified the effects associated with $\underline{\Gamma}_i^{ij}(\varphi)$ as 'explicit' because the diffusion coefficients in all the valleys are coupled together through the presence of $G_{ij}(\varphi)$ (for $i \neq j$) and its derivatives in the diffusion equations (2.3). These latter terms describe a multivalley effect which is not explicitly a diffusion effect; they merely express the interdependence of the perturbations to the moments in all the valleys through intervalley scattering, whether or not the perturbations are produced by a density gradient. We shall return to a fuller discussion of these points in the next section. In the remainder of this section some results will be derived for purely thermal diffusion. These apply to the cases of a single valley, or a set of equivalent valleys. In the former there can obviously be no multivalley effects, and in the latter, we see that the coupling of the valleys is broken in (2.3) when we set $\underline{D}(p_j) \equiv \underline{D}(p_i)$, $\underline{D}(\psi_j) \equiv \underline{D}(\psi_i)$, and $\partial G_{ij}(\varphi)/\partial \psi_j \equiv \partial G_{ji}(\varphi)/\partial \psi_i$, i.e. the equations are reduced to a form in

each of which the diffusion coefficients and moments of only one valley are referred to . Moreover $\underline{\Gamma}_i^{ij}(\varphi)$ is obviously zero when $\underline{v}_i = \underline{v}_j$.

Without solving the diffusion equations (2.3) certain useful results can be derived for the case when only thermal diffusion is important. We proceed by comparing these equations for the diffusion coefficients with the corresponding equations for the coefficients $\underline{d}(p_i)$ and $\underline{d}(\varphi_i)$ which determine the perturbations of p_i and φ_i produced in a homogeneous system by a small constant increment $\delta\underline{F}$ in the applied electric field. These 'field-gradients' are defined by equations analogous to (1.14), i.e.

$$\delta p_i = \underline{d}(p_i) \cdot \delta\underline{F} \qquad (2.7a)$$

$$\delta\varphi_i = \underline{d}(\varphi_i) \cdot \delta\underline{F} \qquad (2.7b)$$

The field-gradients have the same symmetry properties as the corresponding diffusion coefficients and the equations from which they can be determined are obtained by linearising the moment balance equations (1.9) in terms of the perturbations and $\delta\underline{F}$ and setting all space and time derivatives to zero, giving:

$$\sum_{\Psi}\sum_{j}^{N} p_j \frac{\partial G_{ij}(1)}{\partial \Psi_j}\,\underline{d}(\Psi_j) + \sum_{j}^{N} G_{ij}(1)\,\underline{d}(p_j) = 0 \qquad (2.8a)$$

$$\sum_{\Psi}\sum_{j}^{N} p_j \frac{\partial G_j(\varphi)}{\partial \Psi_j}\,\underline{d}(\Psi_j) + p_i^{-1}\sum_{j}^{N} G_{ij}(1)\left[p_i\underline{d}(p_j) - p_j\underline{d}(p_i)\right] + \frac{ep_i}{m}\sum_{\alpha}\underline{F}_\alpha\,\underline{d}\left(\left\langle\frac{\partial\varphi}{\partial k_\alpha}\right\rangle\right)$$

$$= \frac{ep_i}{m}\langle\underline{\nabla}_k\varphi\rangle_i \quad \text{for } \varphi \neq 1 \qquad (2.8b)$$

We see by inspection that these equations differ from the diffusion equations (2.3) only in that the inhomogeneous term $-p_i\underline{\Gamma}_i(\varphi)$ in (2.3) is replaced by $-p_i(e/m)\langle\underline{\nabla}_k\varphi\rangle_i$ in (2.8). In table I we compare the components of

$<\underline{\nabla}_k \varphi>_i$ with those of $\hbar\underline{\Gamma}_i^{th}(\varphi)$ for all moments up to second order. The coordinate axes have been chosen to coincide with the principal axes of the effective mass tensor. The third moments about the mean, $C^{(i)}_{\alpha\beta\beta}$ and $C^{(i)}_{\alpha\alpha\alpha}$; vanish if the steady state distribution is an even function of $(k_\alpha - k_{\alpha i})$. They may be expected to be small in any case and we shall neglect them hereafter. We then see from the table that the α-components of $<\underline{v}_k\varphi>_i$ and $\hbar\underline{\Gamma}_i^{th}(\varphi)$ differ only by a common factor $k_B T_{\alpha i}$, where k_B is Boltzmann's constant and $T_{\alpha i}$ is the temperature of valley i associated with the α-axis, defined as:

$$T_{\alpha i} = \frac{m_i}{k_B} <(v_\alpha - v_{\alpha i})^2> \qquad (2.9)$$

For a single valley where $\underline{\Gamma}_i(\varphi) = \underline{\Gamma}_i^{th}(\varphi)$, the inhomogeneous terms of the α-components of the diffusion and field gradient equations differ therefore by a constant vector $k_B T_{\alpha i}$. Since these equations form a closed set for the α-components of the coefficients $\underline{D}(\varphi_i)$ and $\underline{d}(\varphi_i)$, we have therefore the generalised Einstein relations;

$$D_\alpha(\varphi_i) = \frac{k_B T_{\alpha i}}{e} d_\alpha(\varphi_i) \qquad (2.10)$$

(We have kept the valley subscript i simply to differentiate $\varphi = \varphi(\underline{k})$ and $\varphi_i = <\varphi>$.)

We recall that the Einstein formula for the velocity diffusion constant D for electrons in thermal equilibrium with the lattice is $D = \mu k_B T/e$ [18] where μ is the mobility of the electrons and T their temperature.

The interpretation of the generalised Einstein relations is straightforward when the effective mass is isotropic. In this case the moment functions $\varphi(\underline{k})$ in valley i can be replaced by $\varphi(\underline{v})$ since the components of $\underline{v}$ and $\underline{k}$ differ by the same constant m_i/h. Moreover, the system has cylindrical symmetry about the direction of the applied electric field which we relabel the z-axis. It therefore follows that the

velocity diffusion tensor, $\tilde{D}_{\alpha\beta}(\underline{v}_i)$, formed by the components $D_\alpha(v_{\beta i})$, is invariant under all proper and improper rotations which leave the $\hat{z}$-axis invariant. In order to comply with these transformation properties, the tensor must be diagonal, with components

$$D_{xx}(\underline{v}_i) = D_{yy}(\underline{v}_i) \neq D_{zz}(\underline{v}_i) \tag{2.11}$$

where $D_{xx}(\underline{v}_i) = D_x(v_{x_i})$ etc. Similarly, the same transformation properties which must apply for the vector $\underline{D}(p_i)$ and the third rank tensor $D_\alpha(<v_\beta v_\gamma>_i)$ requires that $\underline{D}(p_i)$ has only one non-zero component $D_z(p_i)$*; and of the other diffusion coefficients which constitute the third rank tensor $D_\alpha(<v_\beta v_\gamma>_i)$, there are only seven non-zero components of which only three are independent:

$$\begin{aligned} &D_z(<v_z^2>_i), \\ &D_z(<v_x^2>_i) = D_z(<v_y^2>_i), \\ &D_x(<v_x v_z>_i) = D_x(<v_z v_x>_i) = D_y(<v_z v_y>_i) \end{aligned} \tag{2.12}$$

It is worthy of note that the average energy of the electrons (equal to $m_i<v^2>/2$) is unperturbed by a density gradient transverse to the electric field.

The symmetry properties of the field gradient coefficients $\underline{d}(\varphi_i)$ follow identically those of the corresponding diffusion coefficients $\underline{D}(\varphi_i)$. Moreover, the longitudinal components may be expressed immediately in terms of the derivatives of the steady state moments with respect to the magnitude of the electric field i.e. $d_z(v_{z_i})$ is just the differential mobility $\frac{d}{dF}(v_{z_i})$ while $d_z(<v_z^2>_i)$ and $d_z(<v_x^2>_i)$ are given by $\frac{d}{dF}(k_B T_{1i}/m_i + v_{zi}^2)$ and

* For a single valley $D_z(p_i)$ must also be zero since $p_i \equiv 1$. For equivalent valleys $D_z(p_i)$ is zero from $D_z(p_i) = D_z(p_j)$ and (2.4).

$\frac{d}{dF}(k_B T_{ti}/m_i)$ respectively. The transverse components of the field gradients can also be expressed in terms of the steady state characteristics when one exploits fully the isotropy of the system with respect to the field orientation. In appendix III we show that $d_x(v_{xi})$ and $d_x(\langle v_x v_z \rangle_i)$ are equal to $\frac{v_{zi}}{F}$ and $\left[\frac{k_B(T_{li}-T_{ti})}{m_i} + v_{zi}^2\right]/F$ respectively. Hence in the case of a single isotropic valley, we have the results

$$D_{zz}(v_i) = \frac{k_B T_{li}}{e} \frac{dv_{zi}}{dF} \tag{2.13}$$

$$D_{xx}(v_i) = \frac{k_B T_{ti}}{e} \frac{v_{zi}}{F} \tag{2.14}$$

$$D_z(\langle v_z^2 \rangle_i) = \frac{k_B T_{li}}{e} \frac{d}{dF}\left(\frac{k_B T_{ti}}{m_i} + v_{zi}^2\right) \tag{2.15a}$$

$$D_z(\langle v_x^2 \rangle_i) = \frac{k_B T_{li}}{e} \frac{d}{dF}\left(\frac{k_B T_{ti}}{m_i}\right) \tag{2.15b}$$

$$D_x(\langle v_x v_z \rangle) = \frac{k_B T_{ti}}{e}\left[k_B(T_{li}) + v_{zi}^2\right]/F \tag{2.15c}$$

The generalised Einstein relations take the simple form (2.13) -(2.15) for a single isotropic valley when the truncation scheme to second order and the neglect of third moments are valid. They are therefore strictly valid for the case when the steady state distribution function is a displaced Maxwellian, and may be considered approximately true for the general case.

We note that the expression for the transverse velocity diffusion coefficient (2.14) is identical to the Einstein relation for electrons in thermal equilibrium with the lattice. This result is not totally unexpected since a density gradient transverse to the applied field does not produce any heating of the electrons ($D_x(\langle v^2 \rangle_i) = 0$). When the density gradient is parallel to the applied field, the average electron energy is perturbed, so the expression for thermal equilibrium is no longer valid. What is perhaps surprising is the simple result (2.13). The field gradients coefficients $d_x(v_{xi})$ are respectively the chord and

differential mobilities precisely because the perturbation δF produces additional heating in the latter case but not in the former. It appears that because of the structural similarity between the diffusion and field-gradient equations, exactly the same correction is applicable to the diffusion coefficients.

§ 2.4 Multivalley effects

When several non-equivalent valleys are populated, the perturbation produced by a density gradient on the moment $\bar{\varphi}$, where the averaging sign denotes an average over all the valleys, is given by:

$$\delta\bar{\varphi} = \sum_i \left[p_i \delta\varphi_i + \varphi_i \delta p_i \right]$$

$$= \sum_i \left[p_i \underline{D}(\varphi_i) + \varphi_i \underline{D}(p_i) \right] \cdot \underline{w} \qquad (2.16)$$

The term containing $\underline{D}(p_i)$ expresses the direct contribution of intervalley scattering to the diffusion process involving $\bar{\varphi}$ while the other diffusion coefficient $\underline{D}(\varphi_i)$ also contains contributions from intervalley scattering as a result of the coupling together of the diffusion coefficient $\underline{D}(\Psi_j)$ for all Ψ and j, and the presence of the intervalley part of the inhomogeneous term $\underline{\Gamma}_i^{ij}(\varphi)$, in the diffusion equations (2.4). In general there is no way of isolating thermal and multivalley effects but for the case of isotropic valleys certain simplifications can be achieved.

Consider then isotropic valleys for each of which one can apply the symmetry arguments of the previous section. We note that $\underline{D}(p_i)$ and $\underline{\Gamma}_i^{ij}(\varphi)$ are purely longitudinal in this case. (The latter follows from (2.6) when all the average velocities $\underline{v}_j$ are parallel to the field for isotropic valleys.) For the longitudinal direction one does not therefore expect the Einstein relations (2.13 - 2.15) to hold because the inhomogeneous terms in the diffusion and field gradient equations no longer differ by a constant factor: the diffusion equa-

tions contain the intervalley part $\underline{\Gamma}_i^{ij}(\varphi)$ which has no counterpart in the field gradient equations, and moreover, even when $\underline{\Gamma}_i^{ij}(\varphi)$ can be ignored, the constant of proportionality for the inhomogeneous terms ($k_B T_i/e$) is different for each valley i, and the equations for all the valleys are coupled together.

For the transverse direction, the symmetry arguments of the previous section show that there are two non-zero components of the diffusion coefficients, $D_{xx}(\underline{v}_i)$ and $D_x(\langle v_x v_z \rangle_i)$, for each valley i, and we may therefore form a close set of equations for these components by taking the x-component of the diffusion equations for $\varphi = v_x$, $v_x v_z$. (In fact all other choice of φ would lead to the trivial identity 0 = 0.) In these equations the inhomogeneous term contains the thermal part $\underline{\Gamma}^{th}(\varphi)$ only, because $\underline{\Gamma}_i^{ij}(\varphi)$ is purely longitudinal and moreover, the equations for the different valleys are decoupled because $G_{ij}(\varphi)$ for $i \neq j$ is identically zero for all φ which are odd functions of v_x. (This follows from (1.6) and (1.2b) when $B_{ji}(\underline{v}', \underline{v})$ contained therein is an even function of v_x according to table II in § 2.5) The equations take therefore the same form as those of distinct single valleys. The same considerations must apply for the field gradient equations and we may evaluate $D_{xx}(\underline{v}_i)$ and $D_x(\langle v_x v_z \rangle_i)$ using the generalised Einstein relations (2.14 -15). Putting $\varphi = v_x$ in (2.16) we have from (2.14)

$$D_t = \sum_i p_i \frac{k_B T_{ti}}{e} \frac{v_{zi}}{F} \qquad (2.17)$$

Where D_t is the transverse velocity diffusion coefficient or the transverse diffusion constant in the usual nomenclature. It is simply the average of the diffusion coefficients in each valley as given by the Einstein relation for thermal equilibrium at the respective electron temperatures T_{ti}. This result was anticipated by Butcher, Fawcett and Ogg [19] completely intuitively. Their assumption that this result holds also for the longitudinal direction is of course erroneous.

Some progress can be made with the evaluation of the longitudinal components only when very drastic approximations are made. We shall consider the case when intervalley scattering effects are weak, in the sense that

(i) $G_{ij}(\varphi) \ll G_{ii}(\varphi)$

for all φ except $\varphi = 1$ since $G_{ii}(1)$ is purely intervalley, and

(ii) $\underline{\Gamma}_i^{ij}(\varphi) \ll \underline{\Gamma}_i^{th}(\varphi)$

for all φ except $\varphi = 1$ because $\underline{\Gamma}_i^{th}(1)$ is zero.

When the conditions (i) and (ii) are valid, and we neglect $G_{ij}(\varphi)$ and $\underline{\Gamma}_i^{ij}(\varphi)$ in comparison with $G_{ii}(\varphi)$ and $\underline{\Gamma}_i^{th}(\varphi)$ respectively, the equations for $\varphi \neq 1$ for each valley i are decoupled from the other valleys and all the diffusion coefficients except $\underline{D}(p_i)$ can be evaluated using the generalised Einstein relations. (The equation for $\varphi = 1$ is a trivial identity for single valleys and does not form part of the close set of equations for $\underline{D}(\varphi_i)$.) Since the generalised Einstein relations express purely thermal effects the sole effect of intervalley scattering in (2.16) is therefore contained in the term involving $\underline{D}(p_i)$ in the present approximation. The equations for $\varphi = 1$ allow the $\underline{D}(p_i)$ is to be determined, subject to the condition that $\sum_i \underline{D}(p_i) = 0$ (2.5). When only two valleys are populated we have from (2.3a), for i = 1:

$$D_Z(p_i) = (G_{12}(1) - G_{11}(1))^{-1}\left[p_1 p_2 (v_{Z_1} - v_{Z2}) + \sum_{\Psi} \sum_{j=1,2} p_j \frac{\partial G_{ij}(1)}{\partial \Psi_j} G_Z(\Psi_j)\right] \quad (2.18)$$

where the result $p_1 G_{11}(1) + p_2 G_{12}(1) = 0$ from the steady state equations (1.12) and (2.6) have been used. The second term on the right-hand side of (2.18) expresses the effect of the perturbations $\delta\Psi_j$ on the intervalley transition rates $G_{11}(1)$ and $G_{12}(1)$ and hence also the fractional population p_i. The first term arises from a finite intervalley relaxation time and the difference of average velocities in the valleys, and was referred to previously as the explicit intervalley diffusion effect. We shall concentrate on this first term and ignore for the moment the rest of the right-hand side of (2.18). When $D_Z(p_i)$ is then substituted into (2.16) for $\varphi = v_Z$, we obtain the intervalley contribution to velocity diffusion in the longitudinal direction which is characterised by an equivalent diffusion constant

$$D_{\text{intervalley}} = \frac{p_1 p_2}{[G_{12}(1) - G_{11}(1)]} (v_{Z1} - v_{Z2})^2 \quad (2.19)$$

The expression (2.19) has been obtained previously by Shockley, Copeland and James [20] and by Ohmi and Hasuo [21]. We note that $G_{12}^{-1}(1)$ and $-G_{11}^{-1}(1)$ are the principal intervalley relaxation times from valley 2 to 1 and vice versa. The equivalent diffusion constant is therefore simply the product of the square of the velocity difference between the valleys and a measure of the transition probability between them. This result is not difficult to reproduce from heuristic arguments. The important assumptions that have been made to obtain (2.19) are the neglect of firstly, intervalley transfer in the balance of all the moments except electron number and secondly, the changes in the intervalley relaxation times produced by the density gradient.

We see therefore that in general, multivalley effects are extremely complicated for the longitudinal orientation. The truncated diffusion equations will always yield analytical solutions for the diffusion coefficients but a simple interpretation of the terms contained therein is impossible because of their interdependence. In the next three sections we shall present the results of the complete solution of the truncated equations for gallium arsenide where the conduction band may be approximated by two sets of non-equivalent, isotropic minima.

§ 2.5 Application to gallium arsenide - band model and scattering mechanisms.

The model of the conduction band of gallium arsenide which we shall adopt consists of two types of minima. The first is a single isotropic valley of effective mass m_1, situated at the centre of the Brillouin zone. The second is composed of three equivalent satellite valleys situated at the edge of the Brillouin zone along the (100) directions at an energy Δ above the central minimum. Although the X_1 symmetry of these minima requires the constant energy surfaces to be ellipsoidal in their neighbourhood, we shall assume that they are isotropic with effective mass m_2. This approximation is justified on the grounds that data for the effective masses in these minima are uncertain and anisotropic effects are not expected to be important because of the strong intervalley scattering between these valleys.

(The relation between intervalley scattering and anisotropic effects will be discussed in full in the next chapter.) The minima situated at the X_3 and L_1 points of the Brillouin zone are ignored in this band model. They are situated at a higher energy above the central minima than the X_1 valleys, and are unlikely to be populated to any extent in the range of electric fields we shall consider since electrons in the X_1 valleys are only slightly heated at these field strengths. A detailed discussion concerning the band structure of gallium arsenide and the approximations made here is given by Fawcett, Boardman and Swain [4] in connection with their Monte Carlo calculation. The band model as described is similar to the one adopted in [4].

The scattering mechanisms we shall include are polar optical phonon and acoustic phonon intervalley scattering, and non-polar optical phonon intervalley scattering for central-satellite and satellite-satellite transitions. Ionised impurity scattering and electron-electron collisions have been omitted throughout, i.e. we shall concern ourselves with high purity samples of low electron concentration. Moreover, we note that electron-electron scattering, which conserves electron momentum and energy, plays no part in the balance of these moments for the electron distribution as a whole. The transition probabilities $A_{ii}(\underline{k}, \underline{k}')$ and $B_{ij}(\underline{k}, \underline{k}')$ as defined in (1.2) for intravalley and intervalley scattering respectively are listed in Table II. These results are obtained from first order time-dependent perturbation theory for plane-wave electron wave-functions.

The formula for polar optical phonon scattering, which is based on the Coulomb interaction between the electron and electric field associated with the polar phonons, was given by Ehrenreich [22] who showed that this process is primarily responsible for limiting the low field mobility of good quality n-type crystals of III-V compounds at room-temperature. The material parameters contained in the formula are ϵ_∞ and ϵ_s, the high frequency and static dielectric constants respectively of gallium arsenide, and ω_o, the polar optical phonon frequency which may be assumed to remain

constant in the range of phonon wavelengths relevant to intravalley transitions. The transition probabilities for acoustic and non-polar optical phonon scattering are derived from deformation potential scattering theory. For long wavelength acoustic phonons, the coupling between electrons and phonons is characterised by a deformation potential tensor through which the shift of the conduction band minimum is related to strains produced in the lattice by the phonons. In isotropic material, the tensor reduces to a scalar deformation potential Ξ_a and only the longitudinal branch of the acoustic phonons are coupled to the electrons. From these considerations the formula given in Table II results [23] in which ρ and s are respectively the density and longitudinal sound velocity. In the case of intervalley scattering, essentially the same formula applies. The wave-vector $(\underline{k} - \underline{k}')$ of the phonon involved in the transitions between valleys i and j is however of an approximately fixed value equal to the separation of the centres of the valleys $(\underline{k}_i - \underline{k}_j)$. We may therefore ignore the dependence of the phonon frequency w_{ij}, the occupation number N_{ij} and hence the transition probability on $\underline{k}$ and $\underline{k}'$. To obtain the final expression for intervalley scattering, we introduce after Reik [24] as a matter of convention D_{ij}, the deformation potential field for the phonon associated with the intervalley transition, in place of $\Xi_a(\underline{k}' - \underline{k})$, and ω_{ij} in place of $(\underline{k}' - \underline{k})$ s, in the formula for acoustic phonon scattering. The values of these and other parameters used in the calculations for gallium arsenide are given in Table III. A discussion of the choice of these values is given in [4] and [32]. The calculations to be described are carried out for a lattice temperature of 300°K.

§ 2.6 The steady state distribution functions

As a first test of the theory of diffusion, we shall apply it to the case where the steady state distribution functions in the two types of valleys are displaced Maxwellians, i.e.

$$f_i(\underline{k}) = n p_i \frac{\hbar^3}{(2\pi m_i k_B T_i)^{3/2}} \exp\left\{\frac{-\hbar^2(\underline{k} - \underline{k}_i)^2}{2m_i k_B T_i}\right\} \qquad (2.20)$$

where $\underline{k}_i = (0, 0, k_{z_i})$, $\hat{z}$ being the direction of the electric field, and the wave vector $\underline{k}$ is measured from the centre of valley i. Although displaced Maxwellians are known to give a poor representation of the steady state, we shall proceed on the grounds that the mathematics is simple in this case and that the theory of diffusion is strictly valid for distribution functions of this form. For a given field $\underline{F}$, the parameters p_i, k_{z_i} and T_i in (2.20) are determined by inserting $\varphi = 1$, v_z and E, where $v_z = \hbar k_z/m_i$ and $E = \hbar^2 k^2/2m_i$ for valley i, into the steady state equations (1.12) and solving the resultant equations which take the form:

$$\sum_i p_j G_{ij}(1) = -p_i/\tau_i + p_j/\tau_j = 0$$

$$G_{ii}(v_z) = -v_{z_i}/\tau_p = -\frac{eF}{m}$$

$$\sum_j p_j G_{ij}(E) = -W_i p_i + U_j p_j = -eF v_{z_i} p_i \qquad (2.21a)$$

where for clarity we have written

$$-G_{ii}(1) = G_{ji}(1) = 1/\tau_i$$
$$G_{ii}(v_z) = -v_{z_i}/\tau_i,$$
$$G_{ii}(E) = -W_i$$
$$G_{ji}(E) = U_i \qquad (2.21b)$$

The terms on the right-hand side of (2.21b) are respectively the intervalley relaxation time τ_i, the momentum relaxation time τ_{pi} in valley i, the total rate of energy loss in valley i per electron W_i, and the total rate of energy gain U_i in valley j by transfer from valley i per electron therein. These are all functions of k_{z_i} and T_i. We have already noted in § 2.4 that $G_{ii}(v_z)$ is identically zero. The physical interpretation is that electrons entering

valley i from valley j populate momentum space in valley i completely randomly so that generation rate for momentum is zero.

The transverse diffusion coefficients are then given simply by (2.14 - 15) in terms of the steady state parameters. The transverse temperature T_{t_1} is simply T_1 in this case.

When the distribution function is assumed to be a displaced Maxwellian, the number of independent diffusion coefficients in the longitudinal direction is further reduced by virtue of the isotropy of the distribution function about the displaced centre $\underline{k}_1$, viz.

$$D_Z(<v_Z^2>_1) = D_Z(<(v_Z - v_{Z1})^2>_1) + 2v_{Z1}D_Z(v_{Z1})$$
$$= D_Z(<v_X^2>) + 2v_{Z1}D_Z(v_{Z1}) \qquad (2.22)$$

We shall rewrite the three remaining independent diffusion coefficients as $D_Z(p_1)$, $D_Z(v_{Z1})$ and $D_Z(E_1)$ where

$$E_1 = \frac{\hbar^2}{2m_1} <k^2>_1$$
$$= 3/2\, k_B T_1 + \tfrac{1}{2} m_1 v_{Z1}^2, \qquad (2.23)$$

is the total average energy of the electrons in valley i and

$$D_Z(E_1) = \frac{3m_1}{2} D_Z(<v_X^2>_1) + m_1 v_{Z1} D_Z(v_{Z1}) \qquad (2.24)$$

The purpose of putting the diffusion coefficients in this form is that to obtain a closed set of equations for them, one simply inserts into the diffusion equations (2.4) the same moment functions ($\varphi = 1$, v_Z and E) as those inserted into (1.12) to determine the steady state. i.e. These equations take the form:

$$-p_1 \frac{\partial \bar{\tau}_1^{-1}}{\partial E_1} D_Z(E_1) - p_1 \frac{\partial \bar{\tau}_1^{-1}}{\partial v_{Z1}} D_Z(v_1) + p_2 \frac{\partial \bar{\tau}_2^{-1}}{\partial E_2} D_Z(E_2)\; p_2 \frac{\partial \bar{\tau}_2^{-1}}{\partial E_2} D_Z(v_2) - \frac{1}{\tau_1} D_Z(p_1)$$
$$= p_1 p_2 (v_{Z1} - v_{Z2}) \qquad (2.25)$$

for $\varphi = 1$ in valley 1 and so forth.

This procedure is not strictly necessary but it does allow the same moment generation functions $G_{ij}(\varphi)$ to be used in both parts of the calculation. The $G_{ij}(\varphi)$'s for the relevant scattering mechanisms are listed in Appendix II. They are functionals of the normalised distribution function f_j/np_j and are therefore functions of k_{zj} and T_{zj}. From (2.23) and $v_{zi} = \hbar k_{zi}/m_i$, the derivatives of $G_{ij}(\varphi)$ with respect to the moments v_{zj} and E_j are given by

$$\frac{\partial G_{ij}(\varphi)}{\partial v_{zj}} = \frac{m_j}{\hbar} \frac{\partial G_{ij}(\varphi)}{\partial k_{zj}}$$

$$\frac{\partial G_{ij}(\varphi)}{\partial E_j} = \frac{2}{3k_B} \frac{\partial G_{ij}(\varphi)}{\partial T_j} + \frac{m_j}{\hbar^2 k_{zj}} \frac{\partial G_{ij}(\varphi)}{\partial k_{zj}} \qquad (2.26)$$

$G_{ij}(\varphi)$ and its derivatives are evaluated numerically. Numerical differentiation is straightforward since $G_{ij}(\varphi)$ varies smoothly with k_j and T_j.

We shall also consider the distribution function:

$$f_i(\underline{k}) = \frac{n p_i \hbar^3}{(2\pi m_i k_B)^{3/2} T_{ti} T_{li}^{\frac{1}{2}}} \exp - \left\{ \frac{\hbar^2}{2m_i} \left[\frac{k_x^2 + k_y^2}{k_B T_{ti}} + \frac{(k_z - k_{zi})^2}{k_B T_{li}} \right] \right\} \qquad (2.27)$$

We refer to this distribution function as a 'two-temperature displaced-Maxwellian' where the parameters T_{li} and T_{ti} are respectively the electron temperatures associated with the longitudinal and transverse directions. As with the displaced Maxwellian, truncation to second order is strictly valid if the steady state distribution function is of the form given by (2.27). To determine the values of the parameters for the steady state, we shall consider the balance of the moments $\varphi = 1$, v_z, E and E_z where $E_z = \hbar^2 k_z^2/2m_i$ in valley i. The diffusion coefficients in the transverse direction can be evaluated using (2.14 -15) as before. In the longitudinal direction, the independent diffusion coefficients are $D_z(p_i)$, $D_z(v_i)$, $D_z(E_i)$ and $D_z(E_{zi})$ where

$$E_i = k_B T_{ti} + \tfrac{1}{2} k_B T_{li} + \tfrac{1}{2} m_i v_{zi}^2 \qquad (2.28a)$$

$$E_{zi} = \tfrac{1}{2}k_B T_{1i} + \tfrac{1}{2} m_i v_{zi}^2 \qquad (2.28b)$$

$$D_z(E_i) = \left[2D_z(\langle v_x^2 \rangle) + D_z(\langle v_z^2 \rangle)\right]^{m_i/2} \qquad (2.29a)$$

and $$D_z(E_{zi}) = D_z(\langle v_z^2 \rangle)\, m_i/2 \,, \qquad (2.29b)$$

and the close set of diffusion equations are obtained for $\varphi = 1$, v_z, E and E_{zi}.

The two-temperature displaced Maxwellian is expected to be an improvement on the simple displaced Maxwellian in representing the steady state where the anisotropy between the longitudinal and transverse directions is inadequately described by just a drift in momentum space [5]. We note that if electron-electron collisions are included then they will contribute towards the balance of E_z although we have not included this type of scattering in the calculation.

Finally we shall make use of the data obtained for the steady state by the Monte Carlo method [4, 5, 33], the essence of which is a ~~complete~~ simulation of the flight of an electron in momentum space. The value of the distribution function $f(\underline{k})$ at a point $\underline{k}$ is given by the total time spent by an electron in the neighbourhood of $\underline{k}$, expressed as a fraction of the time duration of a flight which includes a large number of scattering events, and averaged over many flights. The results of such a calculation are usually presented in two ways. The first is to take a value of the electric field and display the profiles of $f(\underline{k})$ in the directions perpendicular and parallel to the applied field; and by expanding $f(\underline{k})$ in terms of spherical harmonics, to obtain the energy dependence of the coefficients. The second is to obtain the fractional population p_i, the average velocities v_i and the average energies E_i for each of the two-valleys and tabulate these as a function of the electric field. It is the second form of the results that we shall incorporate into our calculations. In [4], results have been obtained assuming that the central valley is parabolic and also for the case when non-parabolicity is accounted for. We shall use the results for parabolic

bands to be consistent with our band model (§ 2.5) and also with the calculation of the diffusion constants by a direct Monte Carlo method by Fawcett and Rees [1]

An examination of the results of the Monte Carlo calculation shows that it is not a realistic objective to obtain a parameterised distribution containing a small number of parameters that will approximate the central valley distribution function, as derived by the Monte Carlo method for the electric field range of 1-20 kV/cm. This distribution function is highly anisotropic as a result of the presence of a threshold energy for intervalley scattering [34]. However, the theory of diffusion we have developed does assume as one of its basic postulates that it is unnecessary to have full knowledge of the distribution function. More specifically, we need to know only the dependence of the moment generation function $G_{ij}(\varphi)$ on the moments ψ_i for moment functions up to second order. From the values of p_1 v_{z1} and E_1 given by the Monte Carlo calculation as functions of the electric field, we shall estimate the values of $G_{11}(1)$, $G_{11}(v_z)$, $G_{11}(E)$ and $G_{21}(E)$ by assuming that they have the following functional dependence:

$$G_{11}(1) = \tau_1^{-1}(T_1), \tag{2.30a}$$

$$G_{11}(v_z) = -v_{z1}\tau_{p_1}^{-1}(T_1) \tag{2.30b}$$

$$G_{11}(E) = -W_1(T_1) \tag{2.30c}$$

$$G_{21}(E) = U_1(T_1) \tag{2.30d}$$

where T_1 = 2/3 x thermal energy/k_B and τ_1 etc are defined in (2.21). Further we shall assume that the distribution function in the satellite valley is a displaced Maxwellian. For a given field F, the moment generation functions in the satellite valley may then be evaluated immediately by putting the Monte Carlo value for the average velocity and temperature ($k_B T_2 = E_2 - m_2 v_{z2}^2/2$) into the displaced Maxwellian. The moment generation functions in the central valley at the temperature T_1, corresponding to an electric field F, is then given by the steady state equations (2.21a).

The relations (2.30) cannot be justified rigorously although one should expect the intervalley and momentum relaxation times, and the rates of energy loss through intravalley and intervalley processes to be strongly dependent on the thermal energy of the electrons. (The energy associated with the average drift, $m_i v_i^2/2$, is at most only about one tenth of the thermal energy). The assumption of a displaced Maxwellian for the distribution function in the satellite valley is a much better approximation. Strong intervalley scattering between the satellite valleys and the absence of a threshold energy for intervalley processes imply that the anisotropy found in the central valley distribution function is not expected to be present in the satellite valleys. (This is confirmed by the Monte Carlo calculation.) Moreover, the electron mobility calculated by assuming a displaced Maxwellian distribution function does not differ significantly from that calculated by the Monte Carlo method when the average velocity and temperature inserted into the displaced Maxwellian are equal to those calculated by the Monte Carlo method.

The calculation of the diffusion coefficients follows exactly that for displaced Maxwellians. By assuming the functional dependence of the moment generation functions (2.30) one has effectively reduced the behaviour of the distribution to that of one which is isotropic about a drifted centre, i.e. only the average velocity and an isotropic second moment (the average energy) are important in determining the values of $G_{ij}(\varphi)$.

In diagrams 2.1-4 we show respectively the average velocity, the fractional population in the satellite valleys, the drift velocity and temperatures of the central and satellite valleys as calculated by assuming displaced-Maxwellian distribution functions (2.20) (dashed curves), two-temperature displaced-Maxwellians (2.27) (broken curves), and by the Monte Carlo method of reference [4]. (full curves). (In diagram 2.4 where the temperatures are displayed, the longitudinal and transverse temperatures from the two-temperature displaced-Maxwellian calculation are labelled respectively by T_l and T_t; in the other two calculations such a distinction is of course unnecessary). As was pointed out in Table III, the values of the effective mass

in the satellite valley m_2, and the deformation potential field D_{12} used in the first two calculations are different from those used in the third. This choice of parameters allows the velocity-field characteristics to agree (diag.2.1) but the fractional population, velocity and temperature of the central valley are quite obviously different for the two types of calculations. This is a reflection of the fact that the distribution function in the central valley is poorly approximated by either of the Maxwellian distributions. The behaviour of the drift velocity in the central valley is in particular of crucial importance with reference to the diffusion calculations as will be seen later. In the Monte Carlo calculation, one observes that when the electrons are sufficiently heated, at fields exceeding $\sim$ 4kV/cm, the drift velocity remains fairly constant, while for the case of the Maxwellians, it continues to rise after a slight reduction in the rate of increase at about 4kV/cm. This disagreement is reduced only slightly when m_2 and D_{12} are taken to be of the same value as in the Monte Carlo calculation, but in this case the fractional population curve for the Maxwellians would be shifted below that for the Monte Carlo calculation (diagram 2.2), with the result that the agreement in the velocity characteristic is lost. The saturation of the central valley velocity is evidently a result of some abrupt change in the behaviour of the distribution function at the threshold energy for intervalley scattering. One should not expect a distribution function which takes no account of this threshold to reproduce the same effect.

The results for displaced-Maxwellian and two-temperature displaced Maxwellian distribution functions do not differ very significantly. Although in the latter case the longitudinal and transverse temperatures, T_l and T_t, and differ by as much as 20% in the central valley, the average $(T_t^2 T_l)^{1/3}$ is nearly always equal to the temperature in the displaced Maxwellian. In the satellite valleys, the results are so nearly equal that the curves for the two cases are indistinguishable.

Before closing this section we include a brief

comment on one further type of parameterised distribution for the central valley. The abrupt change in the shape of the central valley distribution function at the threshold energy for intervalley scattering suggests that it is perhaps a good approximation to use a parameterised distribution function containing two temperatures for the energy range above and below the threshold. An attempt has been made, unsuccessfully, to carry out such a calculation. In the calculation, the distribution function was assumed to be composed of two displaced-Maxwellian with independent temperatures for energies above and below the threshold. From the requirement that the distribution function is continuous at the threshold energy, only one of the average drifts in the displaced Maxwellians is independent; the other is a function of the first average drift and the temperatures in the two energy ranges. Thus in the central valley, the distribution function contains three adjustable parameters plus the fractional population therein. To obtain values for these, and the average drift and temperature in the satellite valley for a given electric field, two types of calculation were carried out. The first is to consider the balance of number, momentum and energy for each valley. Since there are only five equations, the equation for the balance of number being the same equation for the two valleys, it is necessary to remove one of the unknowns. For strong intervalley scattering it was thought justifiable to equate the temperature in the central valley above the threshold to the satellite valley temperature, or, since the satellite valley is known to be only slightly heated, to assume that it remains fixed at the lattice temperature. In neither case as it happens, could the balance equations be satisfied above a field strength of about 4kV/cm. This failure is a result of the contraints placed on the intervalley number and energy transfer rates by the approximations. In the first case the relative transfer between the two valleys is in effect fixed since the electrons in the central valley that can undergo intervalley scattering are always at the same temperature as those in the satellite valley; their average velocities being independent is of little consequence to the transfer

rates. In the second case, the balance of number and energy in the satellite valley proves to be unachievable when the temperature is fixed.

In the second type of calculation, an additional equation, that for the balance of k_z^2 in the central valley, was included and all the independent parameters were allowed to vary freely. The inclusion of this equation requires a large inequality between the moments $<v_x^2>$ and $<(v_z-v_{z1})^2>$, and the longitudinal and transverse temperatures of the two-temperature Maxweelian (2.27) do in fact differ by some 30% in order to satisfy this equation (see diagram 2.4). In the present case, it was found impossible to satisfy simultaneously all the balance equations because such a large temperature anisotropy cannot be achieved within the allowed form of the distribution function.

The approach adopted here to take account of the threshold is by no means unique. One might for instance seek the balance of electrons, momentum and energy in each of the two energy ranges above and below the threshold in the central valley. However, such a line of attack would greatly increase the complexity of the calculation and it was not thought worthwhile to take what is after all an approximate scheme to such elaborate ends.

§ 2.7 Results and Discussion

The diffusion constants commonly referred to in transport theory are the diffusion coefficients of the components of the average velocity parallel and normal to the applied electric field. In the theory of diffusion developed in this chapter these and other diffusion coefficients have been evaluated by neglecting space-charge effects and by an approximate solution of the Boltzmann Equation in the regime of small and slowly-varying density fluctuations. Accordingly, we shall present and discuss the results of the calculations with reference firstly to the physical region within which the theory is expected to apply, then to a Monte Carlo calculation by Fawcett and Rees [17] in which the diffusion constants are

calculated in the absence of space-charge effects by an exact solution of the Boltzmann Equation, and finally to experimental findings.

To estimate the upper limits of the density fluctuations for which the theory of diffusion is valid, we shall consider the requirements (from § 2.1):

$$\frac{\delta\varphi_1}{\varphi_1} = \frac{\underline{D}(\varphi_1)\cdot\underline{w}}{\varphi_1} \ll 1 \qquad (2.31a)$$

where $\underline{w} = -n^{-1}\underline{\nabla} n$ and

$$\frac{\delta F}{F} \ll 1 \qquad (2.31b)$$

The first condition imposes no restriction on the absolute magnitude of the density fluctuations but requires that they vary sufficiently slowly. The results of the calculations show that in all cases $D(\varphi_1)/\varphi_1 \lesssim 10^{-7}$ m so that (2.31a) is satisfied if $\underline{w} \ll 10^{-7}\ m^{-1}$ i.e., if $\underline{w} \sim 10^{-5}\ m^{-1}$ is sufficiently small, then the electron desnity can vary by as much as 100% over a distance of several microns without violating the condition (2.31a). For instance, a gaussian pulse several microns wide would satisfy this condition. The propagation properties of such a pulse is of special interest because both the Monte Carlo calculation and the experimental measurement of the diffusion constants are based on the spread of a pulse with time. The condition (2.31b) does impose an upper limit in the absolute value of the fluctuations. From Gauss's theorem, for a pulse of width l, the difference in the electric field going from one side of the pulse to the other in the direction of the field is given by:

$$\delta F = \frac{\bar{n}\, e}{\epsilon\epsilon_0}\, l \qquad (2.32)$$

where $\bar{n}$ is the average density of the pulse. If $l \sim 5\mu$m and $F \sim 5\times10^5$ V/m (the field range of interest in gallium arsenide being $1\text{-}20 \times 10^5$ V/m) then

$\bar{n}$ must be less than 10^{18} m^{-3} if $\delta F/F$ is to be of the order of a percent. When this condition of low space-charge accumulation is attained, then the sole effect of space-charge is to cause the pulse to spread in the direction of the field as a direct consequence of the field difference, hence velocity difference, going from one side of the pulse to the other. Under these circumstances we are justified as we have done to neglect space-charge effects at the first instance in the theory of diffusion, and to include a correction for the velocity difference on either side of the pulse in the direction of the field.

The Monte Carlo calculation by Fawcett and Rees [17] of the diffusion coefficients is based on a simulation of the spread of a pulse of electrons with time, neglecting space-charge effects and assuming that both the central and satellite valleys have isotropic, constant effective masses. The results thus obtained should therefore be in agreement with results obtained from the theory of diffusion, using steady state values obtained by the Monte Carlo method based on the same band model. [4] In the transverse direction, the Einstein's relation is valid for each valley (2.17) so that the diffusion coefficients can be evaluated directly from the steady state characteristics. In the longitudinal direction further manipulation of the steady state data was necessary in order to obtain the moment generation functions $G_{11}(\varphi)$ as functions of v_1 and T_1 (2.30). The drastic approximations made in this latter process imply that one should no longer expect quantitative agreement in the longitudinal direction but in the transverse direction fair agreement should be achieved.

In diagram 2.5a the transverse velocity diffusion coefficients obtained from the theory of diffusion using Monte Carlo data for the steady state (full curve), and by the direct Monte Carlo method (broken curve) are displayed as functions of the electric field. The agreement between the curves is good and the general shape of the curves can be interpreted as follows. The initial increase of the diffusion coefficient can be attributed to the increase in electron temperature in the central valley, and the decrease

at higher fields to the transfer of electrons to the satellite valleys where both the electron mobility and temperature are considerably lower than the central valley. The curves derived from the theory of diffusion starting from displaced Maxwellians (2.20) and two-temperature displaced Maxwellians (2.27) show that same qualitative behaviour (disgram 2.5b). The curve for the two-temperature displaced Maxwellian lies below that for the displaced Maxwellian at low field mainly because the transverse temperature T_t in (2.27) is lower than T in (2.20). At high fields, this is compensated by the inequality in the transfer from the central to satellite valleys. (see diagrams 2.2 and 2.4). Since the material parameters used in these latter calculations are not identical to those used in the Monte Carlo calculation, qualitative comparison between the curves is not really meaningful. It is worthy of note that the peak in all the diffusion curves occur at an electric field of about 3.5 kV/cm, close to the maximum in the velocity-field characteritic (diag. 2.1) and where the fractional populations in the two sets of valleys become comparable in magnitude.

The curves for the diffusion coefficients in the longitudinal direction are shown in diagrams (2.6a) and(2.6b). The agreement between the curves calculated from the theory of diffusion using Monte Carlo steady state data and by the direct Monte Carlo method is poor (diag.2.6a) in comparison with that achieved in the transverse direction. The largest disparity occurs in the field range 3 - 10 kV/cm and the diffusion constant calculated by the theory of diffusion has a negative value between 4 - 7 kV/cm! However, there are subtle similarities between the curves that merit comment, and the theory of diffusion seems able to provide a qualitative explanation for two important features in the direct Monte Carlo results: firstly, that D_l is a much lower value than D_t, and secondly, the peak in D_l occurs at a lower field.

To discuss in detail the behaviour of D_l we refer to equations (2.16) and (2.18) which can be written as

$$D_{\ell} = p_1 D_Z(v_{Z_1}) + p_2 D_Z(v_{Z_2}) + (v_1 - v_2) D_Z(p_1) \qquad (2.33)$$

$$\text{and } D_Z(p_1) = \tau_2 p_1^2 (v_1 - v_2) - \tau_2 p_1^2 \frac{\partial \tau_1^{-1}}{\partial T_1} D_Z(T_1)$$

$$+ \tau_2 p_1 p_2 \left[\frac{\partial \tau_2^{-1}}{\partial T_2} D_Z(T_2) + \frac{\partial \tau_2^{-1}}{\partial v_{Z2}} D_Z(v_{Z2}) \right] \qquad (2.34)$$

where we have used the relations (2.4), (2.21) and (2.30). Since the intervalley relaxation time τ_2 is nearly a constant, the last two terms in the right-hand side of (2.34) are small and the sign and magnitude of $D_Z(p_1)$ depends on the first two terms only. The first of these has been identified in § 2.5 and gives rise to an equivalent diffusion constant

which is always positive. The second term on the other hand is always negative since the intervalley scattering rate increases always with the central valley temperature as does the latter in the presence of the diffusion driving force _. As it turns out, $D_Z(p_1)$ is always negative in the field range considered and has the largest absolute value in the range 4 - 7 kV/cm. (At low fields $D_Z(p_1)$ is small because both p_2 and $\partial \tau_1^{-1}/\partial T_1$ are small, and at high fields, p_1 is small and the two contributions of opposite signs are nearly equal.) This behaviour of $D_Z(p_1)$ is partly responsible for the low (and negative) values of D_1 in the intermediate fields.

For a single valley, the Einstein relation (2.15) is valid and $D_Z(v_{Z_1})$ is proportional to the differential mobility dv_{Z1}/dF. In the many valley situation, this relationship is no longer strictly valid but the variations of the two quantities are still correlated to some extent especially at low field where intervalley scattering is relatively unimportant. From this effect we again expect the longitudinal diffusion constant to be smaller than the transverse diffusion constant. Moreover, the respective occurence of a maximum and a sudden change in slope on the two curves at about 3kV/cm may be attributed to the onset of velocity saturation in the central valley, causing $D_Z(v_{Z_1})$ to decrease rapidly. (see also diag. 2.3).

$D_z(v_{z1})$ does not in fact become negative at any particular field but it may take small enough values for the term containing $D_z(p_1)$ to dominate the behaviour of D_1. The departure of $D_z(v_{z1})$ from the Einstein relation (2.13) when intervalley scattering becomes important is reflected through a gradual increase of this quantity after the initial decrease in the onset of velocity saturation. At high fields when transport processes in the central valley become less important, the curves are in good agreement. Thus qualitatively the two curves exhibit some common characteristics. The quantitative disagreements may be attributed to the various approximations made in the reduction of the functional dependence of the moment generation functions to the form (2.30). Since the various terms in (2.33) and (2.34) are often of the opposite sign and of nearly equal magnitude, the value of D_1 is very sensitive to any over- or underestimation of their values.

The curves calculated from the theory of diffusion using the two types of displaced Maxwellians (diag. 2.6b) show again the initial decrease of D_1 from the change in slope of the central valley velocity. However another peak follows closely at slightly higher fields and brings D_1 to values exceeding D_t. The second peak and subsequent behaviour of D_1 is a result of $D_z(p_1)$ being positive and large. In these latter calculations the strength of intervalley scattering is decreased by approximately a factor of four since the deformation potential field D_{12} is decreased from 10^9 eV/cm to 5.3×10^8 eV/cm. Consequently both the intervalley relaxation times τ_1 and τ_2 are increased fourfold. In (2.34) then, the first term on the right-hand side dominates the behaviour of $D_z(p_1)$ since the other terms are unchanged by the increase in the intervalley relaxation times.

Comparison of the theory with experiment is hindered by the scarcity of experimental data. Only the longitudinal diffusion constant has been measured in gallium arsenide (Ruch and Kino [31]). The results were obtained by a time-of-flight method designed principally to measure the velocity of a pulse of electrons through semi-insulating material. Electron-hole pairs are created near the cathode of a sample of GaAs by a

short burst from an electron-gun. If the holes are swept out of the sample in a short time because of their close proximity to the cathode, the current induced in the external circuit may be entirely attributed to the flow of electrons through the sample. The duration of the current gives a direct measure of the transit-time of the electrons, and the rise and fall times of the current give a measure of the width of the electron pulse at the time of its creation and as the electrons make their exit through the anode the spread of the pulse, providing then an estimate of the diffusion constant. Although the experimental conditions seem to conform with those set out at the beginning of this section regarding space-charge effects, the values obtained for D_1 are approximately three times as high as thoseobtained by the Monte Carlo calculation showing a peak of $\sim 900 cm^2/sec$ at $\sim 3.5 kV/cm$.

Ohmi and Hasuo [21] have managed to obtain some limited agreement with experiment by adding to the transverse Einstein relation (2.17) the intervalley contribution (2.19). This procedure is clearly unjustifiable on the basis of the theory of diffusion developed in this chapter. Fawcett and Rees [17] proposed that impurity scattering would tend to reduce the anisotropy between the longitudinal and transverse directions, whereby the longitudinal diffusion constant would be decreased. However, even if this were the case, the longitudinal diffusion constant would at most be equal to the transverse constant, which is still too small.

There is, however, a possible source of error in the experiment that has not been given full consideration. In estimating the rise-time t_R of the electron current, the presence of the hole current has been neglected. We show schematically in diagram 2.8 how this can give rise to a considerable underestimation of t_R even though the hole current is typically only a twentieth the value of the electron current. In diagram 2.7 the curves (a) and (b) represent respectively the variation of the electron and hole currents with time. Between the times t_0 and t_1, electron-hole pairs are being created near the cathode. At the completion of this process

the electron current reaches its maximum value so the true rise-time corresponding to the width of the electron pulse is given by $(t_1 - t_0)$. In the meantime, as they are being created, the holes are swept out of the sample under the influence of the electric field. The maximum hole current occurs therefore at a time $< t_1$. Since the low field mobility of holes in gallium arsenide is approximately 400 cm^2/Vsec [34] while that for electrons is 9000 cm^2/Vsec [31] the maximum hole current is roughly 5% that of the maximum electron current. The curve (c) giving the total current is obtained simply by the addition of (a) and (b). Thus if the rise time of (c) $(t_1' - t_0)$ is taken to be the rise time t_R of the electron current, then it is seen from the diagram that t_R will be underestimated consistently by anything up to 25% depending on the exact location of the maximum in the hole current. The diffusion constant was evaluated in reference [31] using the expression

$$D_1 = \frac{v^3 (t_F^2 - t_R^2)}{21.9\, l}$$

where t_R and t_F are the rise- and fall-times of the electron current, v the electron velocity and l the sample length. If $t_R = 0.3$ n sec (a reasonable estimate from [31]) and $\Delta t_R = + 0.06$ n sec, thus the diffusion constant at 3.5 kV/cm is reduced from 900 cm^2/sec to about 260 cm^2/sec, which is close to the value predicted by theory (diag. 2.6a).

We conclude that the behaviour of the diffusion constants in gallium arsenide is probably fairly accurately predicted by the Monte Carlo calculation of Fawcett and Rees [17]. The theory of diffusion we have developed is able to obtain quantitative agreement with the Monte Carlo results only in the direction transverse to the electric field. In the longitudinal direction, certain features of the curve can be explained in terms of contributions to diffusion from intervalley scattering and intravally thermal processes. The inability to achieve quantitative agreement is a result of the poor representation of the steady state distribution function in the central valley of gallium arsenide through parameterised distributions.

TABLE I Comparison of $\langle \nabla_k \phi \rangle_i$ and $\hbar \Gamma_i^{th}(\phi)$

ϕ	$\langle \frac{\partial \phi}{\partial k_x} \rangle_i$	$\hbar \Gamma_{ix}^{th}(\phi)$	$\langle \frac{\partial \phi}{\partial k_y} \rangle_i$	$\hbar \Gamma_{iy}^{th}(\phi)$	$\langle \frac{\partial \phi}{\partial k_z} \rangle_i$	$\hbar \Gamma_{iz}^{th}(\phi)$
1	0	0	0	0	0	0
k_x	1	$k_B T_{xi}$	0	0	0	0
k_y	0	0	1	$k_B T_{yi}$	0	0
k_z	0	0	0	0	1	$k_B T_{zi}$
k_x^2	$2k_{xi}$	$2k_{xi} k_B T_{xi} + C_{xxx}^{(i)}$	0	$C_{yxx}^{(i)}$	0	$C_{zxx}^{(i)}$
k_y^2	0	$C_{xyy}^{(i)}$	$2k_{yi}$	$2k_{yi} k_B T_{yi} + C_{yyy}^{(i)}$	0	$C_{zyy}^{(i)}$
k_z^2	0	$C_{xzz}^{(i)}$	0	$C_{yzz}^{(i)}$	$2k_{zi}$	$2k_{zi} k_B T_{zi} + C_{zzz}^{(i)}$
$k_y k_z$	0	0	k_{zi}	$k_{zi} k_B T_{yi} + C_{yzz}^{(i)}$	k_{yi}	$k_{yi} k_B T_{zi} + C_{yzz}^{(i)}$
$k_z k_x$	k_{zi}	$k_{zi} k_B T_{xi} + C_{zxx}^{(i)}$	0	0	k_{xi}	$k_{xi} k_B T_{zi} + C_{xzz}^{(i)}$
$k_x k_y$	k_{yi}	$k_{yi} k_B T_{xi} + C_{yxx}^{(i)}$	k_{xi}	$k_{xi} k_B T_{yi} + C_{xyy}^{(i)}$	0	0

Notation: $T_{\alpha i} = \frac{m_{xi}}{k_B} \langle (v_\alpha - v_{\alpha i})^2 \rangle_i$, $C_{\alpha\beta\beta}^{(i)} = \langle (v_\alpha - v_{\alpha i})(v_\beta - v_{\beta i})^2 \rangle_i$, $C_{\alpha\alpha\alpha}^{(i)} = \langle (v_\alpha - v_{\alpha i})^3 \rangle_i$

TABLE II. TRANSITION PROBABILITY FOR ELECTRON-PHONON INTERACTIONS.

	PHONON TYPE	ELECTRON TRANSITION PROBABILITY	PHONON DISPERSION RELATIONS
$A_{ii}(\underline{k},\underline{k}')$ (INTRAVALLEY)	POLAR OPTICAL	$\frac{e^2\omega_0}{8\pi^2\epsilon_0}\left(\frac{1}{\epsilon_\infty}-\frac{1}{\epsilon_s}\right)\frac{1}{\lvert\underline{k}-\underline{k}'\rvert^2}F_0^i(\underline{k},\underline{k}')$	$\omega_0(\underline{K}) =$ CONSTANT
	LONG WAVELENGTH ACOUSTIC	$\frac{\Xi_a^2}{8\pi^2\rho s}\lvert\underline{k}-\underline{k}'\rvert F_a^i(\underline{k},\underline{k}')$	$\omega_a(\underline{K}) = KS$
$B_{ij}(\underline{k},\underline{k}')$ (INTERVALLEY)	NON-POLAR OPTICAL	$\frac{D_{ij}^2}{8\pi^2\rho\omega_{ij}}F_{ij}^i(\underline{k},\underline{k}')$	$\omega_{ij}(\underline{K}) =$ CONSTANT

WHERE $F_g^i(\underline{k},\underline{k}')=\left[N_g(\underline{k}-\underline{k}')+1\right]\delta\left[E_i(\underline{k})-E_i(\underline{k}')-\hbar\omega_g(\underline{k}-\underline{k}')\right]+N_g(\underline{k}-\underline{k}')\,\delta\left[E_i(\underline{k}')-E_i(\underline{k})-\hbar\omega_g(\underline{k}-\underline{k}')\right]$,

$N(\underline{K})$ = occupation number of phonon of type g and wave-vector $\underline{K}$

$= \left\{\exp\left[\hbar\omega_g(K)/k_BT_0\right]-1\right\}^{-1}$ for phonons in thermal equilibrium at the lattice temperature T_0,

g = o, a, ij to denote respectively polar optical, long wavelength acoustic and intervalley non-polar optical phonons,

AND $E_i(\underline{k})$ = energy of electron in valley i with wave-vector $\underline{k}$ measured from the centre of valley i.

THE REMAINDER OF THE SYMBOLS ARE DEFINED IN THE TEXT.

TABLE III

VALUES OF MATERIAL PARAMETERS FOR GaAs.

m_1	$0.067\ m_0$	[25]
m_2	$0.35, 0.40\ m_0$	*
Δ	0.36 eV	[26]
ϵ_∞	12.53	[26]
ϵ_s	10.82	[26]
ω_0	5.37×10^{13} rad. s^{-1}	[27]
Ξ_0	7.0 eV	[28,29]
s	5.22×10^5 cm. s^{-1}	[29]
ρ	5.37 g. cm^{-3}	
D_{12}	$0.537, 1.0 \times 10^9$ eV cm^{-1}	*
ω_{12}	4.54×10^{13} rad. s^{-1}	[30]
D_{22}	1.0×10^9 eV cm^{-1}	
ω_{22}	4.54×10^{13} rad. s^{-1}	

* THE TWO SETS OF VALUES QUOTED ARE USED RESPECTIVELY IN DISPLACED-MAXWELLIAN [8] AND MONTE CARLO [4] CALCULATIONS TO OBTAIN THE BEST FIT WITH THE EXPERIMENTAL VELOCITY-FIELD CHARACTERISTIC.

CAPTION TO DIAGRAMS

2.1 The steady state velocity/field characteristic for electrons in gallium arsenide calculated by the Monte Carlo Method (full line) and by the Moment Balance Method using displaced Maxwellians (dashed line) and two temperature displaced Maxwellians (broken line).

2.2 The steady state fractional population in the satellite valleys (n_2/n) calculated as above.

2.3 The average steady state electron velocities in the central and satellite valleys displayed as functions of field. In the satellite valley, the velocities calculated by the two types of displaced Maxwellians are indistinguishable in the scale shown. Note velocity saturation in central valley in the Monte Carlo curve.

2.4 The steady state electron temperatures in the central and satellite valleys displayed as functions of field. T_l and T_t denote respectively the temperature associated with the direction longitudinal and transverse to the electric field. The Monte Carlo temperature is given by 2/3 x average thermal energy/k_B.

2.5 The transverse diffusion coefficient for electrons in GaAs calculated from the theory of diffusion using steady state data dereved by the Monte Carlo Method (full line) and by an independent Monte Carlo calculation (broken curve).

2.5b The transverse diffusion coefficient calculated from the theory of diffusion assuming displaced Maxwellians (dashed line) and two temperature displaced Maxwellians (full line).

2.6a The longitudinal diffusion coefficient calculated as diag. 2.5a.

2.6b The longitudinal coefficients calculated as diag. 2.5b.

2.7 Schematic diagram indicating that the real rise time ($t_1 - t_o$) of the electron current is much longer than the apparent rise time $t'_1 - t_o$ (of the total current) when the hole current is not negligible. (The current rise corresponds to that observed in an insulating sample of semiconductor when electron-hole pairs are created near the p^+ contact by an electron gun or by a laser.)

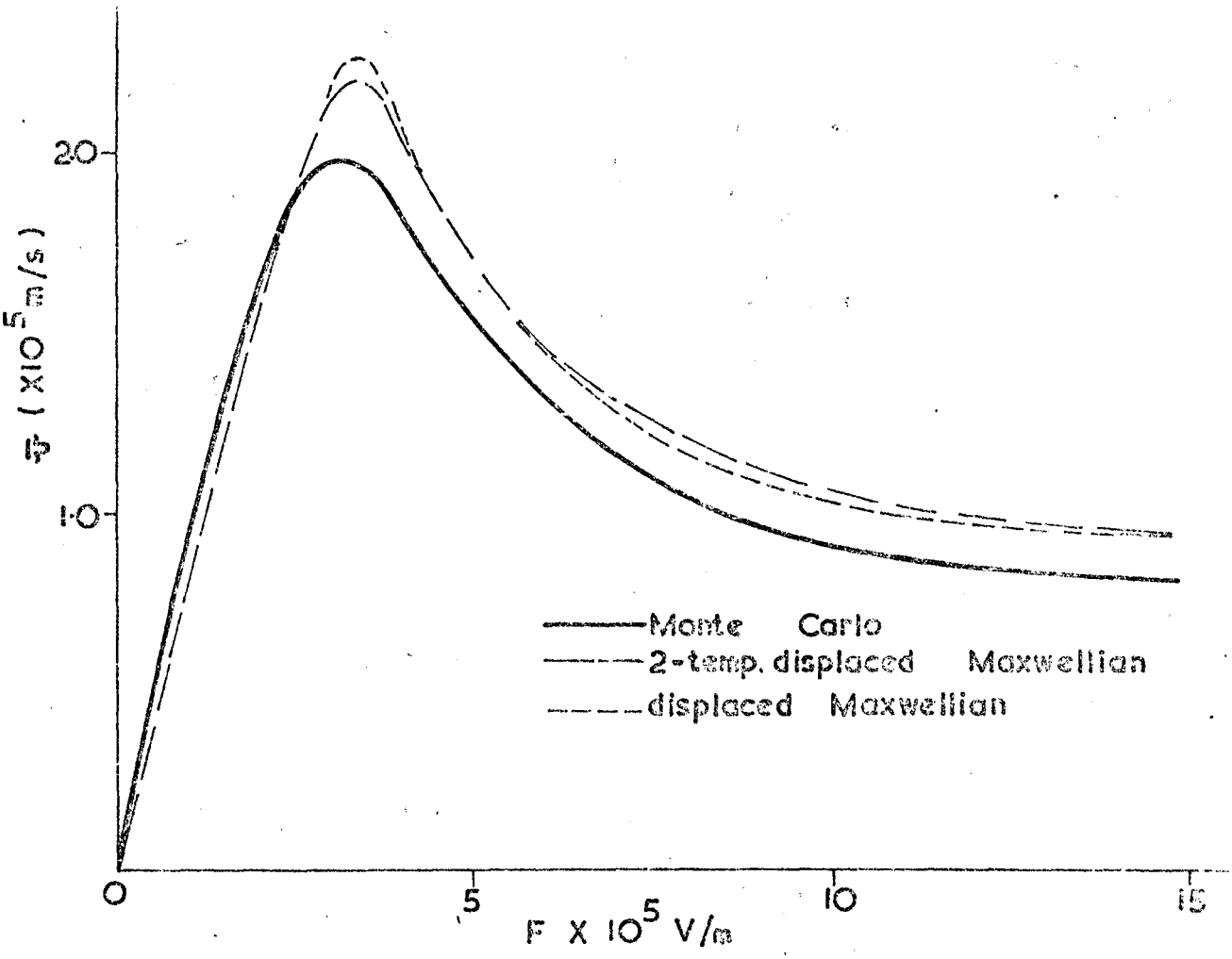
20
1·0
v (x10^5 m/s)
0
5
10
15
F x 10^5 V/m
Monte Carlo
2-temp. displaced Maxwellian
displaced Maxwellian

Diag. 2.1.

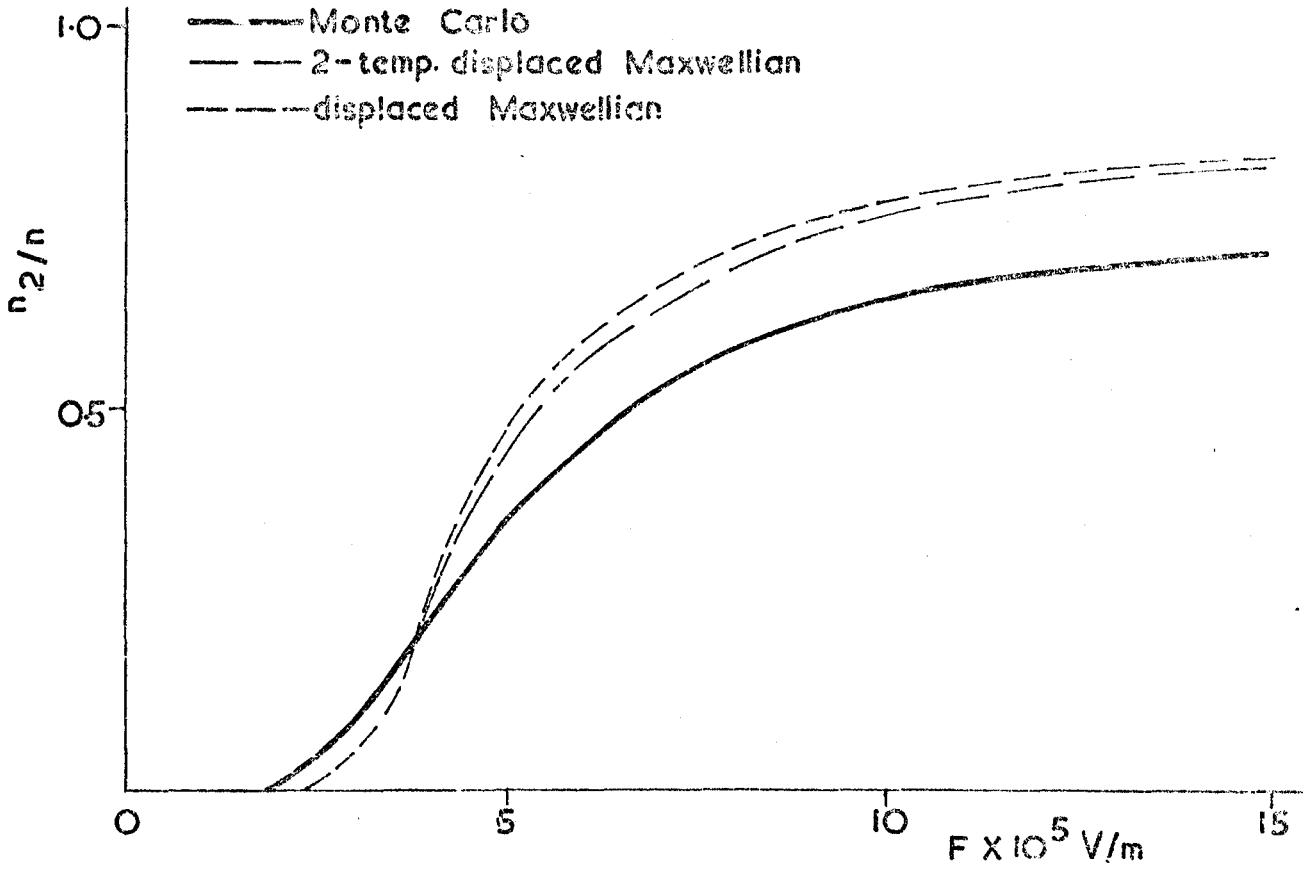
Monte Carlo
2-temp. displaced Maxwellian
displaced Maxwellian
1·0
0·5
n_2/n
0
5
10
15
F X 10^5 V/m

Diag.2.2.

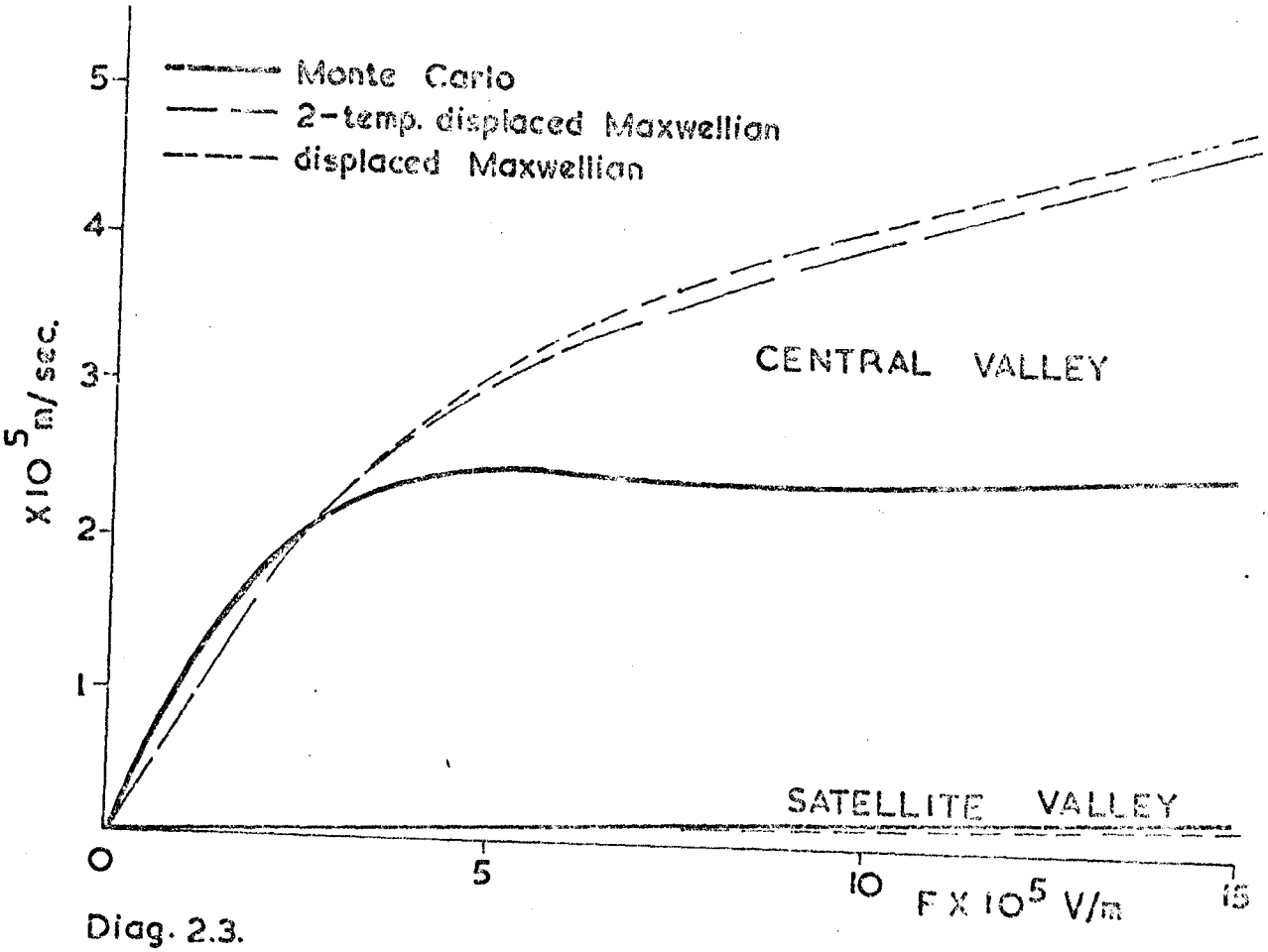
Monte Carlo
2-temp. displaced Maxwellian
displaced Maxwellian
CENTRAL VALLEY
SATELLITE VALLEY
X10^5 m/sec.
F X 10^5 V/m
0
5
10
15
1
2
3
4
5

Diag. 2.3.

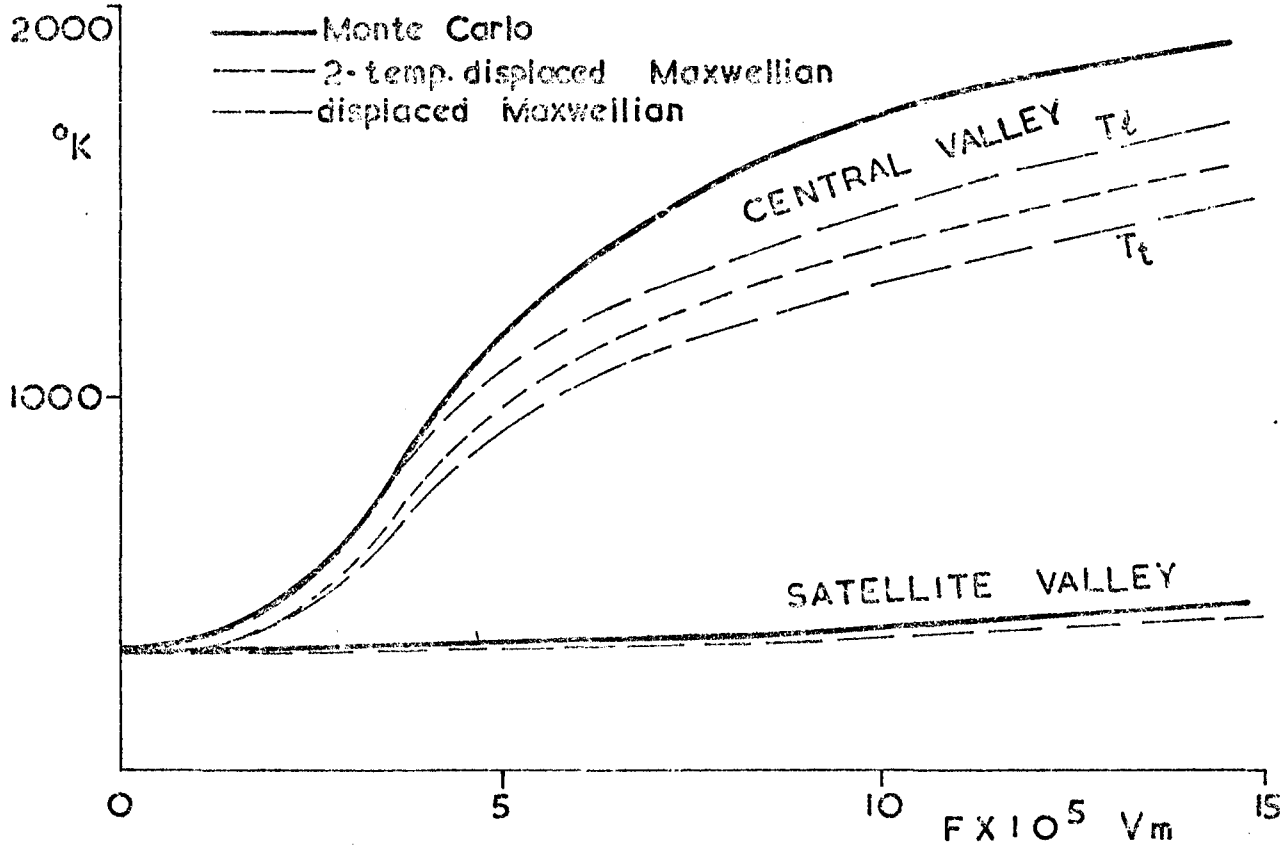
2000
°K
1000
Monte Carlo
2- temp. displaced Maxwellian
displaced Maxwellian
CENTRAL VALLEY
T_ℓ
T_t
SATELLITE VALLEY
0
5
10
15
F X 10^5 Vm

Diag. 2.4.

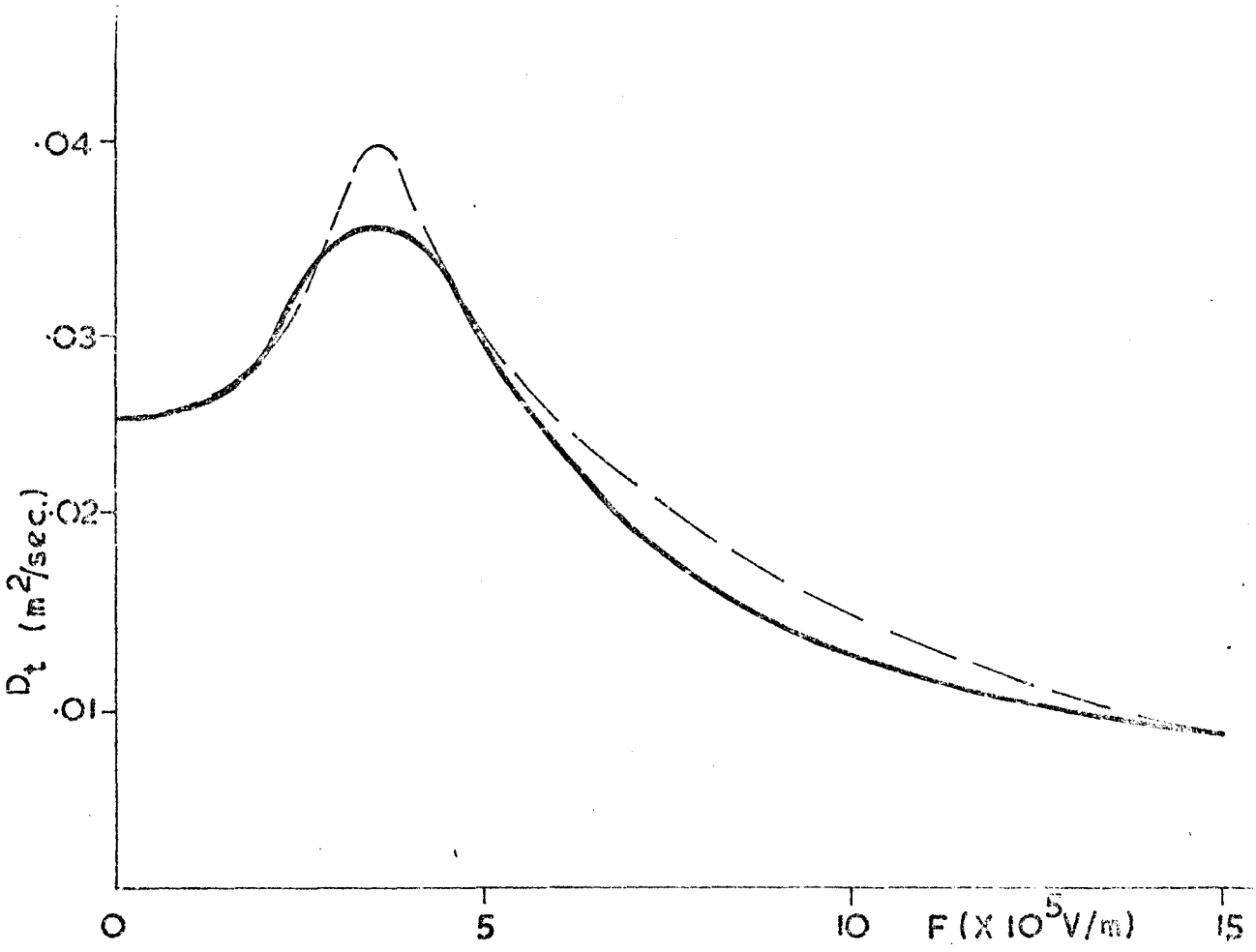

Diag. 2.5 a

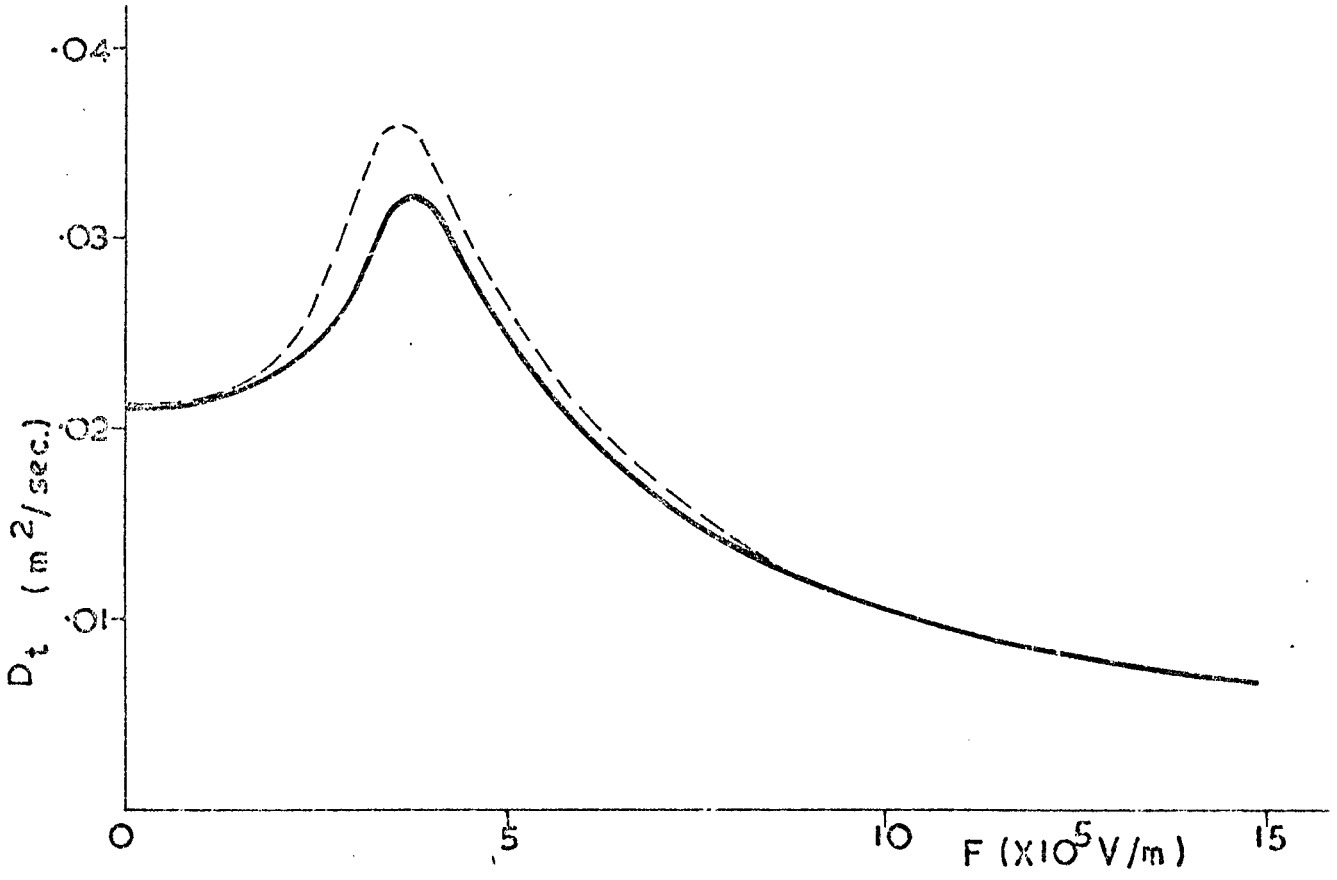

Diag. 2.5b

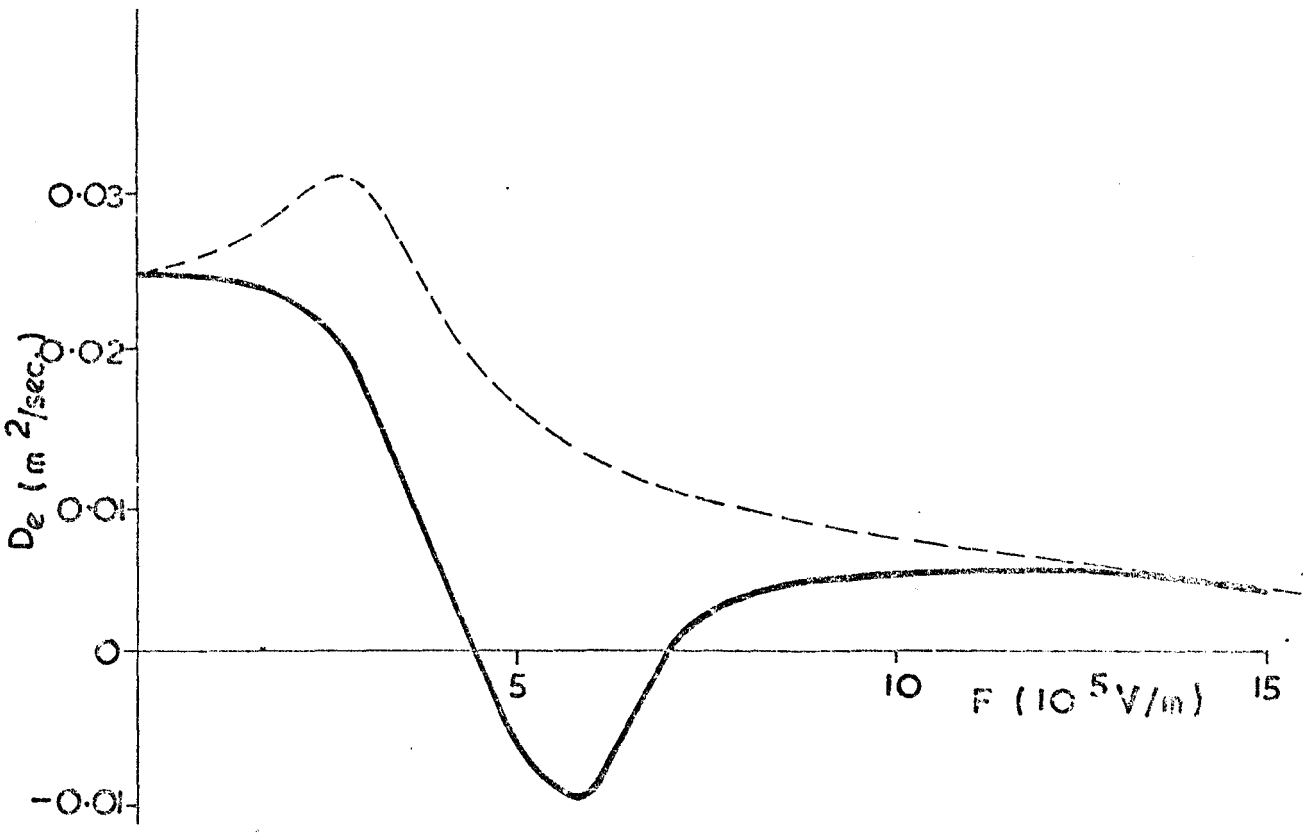

Diag. 2.6a.

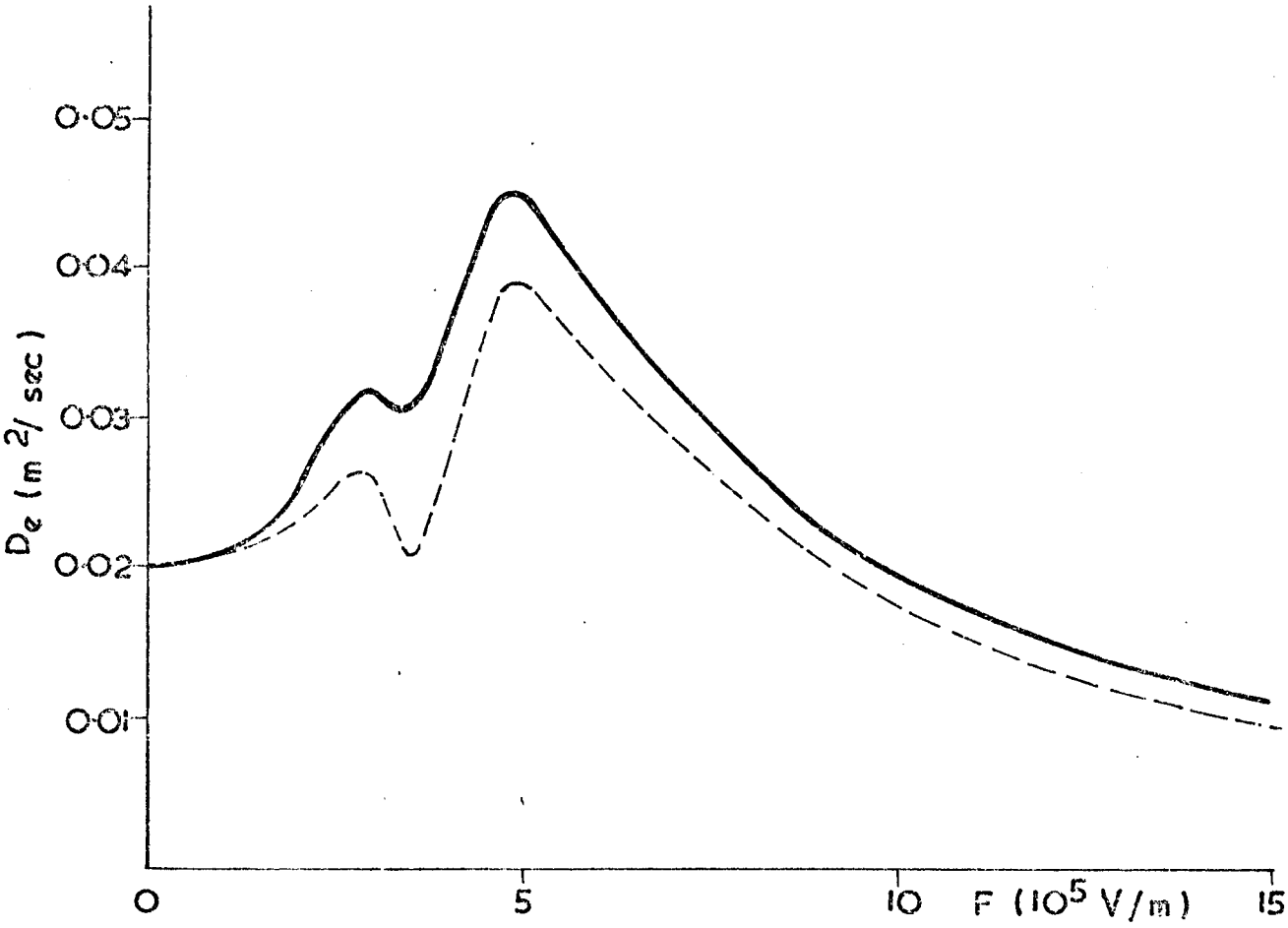

Diag. 2.6b.

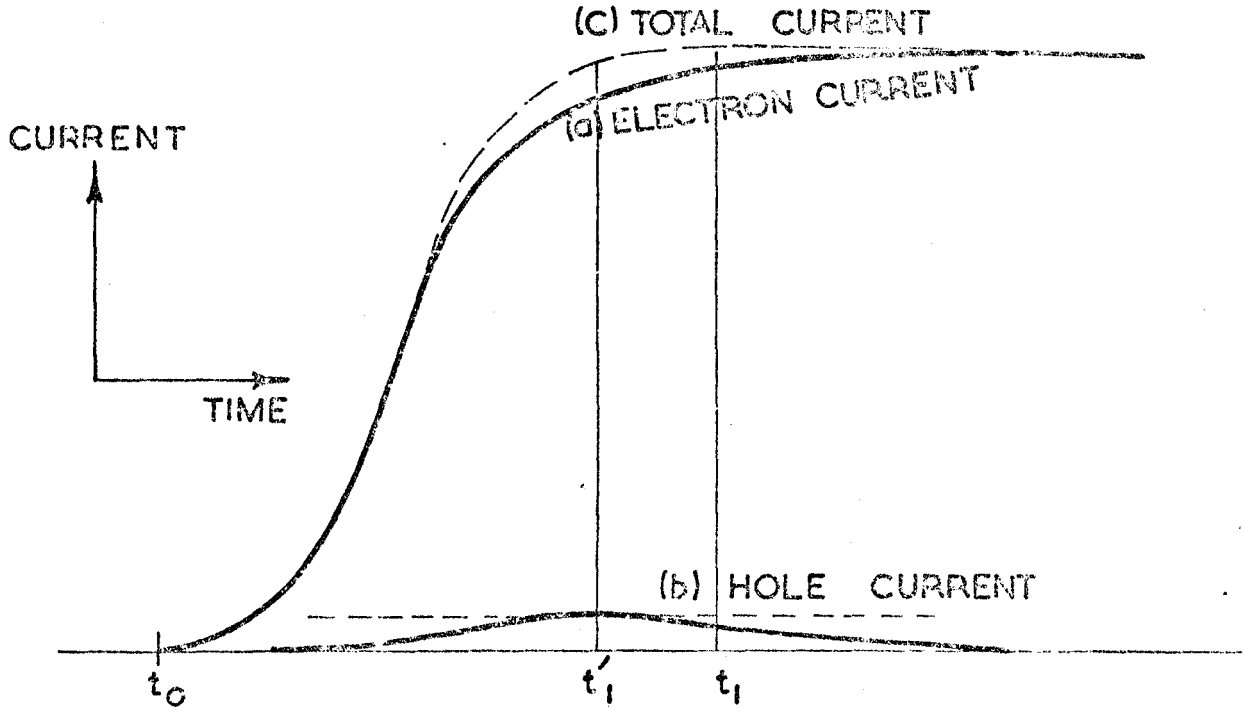
(c) TOTAL CURRENT
(a) ELECTRON CURRENT
CURRENT
TIME
(b) HOLE CURRENT
t_0
t'_1
t_1

Diag. 2.7

Chapter 3. Electronic Diffusion in Silicon

§ 3.1. Introduction

In this chapter we apply the theory of diffusion to electrons in silicon when an external electric field is applied along the <111> - crystallographic axis. This particular orientation of the electric field has been chosen for two reasons. Firstly, all existing experimental data are taken for this orientation, and secondly, the high degree of symmetry allows the calculation to be considerably simplified.

As before, we assume that the steady state distribution function is of a parameterised form which we require to satisfy the appropriate balance equations. Two types of distribution functions, the displaced Maxwellian and the two-temperature displaced Maxwellian have been used. Calculations of the velocity characteristic using displaced Maxwellians have previously been carried out by several authors [11, 55] but the anisotropy of long wavelength acoustic phonon scattering has usually been neglected. In the present work, this feature of the electron-phonon interaction has been incorporated fully into the calculation. Furthermore, in the calculation using the two-temperature displaced Maxwellian, it is possible to include electron-electron scattering explicitly into the balance equations. We took the opportunity to investigate the limit of high electron density when the two-temperature displaced Maxwellian is reduced to a simple displaced Maxwellian by electron-electron scattering.

To exploit fully the symmetry of the electron system, we introduce in § 3.2 the 'equivalent' coordinates. It can be shown later, in § 3.4, that the use of these coordinates enables the many-valley steady state and diffusion equations to be reduced to a form

involving the moments and diffusion coefficients of a single valley only, so that the solution of these equations is greatly simplified. In § 3.2, the symmetry and transformation properties of the velocity diffusion tensor and the other diffusion coefficients are also discussed. We determine from these considerations the number of independent components that are contained in the diffusion coefficients and the relation of these quantities to the experimentally observed diffusion constants.

In §§ 3.3, 3.4 and 3.5 we describe respectively the electron-phonon interactions in silicon (together with a discussion on the choice of material parameters), and the calculations using the two types of distribution functions. In § 3.6 the results of the diffusion calculation are discussed in relation to experiments and Monte Carlo calculations.

§ 3.2. The 'Equivalent' coordinates and symmetry considerations

The conduction band of silicon consists of six minima centred at equivalent points along the <100> - axes (see diagram 3.1). In the neighbourhood of these minima, the constant energy surfaces are prolate ellipsoids of revolution about the respective <100> - axis such that the effective mass tensor for each minimum is diagonal and characterised by the principal effective masses $m_o m_T$ and $m_o m_L$, where m_T and m_L are respectively the effective mass ratios in the directions normal and parallel to the symmetry axis, and m_o is the free electron mass. (Initially we shall assume that m_T and m_L are constants. In § 3.4 we generalise the analysis to the case when m_T is energy dependent[11].) Thus the pairs of valleys sharing the same symmetry axis are strictly equivalent for any orientation of the electric field; for the remainder of this chapter we shall refer to these equivalent pairs as a single valley labelled by an integer i (= 1, 2 and 3.). The non-parallel valleys are on the other hand non-equivalent despite the symmetrical orientation of the electric field for two reasons: the average drift

velocities in the valleys are non-parallel in general, and the response of the electrons in each valley to an arbitrary density gradient is non-identical.

When the electric field is in the <111>-direction, it is possible however, to choose for each valley i, a system of 'equivalent' coordinates, denoted by the bracketed index (i), such that the distribution function $f_i^{(i)}(\underline{k})$ of valley i, as referred to in the equivalent coordinates (i), is identical for all i. The choice of these sets of equivalent coordinates is not unique. In diagram 3.1 we show one particular set which are related to a common coordinate system, the crystal coordinates (c), by the rotational matrices

$$\tilde{T}_{(1)} = \begin{pmatrix} 0 & 0 & 1 \\ 1 & 0 & 0 \\ 0 & 1 & 0 \end{pmatrix}, \quad \tilde{T}_{(2)} = \begin{pmatrix} 0 & 1 & 0 \\ 0 & 0 & 1 \\ 1 & 0 & 0 \end{pmatrix} \text{ and } \tilde{T}_{(3)} = \begin{pmatrix} 1 & 0 & 0 \\ 0 & 1 & 0 \\ 0 & 0 & 1 \end{pmatrix} \tag{3.1}$$

such that the transformation

$$\underline{X}^{(c)} = \tilde{T}_{(i)} \underline{X}^{(i)} \tag{3.1a}$$

applies for a vector quantity $\underline{X}$ for the change of coordinates from (c) to (i). It is evident that the distribution function $f_i^{(i)}(\underline{k})$ is the same for all i because in the equivalent coordinates (i), the field and the symmetry axis of valley i are in the same directions (in this case, the $<111>$ and $<001>$ directions) for all i. Other sets of equivalent coordinates may be generated by applying further rotations identically to each of the set represented by (3.1). Unless otherwise specified, we shall however take equivalent coordinates to mean the set represented by (3.1) because these coincide with the principal axes of the ellipsoidal valleys.

When the distribution function in equivalent coordinates is identical for all the valleys, the same must be true for all moments of the distribution, as well as the diffusion coefficients which depend on the steady state distribution function only. From the transformation properties of the coordinates given by equation (3.1) it is therefore possible to express

all moments and diffusion coefficients in valley j by the moments and diffusion coefficients of valley i. In § 3.4 we shall use this information to simplify the steady state and diffusion equations. For the remainder of this section we shall discuss the symmetry properties of the moments of the distribution function and their respective diffusion coefficients.

(i) The fractional population

The fractional population p_i in valley i in the steady state must be the same for all the valleys since this is obtained by integrating $f_1^{(1)}(\underline{k})$, i.e.

$$p_i = \frac{1}{3} . \qquad (3.2)$$

Since $\sum_i \delta p_i = 0$, and $\underline{D}^{(1)}(p_i)$ is identical for all i, we have for an arbitrary diffusion driving force $\underline{w}$:

$$\sum_i \delta p_i = \underline{w}.\left[\sum_i \tilde{T}_{(1)}{}^{x}\, \underline{D}^{(1)}(p_i)\right]$$

$$= \underline{w}.\left[\begin{pmatrix} 1 & 1 & 1 \\ 1 & 1 & 1 \\ 1 & 1 & 1 \end{pmatrix} x\, \underline{D}^{(1)}(p_i)\right]$$

$$= 0$$

which implies that $\sum_\alpha D_{\alpha\alpha}^{(1)}(p_i) = 0$. Since the x- and y-components of $\underline{D}^{(1)}(p_i)$ must be equal from the symmetry of the x- and y-axes, we may therefore write:

$$\underline{D}^{(1)}(p_i) = D_p\,(-1,\ -1,\ 2) \qquad (3.3)$$

so that $\underline{D}^{(1)}(p_i)$ has only one independent component D_p.

(ii) The average velocity and diffusion tensor

In equivalent coordinates, the average velocity i may be written in the most general form as:

$$\underline{v}_i^{(1)} = (v_T,\ v_T,\ v_L) \qquad (3.4)$$

where the components v_T and v_L in the light and heavy mass directions respectively (i.e. the transverse and longitudinal directions w.r.t. the symmetry axis of the ellipsoidal constant energy surfaces) are to be treated as independent moments of the distribution function when the scattering of electrons is anisotropic. Note that for isotropic scattering the average momentum of the electrons is parallel to $\underline{F}$ (see § 3.5) so that v_T and v_L are in the ratio m_L/m_T and are not independent of each other.

In general therefore, the velocities of the different valleys are non-parallel. Using (3.1) it can be shown that they have components of equal magnitude in the $<111>$-direction and components normal to the $<111>$-direction that are also equal in magnitude but are orientated along the $\{11\bar{2}\}$-directions respectively. Since the fractional populations of the valleys are equal, the average velocity of the entire electron system $\underline{\bar{v}}$ is parallel to the electric field $\underline{F}$, which must be the case when $\underline{F}$ is applied in the $<111>$-direction for a cubic system. The total average velocity $\underline{\bar{v}}$ and the components $\underline{v}_\perp$ in each valley normal to the field are given respectively by:

$$\underline{\bar{v}} = (v_L + 2v_T)\,(1,\ 1,\ 1)/3 \qquad (3.5a)$$

and

$$\underline{v}_\perp = 3^{-\frac{1}{2}}(v_T - v_L)\,\{1\ 1\ \bar{2}\} \qquad (3.5b).$$

Although the component $\underline{v}_\perp$ is unobservable experimentally from measurements of the average velocity, it is an important quantity in relation to intervalley diffusion effects since the difference in average velocity between any two valleys is $2^{\frac{1}{2}}\underline{v}_\perp$.

The diffusion tensore for the average velocity $\underline{v}_1$ can be written in the most general way as

$$\tilde{D}^{(1)}(\underline{v}_1) = \begin{pmatrix} D_T & D_3 & D_1 \\ D_3 & D_T & D_1 \\ D_2 & D_2 & D_L \end{pmatrix} \qquad (3.6)$$

where we have made use of the symmetry between the x- and y-axes to reduce the number of independent components to five. The off-diagonal elements of the are non-zero because in the presence of the electric field, the positive and negative directions along each of the coordinate axes are asymmetrical. For

instance, the velocity induced in the z-direction by a density gradient in the x-direction is given by

$$\delta v_z = D_2 \, w_x .$$

If the positive and negative directions along the x-axis were symmetrical, then changing the sign of w_x should leave δv_z unaltered which is possible only if D_2 is zero. Similarly if the z-axis were symmetrical in the same sense then D_2 must again be zero because for a given w_x there is no preferred direction for δv_z. It does not follow however, that the diffusion tensor $\underline{D}(\bar{\underline{v}})$ for the total average velocity $\bar{\underline{v}}$ is non-diagonal. By definition

$$\delta \bar{\underline{v}} = \sum_i \left\{ p_i \left[\tilde{T}_{(i)} \tilde{D}^{(i)}(\underline{v}_i) \tilde{T}^{-1} \right] x \underline{w} + \underline{v}_i \left[\underline{D}^{(i)}(p_i) . \underline{w} \right] \right\}$$

$$= \tilde{D}(\bar{\underline{v}}) \times \underline{w}$$

If we choose a coordinate system in which the z-axis is parallel to $\underline{F}$, then using (3.1) - (3.6), it can be shown that

$$\tilde{D}(\bar{\underline{v}}) = \begin{pmatrix} D_\perp & 0 & 0 \\ 0 & D_\perp & 0 \\ 0 & 0 & D_{\parallel} \end{pmatrix} \qquad (3.7a)$$

where $D_\perp = (D_L + 2D_T)/3 - (D_1 + D_2 + D_3)/3 + 3D_p(v_L - v_T)$ (3.7b)

and $D_{\parallel} = (D_L + 2D_T)/3 + 2(D_1 + D_2 + D_3)/3$ (3.7c)

i.e. the diffusion tensor for the entire electron system is diagonal and $D_\perp$ and $D_{\parallel}$ are the diffusion constants in the directions normal and parallel to the electric field. (To avoid confusion the symbols $\perp$ and $\parallel$ will be used to denote the directions normal and parallel to the electric field while T and L will continue to signify the respective orientations w.r.t. the symmetry axis of the constant energy surfaces.) This result is again to be expected from the cubic symmetry of the crystal and the orientation of $\underline{F}$. Through equations (3.7b) and (3.7c), the experimentally observed diffusion constants $D_\perp$ and $D_{\parallel}$ are related to the components of the diffusion coefficients of the moments of the distribution function $f_i(\underline{k})$, which are the

quantities to be computed directly from the diffusion equations.

The results (3.2 - 3.7) are derived from the transformation properties of the equivalent coordinates and the symmetry between the x- and y-axes in these coordinates. They are therefore independent of the approximations we make with respect to the shape of the distribution function. The results concerning the diffusion tensor for velocity $\underline{v}_i$ apply moreover to the diffusion tensor of the wave-vector $\underline{k}_i$ since $\underline{v}_i$ and $\underline{k}_i$ are related by the transformation $\hbar k_{\alpha i} = v_{\alpha i}/(m_o m_\alpha)$ which preserves the symmetry between the x- and y- axes ($m_x = m_y = m_T$).

(iii) The second order moments

When the distribution function is assumed to be a displaced Maxwellian, the steady state is determined completely by the balance of one of the second order moments only, namely the average energy E_i. Consequently, in the diffusion equations, only the diffusion coefficient of E_i is involved. From the symmetry of the x- and y-axis in the equivalent coordinate system, we have

$$D_x^{(i)}(E_i) = D_y^{(i)}(E_i) \neq D_z^{(i)}(E_i) \tag{3.8}$$

For the two-temperature displaced Maxwellian calculation, two second order moments are involved. The most convenient pair of moments are E_i and $E_{\|i}$, the latter being the energy associated with the motion in the direction of the field, and is equal to $\langle \hbar^2 k_\|^2 / 2m_o m_c \rangle_i$ where $m_c^{-1} = (m_L^{-1} + 2m_T^{-1})^{-1}$ is the reciprocal of the conductivity effective mass ratio. The diffusion coefficient of $E_{\|i}$ can again be written in the form:

$$D_x^{(i)}(E_{\|i}) = D_y^{(i)}(E_{\|i}) \neq D_z^{(i)}(E_{\|i}) \tag{3.9}$$

§ 3.3. The scattering mechanisms

The electron-phonon interactions of importance in silicon

are known to be acoustic intravalley scattering, and intervalley scattering between perpendicular valleys (f-type), which involves a mixture of two phonons from the LA and TO branches, and between parallel valleys (g-type) which involves a single LA phonon. [35, 36, 37]. In a cubic material such as silicon, the transition probabilities for these electron-phonon interactions are in general anisotropic because the electron effective mass tensor, and the elastic constants are anisotropic [38]. In the present calculation we shall examine in some detail the effects of this anisotropy since they have been ignored in previous calculations of the velocity characteristic [11, 55] and we are uncertain a priori if the values of the diffusion constants are sensitive to these effects.

For intervalley scattering we shall again adopt the deformation potential approach outlined in § 2.5. In the present context, the important approximation made in this treatment is that the phonon involved is assumed to be of a fixed wave-vector equal to the centre-to-centre separation of the relevant valleys. (This is valid because the wave-vector difference within a valley is usually small in comparison with the separation of the valleys.) As a result, however, the transition probability for intervalley scattering (see Table II of chapter 2) is isotropic. This is because the intervalley phonon wave vector is independent of the initial and final states of the electron in the respective valleys so the detail shape of the valleys can in no way influence the transition probability. Moreover, the anisotropy of the elastic constants is irrelevant in this case because essentially the same phonon is involved in all the transitions.

The energies and deformation potential fields of the phonons involved in intervalley scattering that we shall use are given by Costato and Reggiani [11] who have shown that their values of the parameters lead to good theoretical estimates of the velocity characteristic in silicon for a large range of lattice temperatures and electric fields, and for various

orientations of the field. These values are further supported by experimental evidence deduced from photoconductivity [39] and radioactive recombination measurements [40, 41]. In table I where the numerical constants for n-silicon are listed, D_f and D_g are respectively the deformation potential fields for f-type and g-type scattering; $T_f(LA)$, $T_f(TO)$ and $T_g(LA)$ are the energies of the phonons involved expressed in units of a temperature. Since the parallel valleys are strictly equivalent, g-type scattering may be treated as a special case of 'optical' intravalley scattering.

For acoustic intravalley scattering we shall follow the formalism of Herring and Vogt [38]. When the constant energy surfaces are ellipsoidal shear strains as well as dilations of the lattice can produce a shift in the conduction band edge. Herring [42] has shown that when the valleys are centred on the $<100>$ or $<111>$ axes in the Brillouin zone then it is possible by symmetry considerations to relate the band edge shift to the strains in the lattice through two independent deformation potentials Ξ_d and Ξ_u, which are defined by:

$$\delta E_i = \Xi_d (e_{xx} + e_{yy} + e_{zz}) + \Xi_u e_{zz} \qquad (3.10)$$

where $e_{\alpha\beta}$ are the components of the strain tensor and δE_i is the shift of the band edge in valley i. When the phonon wave-vector is parallel to the symmetry directions of the cubic crystal, two of the acoustic modes are purely transverse and the third purely longitudinal so (3.10) may be used without ambiguity to evaluate the transition probability for acoustic phonon scattering. By interpolating between the results for the symmetry directions, Herring and Vogt [38] were able to obtain a general formula for the transition probability which is applicable for all orientations of the phonon wave vector. Following Conwell [43], we omit further some small terms in this formula and obtain the intravalley transition probability (from state $\underline{k}$ to $\underline{k}'$) due to acoustic phonon scattering:

$$A_{11}(\underline{k},\underline{k}') = \frac{(\Xi_d+\Xi_u\cos^2\theta)^2}{8\pi^2\rho s_L}\,|\underline{k}-\underline{k}'|\,F_{LA}^{11}(\underline{k},\underline{k}') +$$

$$\frac{(\Xi_u\cos\theta\sin\theta)^2}{8\pi^2\rho s_T}\,|\underline{k}-\underline{k}'|\,F_{TA}^{11}(\underline{k},\underline{k}') \qquad (3.11)$$

where θ is the angle between the phonon-wave-vector $(\underline{k}'-\underline{k})$ and the z-axis, s_L and s_T are respectively the longitudinal and transverse wave velocities, and $F_{LA}(\underline{k},\underline{k}')$ and $F_{TA}^{11}(\underline{k},\underline{k}')$ are defined in table II of chapter 2. The two contributions to the right-hand side of (3.11) come respectively from the 'longitudinal' and 'transverse' modes. We see that they can be obtained from the formula for isotropic valleys (table II, chapter 2) by replacing the scalar deformation potential Ξ_a with $(\Xi_d+\Xi_u\cos^2\theta)$ and $\Xi_u\cos\theta\sin\theta$ respectively, and substituting for s the appropriate wave velocity. The transition probability according to (3.11) is clearly anisotropic through the θ dependence.

The average rates of change of momentum and energy by an electron of wave-vector $\underline{k}$ due to acoustic phonon scattering are given by

$$\left(\frac{d\underline{P}}{dt}\right)_{\underline{k}} = \hbar\int(\underline{k}'-\underline{k})\,A_{11}(\underline{k},\underline{k}')\,d\underline{k}' \qquad (3.12a)$$

and

$$\left(\frac{dE}{dt}\right)_{\underline{k}} = \int[E(\underline{k}')-E(\underline{k})]\,A_{11}(\underline{k},\underline{k}')\,d\underline{k}' \qquad (3.12b)$$

In order to evaluate the moment generation functions $G_{11}(\varphi)$ for acoustic phonon scattering and for $\varphi = k_\alpha, E$, one simply multiplies (3.12a) and (3.12b) by the distribution function $f_i(\underline{k})$ in valley i and integrates over all $\underline{k}$. Because of the complex structure of (3.11), it is usual to calculate $(d\underline{P}/dt)_{\underline{k}}$ and $(dE/dt)_{\underline{k}}$ for the cases when $\underline{k}$ is parallel and normal to the z-axis only, so that they reduce to functions that depend only on the electron energy, and use an average value of these energy-dependent rates to evaluate $G_{11}(\varphi)$ [43]. In Appendix II we show that it is possible to

evaluate the expressions (3.12) for all orientations of $\underline{k}$. In particular the rate of momentum loss may be written in the form:

$$\left.\frac{d\underline{p}}{dt}\right|_{\underline{k}} = -\frac{p_z \hat{z}}{\tau_L(E,\theta)} - \frac{(p_x \hat{x} + p_y \hat{y})}{\tau_T(E,\theta)} \qquad (3.13)$$

where τ_L and τ_T are relaxation times that depend on the energy of the electron, and the orientation of the wave-vector with respect to the z-axis. Thus the rates of momentum loss in the heavy and light mass directions are not simply unequal, but depend on the orientation of the electron wave-vector as well as the electron energy. The results derived in Appendix II have not been reported in the literature previously.

The deformation potentials Ξ_u and Ξ_d have been determined from electron cyclotron resonance experiments [44, 45, 46]. The values of Ξ_u obtained by the various authors appear to be consistent within the limits of experimental error at 8.5 ($\pm$ 0.4) eV at room temperature. This value of Ξ_u is confirmed by observations involving piezoelectric [47], acoustoelectric [48] and spectroscopic effects [49]. The values of Ξ_d on the other hand, vary between -2.0 and -6.0eV although the higher values are obtained near room-temperature and the lower ones near helium temperatures. In view of this uncertainty we shall use Ξ_d as an adjustable parameter in our calculations, bearing in mind that at room temperature, the higher values are probably the more accurate.

Impurity scattering has been omitted throughout. When displaced Maxwellian distribution functions are assumed and the balance of momentum and energy are considered, electron-electron collisions can make no explicit contribution. For the two-temperature displaced-Maxwellian, electron-electron interaction enters explicitly into the balance of one of the moments. This will be considered in detail in § 3.5. The calculations are carried out at a lattice temperature of 300^{o}K. In table I we give the values of the material parameters used.

§ 3.4. Displaced Maxwellian Calculation - anisotropic scattering

To evaluate the velocity characteric and diffusion constants for electrons in silicon we shall assume that the distribution functions in the steady state are displaced Maxwellians in the transformed space(denoted by an asterisk) in which the constant energy surfaces are spherical, i.e. for valley i, in equivalent coordinates where the coordinate axes coincide with the principal axes of the ellipsoidal constant energy surfaces. we have:

$$f_i^{(1)}(\underline{k}^*) = \frac{n p_i \hbar^3}{(2\pi m_o k_B T_i)^{3/2} m_T m_L^{1/2}} \exp\left\{-\frac{\hbar^2 (\underline{k}^* - \underline{k}_i^*)}{2 m_o k_B T_i}\right\} \qquad (3.14)$$

where $$k^*_\alpha = k_\alpha m_\alpha^{-1/2} \qquad (3.15)$$

such that $$E = \sum_\alpha \frac{\hbar^2 k_\alpha^2}{2 m_\alpha} = \frac{\hbar^2 k^{*2}}{2 m_o} \qquad (3.16)$$

The transformation (3.15) is a well-known procedure to simplify calculations involving ellipsoidal bands; the distribution function is chosen to be a displaced Maxwellian in the transformed coordinates partly for the mathematical reason that computational manipulations are much simpler when carried out in these coordinates. Physically, this choice is also the unambiguous one: if the distribution function were written as a displaced Maxwellian in $\underline{k}$-space, then the difficulty would arise as to which is the correct effective mass to be inserted into the exponential part of the Maxwellian. The usual choice is the conductivity mass [11] but this can at best be considered a good intuitive average.

For a given field strength F, the parameters p_i, $k^*_{\alpha i}$ and T_i in (3.14) are determined by solving the steady state equations (1.12) for the moment functions $\varphi = 1$, k_α and E. It is convenient to transform all the vector quantities into the starred coordinates according to (3.15) so that the equations take the form:

$$\sum_j G_{ij}(1)\, p_i = 0 \qquad (3.17a)$$

$$-m_\alpha^{-\frac{1}{2}} G_{ii}(k_\alpha) = k^*_{\alpha i}/\tau_{p\alpha} = eF^*_\alpha/\hbar \qquad (3.17b)$$

$$\sum G_{ij}(E)p_j + \sum_\alpha (e\hbar/m_o)F^*_\alpha k^*_{\alpha i} = 0 \qquad (3.17c)$$

Except for the anisotropy of the momentum relaxation time ($\tau_{px} = \tau_{py} \neq \tau_{pz}$) the equations (3.17) are identical to the equations for isotropic valleys (2.21) if $\underline{k}^*$, $\underline{F}^*$ and m_o were replaced by $\underline{v}$, $\underline{F}$ and m^* respectively. [N.B. if the momentum relaxation time were isotrocic then $\underline{k}^*$ is parallel to $\underline{F}^*$, or $\underline{k} \| \underline{F}$.]

Equations (3.17) as they stand involve the distribution function of valley i as well as that of valley j through the terms $G_{ij}(1)$ and $G_{ij}(E)$. However, since the distribution functions with respect to equivalent coordinates, $f_j^{(j)}(\underline{k})$, are identical for all the valleys, we must have

$$G_{ij}(1) \equiv G_{ji}(1) \qquad (3.18a)$$

$$G_{ij}(E) \equiv G_{ji}(E) \qquad (3.18b)$$

Using (3.18) then, the equations (3.17) can be written in a form which involves $f_i^{(i)}(\underline{k})$ only and the parameters contained therein may be determined from the condition of self-consistency of the equations. [The equation (3.17a) is trivially satisfied because from symmetry (cf § 3.2) we have $p_i = p_j = 1/3$ and

$$\sum_{j\neq i} G_{ij}(1) = \sum_{j\neq i} G_{ji}(1) = -G_{ii}(1) \qquad (3.18c)$$

is automatically satisfied since the rate of loss of electrons from valley i is always equal to the rate of gain of electrons in the other valleys due to transfer from valley i.] Having determined $k^*_{\alpha i}$, the velocity in valley i is obtained by the transformation:

$$v_{\alpha i} = \frac{\hbar k_{\alpha i}}{m_o m_\alpha} = \frac{\hbar k^*_{\alpha i}}{m_o m_\alpha^{\frac{1}{2}}} \qquad (3.19)$$

from which the average velocity over all the valleys may be evaluated according to equation (3.4).

The diffusion equations (2.3) for $\varphi = 1$, k_α and E are (in equivalent coordinates):

$$\sum_j \sum_\Psi p_j \frac{\partial G_{ij}(1)}{\partial \Psi_j} \underline{D}^{(i)}(\Psi_j) + \sum_j G_{ij}(1)\, \underline{D}^{(i)}(p_j) = -p_i \underline{\Gamma}_i^{(i)}(1)$$

$$\sum_\Psi \frac{\partial G_{ii}(k_{\alpha i})}{\partial \Psi_i} \underline{D}^{(i)}(\Psi_i) = -\underline{\Gamma}_i^{(i)}(k_\alpha)$$

$$\sum_j \sum_\Psi p_j \frac{\partial G_{ij}(E)}{\partial \Psi_j} \underline{D}^{(i)}(\Psi_j) + p_i^{-1} \sum_j G_{ij}(E)\left[p_i \underline{D}^{(j)}(p_j) + p_j \underline{D}^{(i)}(p_i)\right]$$

$$+ \frac{ehp_i}{m_o} \sum_\alpha F_\alpha \underline{D}(k_{\alpha i})\, m_\alpha^{-1} = -p_i \underline{\Gamma}_i^{(i)}(E) \qquad (3.20)$$

where $\Psi_j = k_{\alpha i}$ and E. These again involve the diffusion coefficients of the moments Ψ_i of valley j as well as those of valley i. To reduce the equations to a form involving the coefficients in valley i only, the following substitutions are available (for $\varphi = 1, E$):

$$\frac{\partial G_{ij}(\varphi)}{\partial \Psi_j} = \frac{\partial G_{ji}(\varphi)}{\partial \Psi_i} \qquad (3.21a)$$

and

$$\underline{D}^{(i)}(\Psi_j) = \tilde{T}_{ji} \underline{D}^{(j)}(\Psi_j) = \tilde{T}_{ji} \underline{D}^{(i)}(\Psi_i) \qquad (3.21b)$$

where $\tilde{T}_{ji}$ is the transformation matrix from valley j to i. Equation (3.21a) follows from (3.18), and (3.21b) from the fact that $\underline{D}^{(i)}(\Psi_i)$ is identical for all i. Using (3.21) and (3.18), and the equations (3.5) and (3.1) for $\underline{D}(p_i)$ and the transformation matrices $\tilde{T}_{ji}$ (putting i = 3 for convenience) respectively, the equations (3.20) may be rewritten in terms of quantities in valley i only as:

$$\sum_\Psi \frac{\partial G_{ii}(1)}{\partial \Psi_i} \begin{pmatrix} 1 & -\frac{1}{2} & -\frac{1}{2} \\ -\frac{1}{2} & 1 & -\frac{1}{2} \\ -\frac{1}{2} & -\frac{1}{2} & 1 \end{pmatrix} \underline{D}^{(i)}(\Psi_i) + 9\, G_{ji}(1)\, D_p \begin{pmatrix} 1 \\ 1 \\ -2 \end{pmatrix} = -\Gamma_i^{(i)}(1) \qquad (3.22a)$$

$$\sum_{\Psi} \frac{\partial G_{1j}(1)}{\partial \Psi_1} \begin{pmatrix} 1 & -\frac{1}{2} & -\frac{1}{2} \\ -\frac{1}{2} & 1 & -\frac{1}{2} \\ -\frac{1}{2} & -\frac{1}{2} & 1 \end{pmatrix} \underline{D}^{(1)}(\Psi_1) + 9\, G_{j1}(1) D_p \begin{pmatrix} 1 \\ 1 \\ 2 \end{pmatrix} = -\underline{\Gamma}_1^{(1)}(1) \qquad (3.22a)$$

$$\sum_{\Psi} \frac{\partial G_{11}(k_{\alpha 1})}{\partial \Psi_1} \underline{D}^{(1)}(\Psi_1) = -\underline{\Gamma}_1^{(1)}(k_{\alpha}) \qquad (3.22b)$$

$$\sum_{\Psi} \left\{ \left[\frac{\partial G_{11}(E)}{\partial \Psi_1} - \frac{G_{j1}(E)}{G_{j1}(1)} \frac{\partial G_{11}(1)}{\partial \Psi_1} \right] + \left[\frac{\partial G_{j1}(E)}{\partial \Psi_1} - \frac{G_{j1}(E)}{G_{11}(1)} \frac{\partial G_{j1}(1)}{\partial \Psi_1} \right] \begin{pmatrix} 0 & 1 & 1 \\ 1 & 0 & 1 \\ 1 & 1 & 0 \end{pmatrix} \right\} \underline{D}^{(1)}(\Psi_1)$$
$$+ \frac{e\hbar}{m_o} \sum_{\alpha} F_{\alpha} \underline{D}^{(1)}(k_{\alpha 1}) m_{\alpha}^{-1} = -\left[\underline{\Gamma}_1^{(1)}(E) \frac{G_{j1}(E)}{G_{j1}(1)} - \underline{\Gamma}_1(1) \right] \qquad (3.22c)$$

The unknowns contained in the diffusion coefficients have been deduced in § 3.2 by symmetry arguments so these can be determined from (3.22) by solving the linear algebraic equations. Note that although equations (3.22) contain the diffusion coefficients of a single valley only, they are different in form to the single valley equations because of the effective mass anisotropy and anisotropic scattering. Furthermore, intervalley transfer gives rise to $\underline{\Gamma}^{1j}$ on the right-hand side and the non-diagonal matrix on the left-hand side.

Finally to obtain the velocity diffusion coefficients we have from equation (3.19)

$$\underline{D}(v_{\alpha 1}) = \frac{\hbar}{m_o m_{\alpha}} \underline{D}(k_{\alpha 1}) \qquad (3.23)$$

From the components of $\underline{D}(v_{\alpha 1})$ the experimentally observed diffusion constants $D_{\perp}$ and $D_{\parallel}$ in the directions normal and parallel to the electric field may be evaluated according to equations (3.6) and (3.7).

In order to obtain saturation of the drift velocity at high fields, Costato and Reggiani [50] have shown that it is necessary to take into account the increase of the transverse effective mass ratio $m_{\perp}$ with electron energy. This effect has been observed experimentally by Spradling and Zhukov [44]. Assuming an energy/wave-vector dispersion relation of the form [51]:

$$E(\underline{k}) = -\Delta + \frac{\hbar^2 k_z^2}{2m_L m_o} + \Delta\left[1 + \frac{\hbar^2 (k_x^2 + k_y^2)}{2m_{To} m_o \Delta}\right]^{\frac{1}{2}}$$

where m_L and m_{To} are the longitudinal and transverse effective mass ratios respectively at the bottom of the conduction band and 2Δ is the direct energy-gap between the $<100>$ - minima of the conduction band and the valence band, a temperature-dependent average transverse effective mass ratio can be obtained having the form:

$$m_T = m_{To}(1 - k_B T_1/\Delta)^{-1} \qquad (3.24)$$

which is accurate to first order in $k_B T_1/\Delta$. The expression (3.24) is consistent with the expression for the conductivity effective mass derived by Cardona et al [51] for classical statistics but differs from that of Costato and Reggiani [50] which contains an extra factor of 2 in the term $k_B T_1/\Delta$. The value of 2Δ (the $X_4 \rightarrow X_1$ energy gap in silicon) obtained from Brust [52] is 4.30eV so (3.24) is good for values of T up to $\sim 5000^{\circ}$K. (Costato and Reggiani [50] have taken 2Δ to be 3.6eV which corresponds to the indirect band gap .)

The inclusion of the temperature dependence of m_T into the calculation requires several modifications to the equations apart from substituting m_T by the expression (3.24) throughout. The left-hand side of (3.22c) should now contain an extra term:

$$-\frac{e\hbar}{m_o}\left(\sum_{\vec{\alpha}} F_\alpha k^*_{\alpha 1} \frac{1}{m^2_\alpha} \frac{dm_\alpha}{dk_B T}\right) \underline{D}(k_B T_1) \qquad (3.22d)$$

and equation (3.23) should be modified to

$$\underline{D}(v_{\alpha 1}) = \frac{h}{m_o m_\alpha} \underline{D}(k_{\alpha 1}) - \frac{\hbar k_{\alpha 1}}{m_o m_\alpha}\left(\frac{1}{m_\alpha} \frac{dm_\alpha}{dk_B T_1}\right) \qquad (3.23a)$$

where in (3.22d) and (3.23a), from $kT_1 = \frac{2}{3}(E_1 - \sum_\alpha \hbar^2 k_{\alpha i}^2 / 2m_o m_\alpha)$,

$$\underline{D}(k_B T_1) = \frac{2}{3}\left[\underline{D}(E_1) - \sum_\alpha \frac{\hbar^2 k_{\alpha 1}}{m_o m_\alpha}\,\underline{D}(k_{\alpha_1})\right] \Big/ \left(1 - \frac{2}{3m_T}\frac{dm_T}{dk_B T}\sum_{\alpha \neq z} \frac{\hbar^2 k_{\alpha i}^2}{2m_o m_T}\right)$$

(3.24)

In evaluating the derivatives $\partial G_{j1}(\varphi) / \partial \Psi_1$ the temperature dependence of m must of course be fully accounted for.

In diagram (32) we show the velocity characteristics [curves (a)] calculated for Ξ_d = -6.0, -3.4 and -2.0eV which cover the probable range for Ξ_d, -3.4 eV being the best experimental value at room-temperature [44]. The effect of changing this deformation potential is apparent only at high fields when the energy loss to long wavelength acoustic phonons becomes significant. Comparison with the experimental points of Sigmon and Gibbons [53] at 300°K indicates that the value of Ξ_d is close to the experimental value of -3.4eV.

The curves (b) in diagram 3.2 show the magnitude of the component of velocity normal to the field in a given valley. This component of velocity is unobservable experimentally because the average over all the valleys is zero from equation (3.5b). We show these curves in order to give a further measure of the effect of anisotropic scattering. Although the dependence of these curves in Ξ_d is more pronounced than that of the velocity characteristic, they do not in fact differ by a marked extent. We have noted earlier that the effect of anisotropic scattering is to render $\underline{k}_1^*$ non-parallel to $\underline{F}^*$. In diagram 3.3 we plot the ratio $(\cos\theta_{k^*} - \cos\theta_{F^*}) / \cos\theta_{F^*}$ against field for the various values of Ξ_d where θ_{k_*} and θ_{F^*} are the angles made by $\underline{k}^*_i$ and $\underline{F}^*$ with the $\hat{z}$ - axis. ($\underline{k}^*$ and $\underline{F}^*$ both lie in the (110) - plane from § 3.2, θ_{F^*} is not a constant because of the increase of the effective

mass ratio m_T). We see that the effect of anisotropic scattering is always small. This is because momentum relaxation is dominated by intervalley scattering which is isotropic in the present treatment. Increasing Ξ_d from -6.0 to -2.0eV causes Θ_{k*} to increase from a value $<\Theta_{F*}$ to one $>\Theta_{F*}$. For Ξ_d - -3.4eV, Θ_{k*} is nearly always equal to Θ_{F*}, as if acoustic phonon scattering too were isotropic. We conclude that the neglect of the anisotropy of long wavelength acoustic phonon by previous authors is justified for the purpose of evaluating the velocity characteristic.

The calculated diffusion constants are shown in diagram 3.4 and the electron temperature in diagram 3.5. Experimental points for the longitudinal diffusion constant by Sigmon and Gibbons [53] and the transverse diffusion constant by Persky and Bartelink [54] are included for comparison. The error bars associated with the experimental points are as quoted by the authors (in the former case, an error of about 30% is given for all the points). The agreement between theory and experiment is poor for both the constants: the theoretical estimate appears to be too high for the transverse constant and too low for the longitudinal one. We shall defer the discussion of these results to a later section when the results for the two-temperature displaced Maxwellian calculation are also available for comparison.

§3.5 'Two-temperature' calculation - effects of electron-electron scattering.

The two-temperature calculation can be simplified considerably if the anisotropy of the acoustic phonon scattering rate were neglected. We shall justify the approximation on the grounds that $\underline{k}^*$ is nearly always parallel to $\underline{F}^*$, especially when the most probable values of the deformation potentials are used. Accordingly we shall replace the transition probability for acoustic phonon scattering (3.11) by the expression given in table II of Chapter 2. The single deformation potential Ξ_a contained therein is to be given a value that would lead to a close fit between the calculated velocity characteristic and experimental

data. (The optimum value of $\mathcal{E}_a$ turns out in fact to be 7.0eV which is close to the value quoted in the literature [55].) Neglecting the anisotropy of the scattering would obviously introduce some uncertainty into the calculated diffusion constants. This uncertainty should not however, exceed the variance of the results for the various values of $\mathcal{E}_d$ used for the case when the anisotropy is accounted for fully. From diagram 3.4 we see that this corresponds to an uncertainty of about 10%.

The distribution function assumed to be of the form:

$$f_1^{(i)}(\underline{k}) = A \exp -\frac{\hbar^2}{2m_o}\left\{\frac{(k^*_{\parallel}-k^*_1)^2}{k_B T_{\parallel}} + \frac{k^{*2}_{\perp}}{k_B T_{\perp}}\right\} \qquad (3.25)$$

where $k^*_{\parallel}$ and $k^*_{\perp}$ are respectively the components of $\underline{k}^*$ parallel and normal to $\underline{F}^*$. We have again written the distribution function in the starred-coordinates so that there is no ambiguity concerning the effective mass to be inserted into (3.25).

The distribution function (3.25) is of a simple form (where the orthogonal components of the wave-vector are not mixed) only if it is written in the starred coordinates with the $\hat{z}$-axis running parallel to $\underline{k}^*_1$. Accordingly it is convenient to rewrite the steady state and diffusion equations in this system of coordinates. This is effected by transforming all the components of vector quantities in the equations according to (3.15) and then rotating the z-axis in the (110)-plane through an angle $\tan^{-1}(2m_T/m_L)^{\frac{1}{2}}$. (The rotation aligns the z-axis in the direction of $\underline{k}^*_1$ and preserves moreover the symmetry between the x- and y-axis so that the form of the diffusion coefficients deduced in § 3.2 are still valid.) The calculation is then analogous to that for a displaced Maxwellian. We consider that the steady state and diffusion equations for the moments $\varphi = 1$, k^*_α, E and E_z, where $E_z = \hbar^2 k^{*2}_z / 2m_o$, from which the steady state values of $\underline{k}^*_1$, $T_{\parallel}$ and $T_{\perp}$, and the diffusion coefficients $\underline{D}^*(\varphi_1)$ may be determined. When these quantities have been transformed back into $\underline{k}$-space in equivalent coordinates, the velocity and velocity diffusion coefficients can be obtained as before.

It is to be appreciated that if isotropic scattering were not assumed then the procedure described above would be made much more

complicated for the following reasons. Firstly since $\underline{F}^*$ and $\underline{k}_1^*$ are not parallel, the distribution will be of a more complex form than (3.25), when $\underline{F}^*$ is taken to the symmetry axis for the temperature anisotropy. Secondly, in the rotated coordinates, the transition probability for acoustic phonon scattering will involve the azimuthal angle φ in addition to the polar angle θ of the phonon wavevector. Both these factors imply the evaluation of triple integrals where double integrals would otherwise occur in obtaining the moment generation functions.

In the balance equations for the moment E_z, electron-electron collisions make an explicit contribution. (Unlike momentum and energy, the moment E_z is not conserved for electron-electron collisions.) We have therefore included this scattering mechanism in the calculation, in order to obtain an approximate value for the concentration of electron that is required to reduce the distribution function to a displaced Maxwellian, in the particular case when the departure from this shape takes the form of two unequal temperatures normal and parallel to the electric field. Previous estimates of this critical concentration are based on criteria regarding the relative frequency of electron-phonon and electron-electron collisions [55, 56] or the relative rates of energy exchange for a given electron by the two types of collisions [57]. In none of these calculations was it possible however, to examine the actual effect on the distribution produced by electron-electron collisions.

The transition probability for electron-electron scattering is calculated from first order time-dependent perturbation theory based on plane waves and a screened Coulomb potential of range λ^{-1} where λ^{-1} is to be identified with the Debye screening length. Collective energy losses and inter-carrier Umklapp processes are neglected. The resultant formula for the transition probability per unit time for an electron in state s to a state s' is [57]:

$$P(s,\ s') = \frac{4c\hbar}{\pi}\left(\frac{e^2}{4\pi\epsilon\epsilon_0}\right)^2 \int f(\underline{k}_q)\ \left|\frac{1}{\lambda^2 + (\underline{k}_s - \underline{k}_{s'})^2}\right|^2 \delta(E_s + E_q - E_{s'} - E_{q'})\, d\underline{k}_q \qquad (3.26)$$

$$\underline{k}_{q'} = \underline{k}_s + \underline{k}_q - \underline{k}_{s'}$$

where c is a numerical factor which lies between 1 and 2 according to the likelihood of collisions between electrons of like spin (c = 1 where screening is sufficiently stron so that collisions between electrons of like spin is negligible), ϵ is a suitable dielectric constant for the crystal, and $f(\underline{k}_q)$ is the distribution function of the electrons that are available to collide with the electron in state s. If electron-electron collisions are restricted to carriers in the same valley, then the moment generation function for the moment E_z for this process is given by:

$$G_{ii}^{e-e}(E_z) = \iint f_i(\underline{k}_s)\, P(s,\ s')\, (E_{zs'} - E_{zs})\, d\underline{k}_s\, d\underline{k}_{s'} \qquad (3.27)$$

where in (3.26) and (3.27) the electron distribution function is that of carriers in the valley i. The explicit expression for $G_{ii}^{e-e}(E_z)$ is given in appendix II.

Impurity scattering has been neglected throughout. Our purpose in including electron-electron scattering is to determine the behaviour of the departure of the distribution function from a displaced Maxwellian with respect to electron density. If the electron density change is accompanied by a corresponding change in impurity concentration, then the effect we wish to investigate would be obscured. Experimentally, the condition we have specified may be fulfilled by exciting electrons of varying concentration into a high purity sample.

The results with no electron-electron scattering will be discussed first. The velocity characteristic for the optimised value of Ξ_a(=7.0eV) is nearly identical to that calculated in the previous section so this will not be shown. In diagram 3.5 we show the temperatures $T_\perp$ and $T_{||}$ as a function of the electric field, together with the single temperature obtained from the displaced Maxwellian calculation obtained from the dis-

placed Maxwellian calculation for $\mathcal{E}_d = -3.4$eV. (The electron temperatures calculated for the various values of $\mathcal{E}_d$ differ less than 5% throughout.) We see that the difference between the longitudinal and transverse temperatures is very small (~ 7% at worse) and the departure of the distribution function from the displaced Maxwellian is barely noticeable. The diffusion constants (diagram 3.6) are nevertheless changed by a marked extent from the results of the displaced Maxwellian calculation. There is now a fair agreement between the calculated longitudinal constant and the experimental results of Sigmon and Gibbons [53], although the disparity between theory and experiment for the transverse diffusion constant remains very much unaltered. We shall discuss the results of the diffusion calculation in detail in the next section.

When electron-electron scattering is included no noticeable effect is observable until the electron concentration is increased to 10^{19} cm^{-3} when the difference between the longitudinal and transverse temperatures is reduced by a few degrees e.g. at about 10kV cm^{-1}, the temperatures of roughly 900^{o}K and 960^{o}K for the limit of zero electron concentration are modified to 902^{o}K and 957^{o}K for an electron concentration of 10^{19} cm^{-3}. Increasing the electron concentration beyond 10^{19} cm^{-3} does not reduce the temperature anisotropy significantly further because the increase in the screening reduces the effectiveness of the scattering potential. (In any case, the formula for electron-electron scattering is invalid for higher concentrations because of the onset of degeneracy.) For the given form of the electron-electron interaction, there is therefore a residual anisotropy of a few percent on which electron-electron scattering can make no impression. The effect of electron-electron scattering on the diffusion constants is also negligible. The relative unimportance of electron-electron scattering can be explained by the fact that the departure of the distribution function from a displaced Maxwellian is not large even in the absence of electron-electron scattering.

The effect of electron-electron scattering is to reduce the distribution function to a displaced Maxwellian so that the moment generation functions for electron-electron scattering is zero whatever the moment, if the distribution function is a displaced Maxwellian. (See Appendix II, under electron-electron scattering.) When the departure from a displaced Maxwellian is small, the moment generation functions for electron-electron scattering (in the present case, for the moment E_z) are also small so the contribution of electron-electron scattering to the balance equations is small.

We conclude that the departure of the distribution function from a displaced Maxwellian in the form of a temperature anisotropy is small for silicon, and the effect of electron-electron scattering on this anisotropy is negligible. This does not imply however, that the distribution function is in fact a displaced Maxwellian, nor what the effect of electron-electron scattering will be on departures from this asymptotic form of the distribution function other than the case of a temperature anisotropy.

§ 3.6 Discussion

Before proceeding to discuss the results of the diffusion calculation in relation to experiements and Monte Carlo calculations, we shall outline and attempt at some interpretation of the salient features of the present theory.

The curves obtained for the two types of distribution functions show essentially the same qualitative behaviour. At low fields, the transverse and longitudinal constants are equal, and as the field is increased the transverse constant $D_\perp$ begins to rise monotonically while the longitudinal constant $D_{||}$, after an initial decrease, begins to increase very slowly at about 40kV/cm. There is however no tendency for the curves to coalesce up to the highest field considered ($\sim$ 100kV cm^{-1}.)

From equations (3.7b) and (3.7c) we see that the difference between the longitudinal and transverse constants is equal to the sum of the off-diagonal elements $(D_1 + D_2 + D_3)$ in the diffusion tensor in equivalent coordinates, as given by equation (3.6). (The transverse constant contains a contribution from intervalley scattering which in fact turns out to be small: ~ 2 cm^2 s^{-1}, because the velocity difference between the valleys is small compared to the thermal spread of velocity). As was explained in § 3.2, the off-diagonal elements occur as a consequence of the assymetry introduced by the electric field along the positive and negative directions of the coordinate axes. Thus at zero field, the off-diagonal elements are zero and the diffusion constants $D_\perp$ and $D_\parallel$ are equal. At higher fields the constants are generally unequal, and in the limit of extremely high fields, there is no reason to believe that the curves should coalesce.

The result $D_\perp > D_\parallel$, corresponding to $D_1 + D_2 + D_3 < 0$, can be best understood if we refer to the special case of the two-temperature displaced Maxwellian calculation in which we have transformed the diffusion equations to $\underline{k}^*$-space and rotated the coordinates so that the z-axis is parallel to the electric field. Through these transformations we have reproduced a 'pseudo-isotropic-single-valley' system since the constant energy surfaces in $\underline{k}^*$- space are spherical, the equations involve the coefficients of a single valley only and the scattering has been assumed to be isotropic. The diffusion tensor is thus expected to resemble that for the real isotropic single valley, i.e. the tensor is diagonal with elements given by the Einstein relations (2.13) and (2.14). One 'multivalley-anisotropic' effect remains however, despite the transformations: the average drift in $\underline{k}^*$-space in the various valleys are non-identical (a multivalley effect) and the difference in the average drift is non-parallel to the field (a consequence of anisotropic band).* The effect of the residual multivalley-anisotropic terms in the diffusion equations is to introduce two non-diagonal terms in the diffusion tensor, which then takes the form:

* For isotropic scattering, the average drift $\underline{k}_i$ in the various valleys are parallel but the $\underline{k}^*_i$'s are not because the transformation (3.15) is non-identical for all i.

$$\underline{D}^*(\underline{k}^*) = \begin{pmatrix} D^*_{\perp} & 0 & 0 \\ 0 & D^*_{\perp} & 0 \\ \xi & \xi & D^*_{\parallel} \end{pmatrix} \qquad (3.28)$$

where $D^*_{\perp}$ is given exactly by the Einstein relation $D^*_{\perp} = (k^*_{\perp}/eF^*)k_B T$. Since the difference in the average drift $\underline{k}^*_j$ between the valleys is small compared to the thermal spread of $\underline{k}^*$, ξ is small compared to the diagonal terms and $D^*_{\parallel}$ is given approximately by the Einstein relation $D^*_{\parallel} = (dk^*_{\perp}/dF^*)\, k_B T_{\parallel}/e$. When (3.28) is transformed back into $\underline{k}$-space and equivalent coordinates, we find that the off-diagonal terms sum to:

$$-(D^*_{\perp} - D^*_{\parallel})r(r+1) + \xi(2r+1)(r-1) \qquad (3.29)$$

where $r = (m_L/m_T)^{\frac{1}{2}}$. The sign of (3.29) is dominated by the first term which is negative since $D^*_{\perp} > D^*_{\parallel}$ from the Einstein relations.

When anisotropic scattering is included in the calculation, further small terms appear in the off-diagonal positions in (3.28) because $\underline{k}^*$ and $\underline{F}^*$ are non-parallel. These terms are small because the anisotropy of the scattering is small and the value of the off-diagonal terms in the diffusion tensor of $\underline{k}$ in equivalent coordinates is still dominated by the behaviour of $D^*_{\perp}$ and $D^*_{\parallel}$ which are given approximately by the Einstein relations. Thus we see that the result $D_{\perp} > D_{\parallel}$ is a consequence of the Einstein relations being approximately valid for the tensor $D^*(\underline{k}^*)$ - the physical interpretation for which is that a density gradient in the direction of the field produces heating of the electron system, as was explained in chapter 2.

One last observation that requires some comment is the fact that the value of the diffusion constants depends not only on the form of the steady state distribution function, but also on the degrees of freedom by which the latter is allowed to be perturbed by density gradients. This is illustrated quite clearly by the results for the displaced Maxwellian and the two-temperature displaced Maxwellian calculations. Although the steady state distributions are very nearly equal in the two cases, a sizeable change is

observed in the values of the distribution constants calculated because in the latter case the freedom for the temperatures in the directions normal and parallel to the field to vary independently is included. It is therefore incorrect when evaluating the diffusion constant by any method, to ignore the influence of the density gradient on the distribution function itself. In a calculation of the diffusion constants for holes in germanium by Persky and Bartelink [15] the diffusion constants are evaluated according to:

$$\begin{matrix} D_{\parallel} \\ D_{\perp} \end{matrix} = \frac{2}{3}\int_0^{-0} \tau E^{3/2}\left[n_o + \frac{(1\pm 3)}{10} n_2 \right] dE \;\; m\int_0^{\infty} E^{\frac{1}{2}} n_o dE$$

where $n_o(E)$ and $n_2(E)$ are the energy dependent coefficients of the zeroth and second order terms in a Legendre polynomial expansion of the distribution function, $\tau(E)^{-1}$ the collision frequency, and m the effective mass. The results are invalid for the reason that the effects of a density gradient on the distribution function are ignored. One of the most notable consequences of this error is that $D_{\parallel}$ is always larger than $D_{\perp}$ since ordinarily, n_2 is positive (corresponding to $T_{\parallel} > T_{\perp}$ in a two-temperature displaced Maxwellian.) Moreover, the constants become nearly equal at high fields because the distribution function is nearly isotropic then.

We shall now consider the failure to obtain agreement between theory and experiment. The features of the theoretical curves outlined in the preceding paragraphs are results of fairly general deductions and although some error is to be expected from the theory because it assumes very simple steady state distribution functions, one should be surprised to expect these broad qualitative features of the curves to be seriously affected. A Monte Carlo calculation by Persky and Bartelink [54] does indicate that $D_{\perp} > D_{\parallel}$ as the present theory also predicts, so one suspects that either or both of the two sets of experi-

mental results are in error in giving the reversed negative magnitude.

Our calculation for the two-temperature displaced Maxwellian is in agreement with the results of Sigmon and Gibbons [53], while the Monte Carlo calculation and experiment of Persky and Bartelink [54] seem also to achieve agreement between each other. The Monte Carlo calculation, however, is based on a simplistic band structure in which the energy minima are assumed to be isotropic; and what is more disturbing is that the isotropic effective mass is given a value of $0.61m_o$ which is inconsistent if the well-established values of the conductivity effective mass, even when the increase of m_T with electron temperature is allowed for. (At 5000^oK, m_T increases from 0.1905 to 0.24 approximately according to (3.24), giving a value of $0.33m_o$ for the conductivity effective mass.) The correct velocity characteristic is obtained in spite of the high effective mass value used because the electron-phonon interactions are not treated correctly either. For example, only one intervalley phonon (of high energy) is considered when three phonons, one of which being of comparatively low energy ($\equiv 307^oK$), are involved. Energy loss to long wavelength acoustic phonons are also neglected. The net effect of these inconsistencies is to make calculated average energies become much lower than in reality for a given electric field so that the values of the diffusion constants are also lower. The agreement between theory and experiment may therefore be purely accidental.

We conclude that the discrepancy between theory and experiment is not irresolvable. Further experimental work and a careful Monte Carlo calculation are needed. From the point of view of the interpretation of numerical results, the present theory has been able to give a macroscopic description which would usefully supplement the microscopic explanations obtainable from the Monte Carlo calculation.

TABLE I

VALUES OF MATERIAL PARAMETERS FOR SILICON

m_L	$0.9163\ m_0$
m_T	$0.1905\ m_0$
2Δ	4.30 eV
$T_f(LA)$	540 °K
$T_f(TO)$	680 °K
$T_g(LA)$	307 °K
D_f	3×10^8 eV cm^{-1}
D_g	4.5×10^8 eV cm^{-1}
Ξ_u	8.5 eV
Ξ_d	$-2.0 \sim -6.9$ eV
Ξ_a	7.0 eV
S_L	9.33×10^5 cm s^{-1}
S_T	5.42×10^5 cm s^{-1}
ρ	2.329 g. cm^{-3}

CAPTION TO DIAGRAMS

3.1 The conduction band of silicon and the 'equivalent' coordinates (i) in which the distribution function $f_i^{(1)}$ is identical for all i which the electric field is in the $<111>$-direction.

3.2 The velocity characteristic of silicon for $\underline{F} \parallel <111>$ and anisotropic long wavelength acoustic phonon scattering, assuming displaced Maxwellians in $\underline{k}^*$-space, and various values of the deformation potential Ξ_d [curves (a)]. Curves (b) show the component of velocity in a given valley normal to the electric field.

3.3 The anisotropy ratio, $(\cos\theta_{k^*} - \cos\theta_{F^*})/\cos\theta_{F^*}$, where θ_{k^*} and θ_{F^*} are the angles subtended between the heavy mass axis, and the vectors $\underline{k}^*$ and $\underline{F}^*$ respectively, is plotted for various values of Ξ_d. For isotropic scattering $\theta_{k^*} = \theta_{F^*}$ so the ratio is zero. Thus scattering is nearly isotropic for $\Xi_d = -3.4$ eV.

3.4 The longitudinal and transverse diffusion coefficients for electrons in silicon assuming displaced Maxwellians in $\underline{k}^*$-space and anisotropic scattering. Experimental points for the transverse coefficient by Persky and Bartelink [54] and for the longitudinal constant by Sigmon and Gibbons [53] are shown for comparison. The relative magnitude of the coefficients from theory and experiment are reversed.

3.5 Electron temperature in silicon calculated by assuming displaced Maxwellians in $\underline{k}^*$-space (full curve) and two-temperature displaced Maxwellians (Δ and $\odot$ denote respectively T_t and T_l).

3.6 Diffusion coefficients for electrons in silicon with $\underline{F}\,11 < 111 >$ calculated by assuming two-temperature displaced Maxwellians and isotropic electron-phonon scattering. Fair agreement is achieved between theory and the measurements of Sigmon and Gibbons for the longitudinal coefficient.

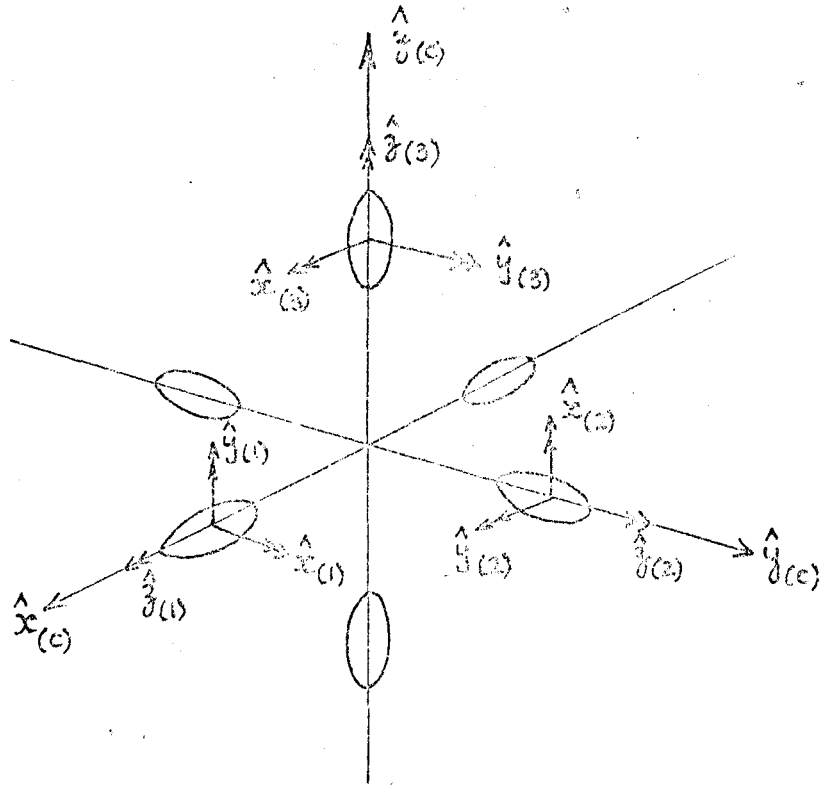
$\hat{z}_{(c)}$
$\hat{z}_{(3)}$
$\hat{x}_{(3)}$
$\hat{y}_{(3)}$
$\hat{y}_{(1)}$
$\hat{x}_{(2)}$
$\hat{x}_{(1)}$
$\hat{y}_{(2)}$
$\hat{z}_{(2)}$
$\hat{y}_{(c)}$
$\hat{z}_{(1)}$
$\hat{x}_{(c)}$

Diag. 3.1.

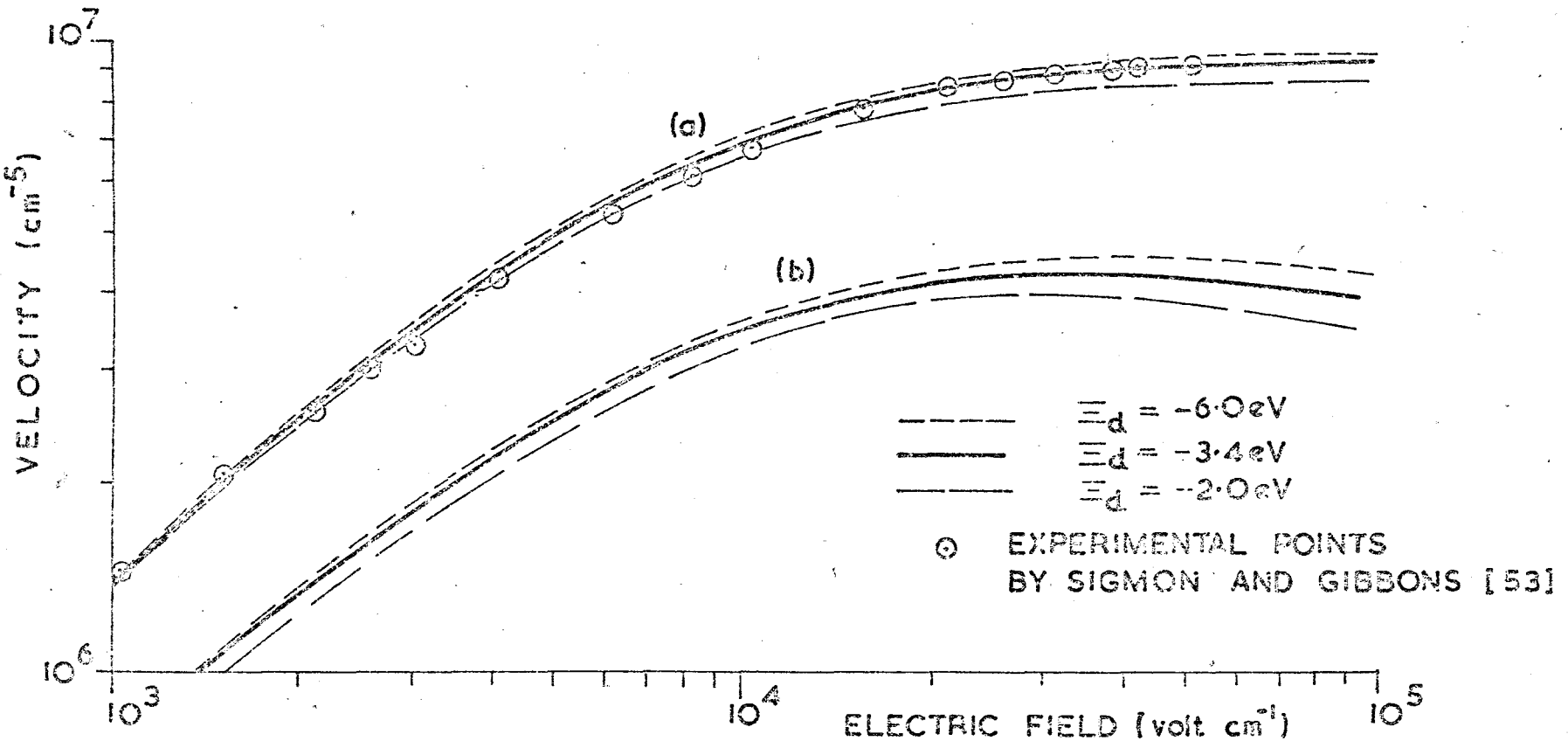
VELOCITY (cm⁻¹)
10⁷
10⁶
(a)
(b)
10³
10⁴
10⁵
ELECTRIC FIELD (volt cm⁻¹)
Ξd = -6·0eV
Ξd = -3·4eV
Ξd = -2·0eV
EXPERIMENTAL POINTS
BY SIGMON AND GIBBONS [53]

Diag. 3.2

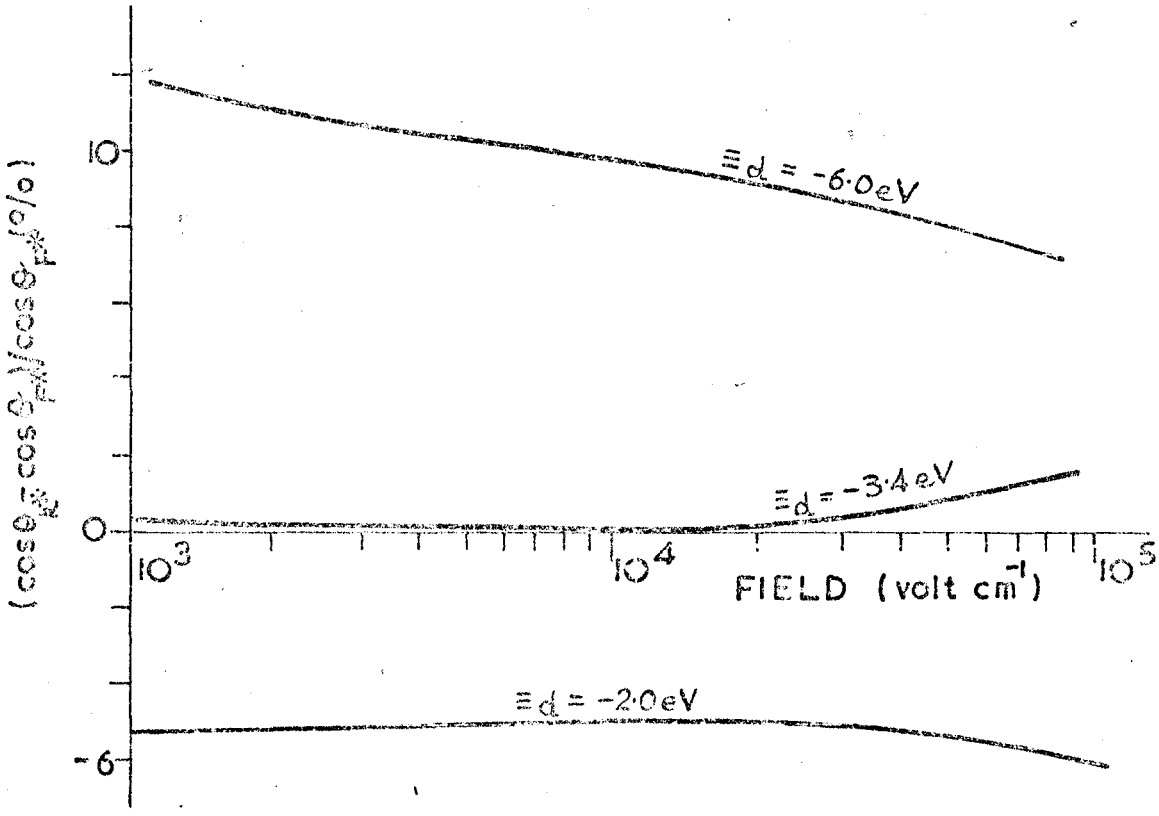
10
0
-6
10^3
10^4
10^5
FIELD (volt cm^{-1})
Ξ_d = -6·0eV
Ξ_d = -3·4eV
Ξ_d = -2·0eV
$(\cos\theta - \cos\theta_{max})/\cos\theta_{max}$ %

Diag. 3.3

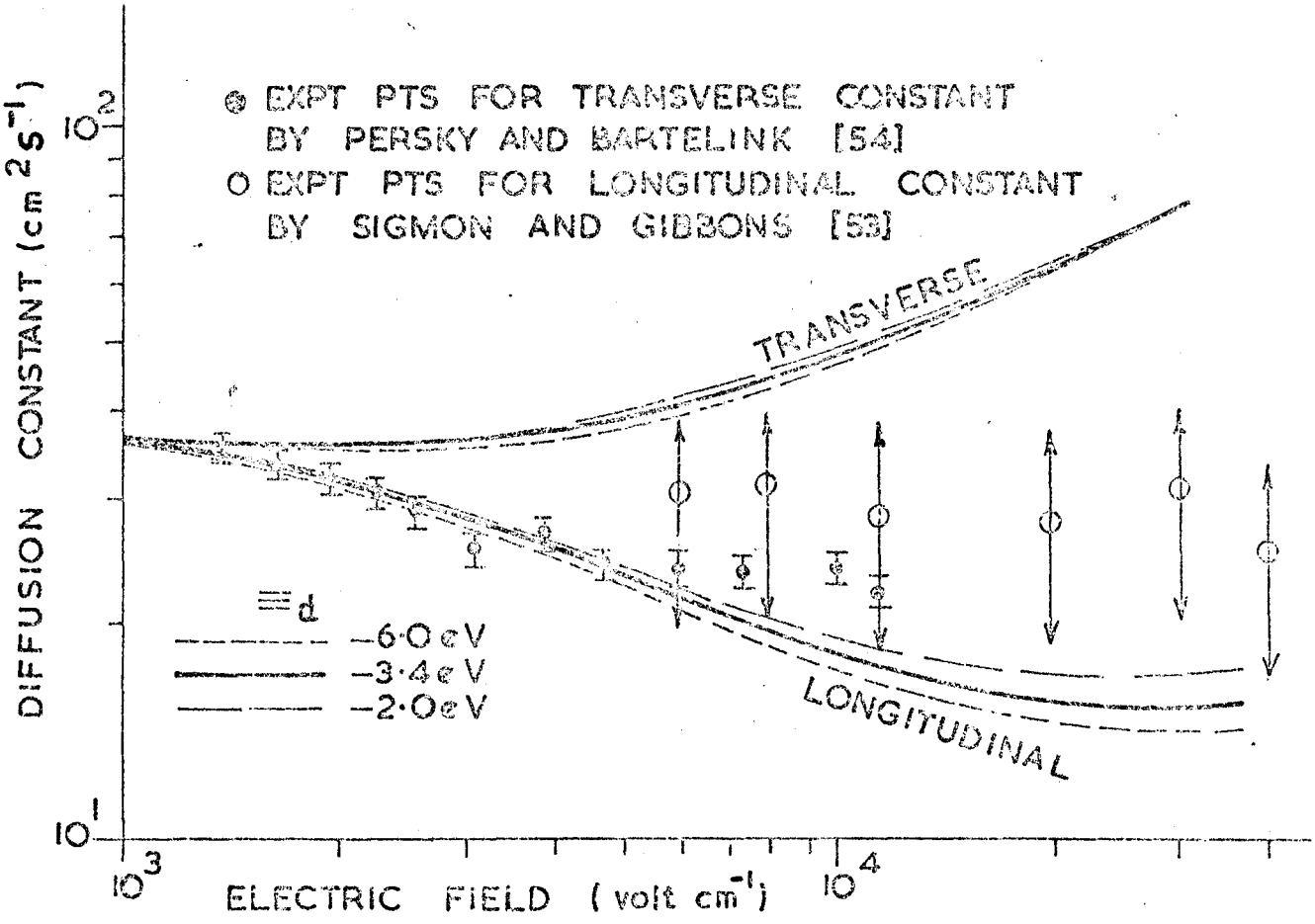
⊗ EXPT PTS FOR TRANSVERSE CONSTANT
BY PERSKY AND BARTELINK [54]
O EXPT PTS FOR LONGITUDINAL CONSTANT
BY SIGMON AND GIBBONS [53]
TRANSVERSE
LONGITUDINAL
≡d
−6·0 eV
−3·4 eV
−2·0 eV
DIFFUSION CONSTANT (cm²s⁻¹)
ELECTRIC FIELD (volt cm⁻¹)
10²
10¹
10³
10⁴

Diag. 3.4

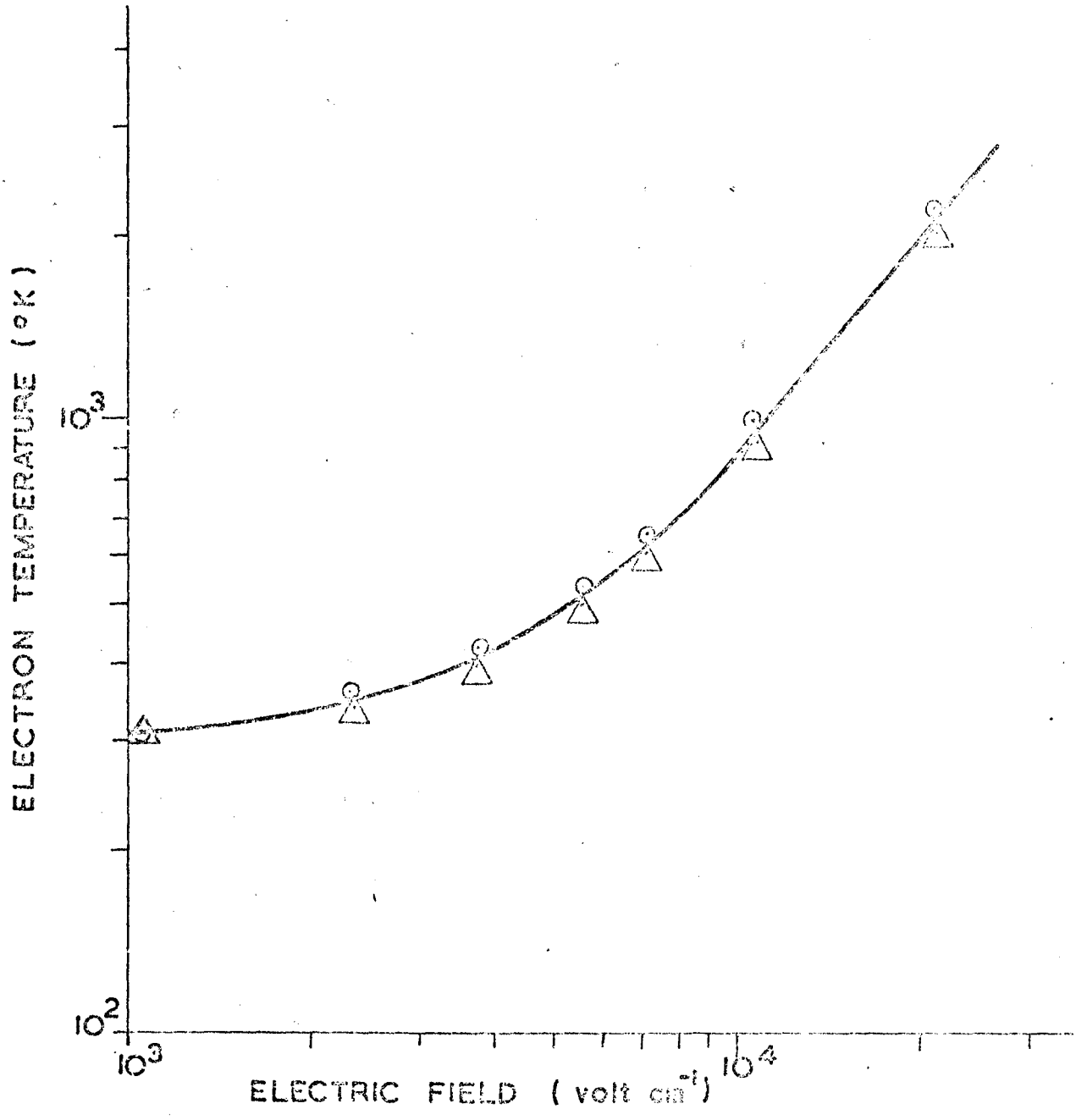
ELECTRON TEMPERATURE (°K)
10^3
10^2
10^3
10^4
ELECTRIC FIELD (volt cm^{-1})

Diag. 3.5

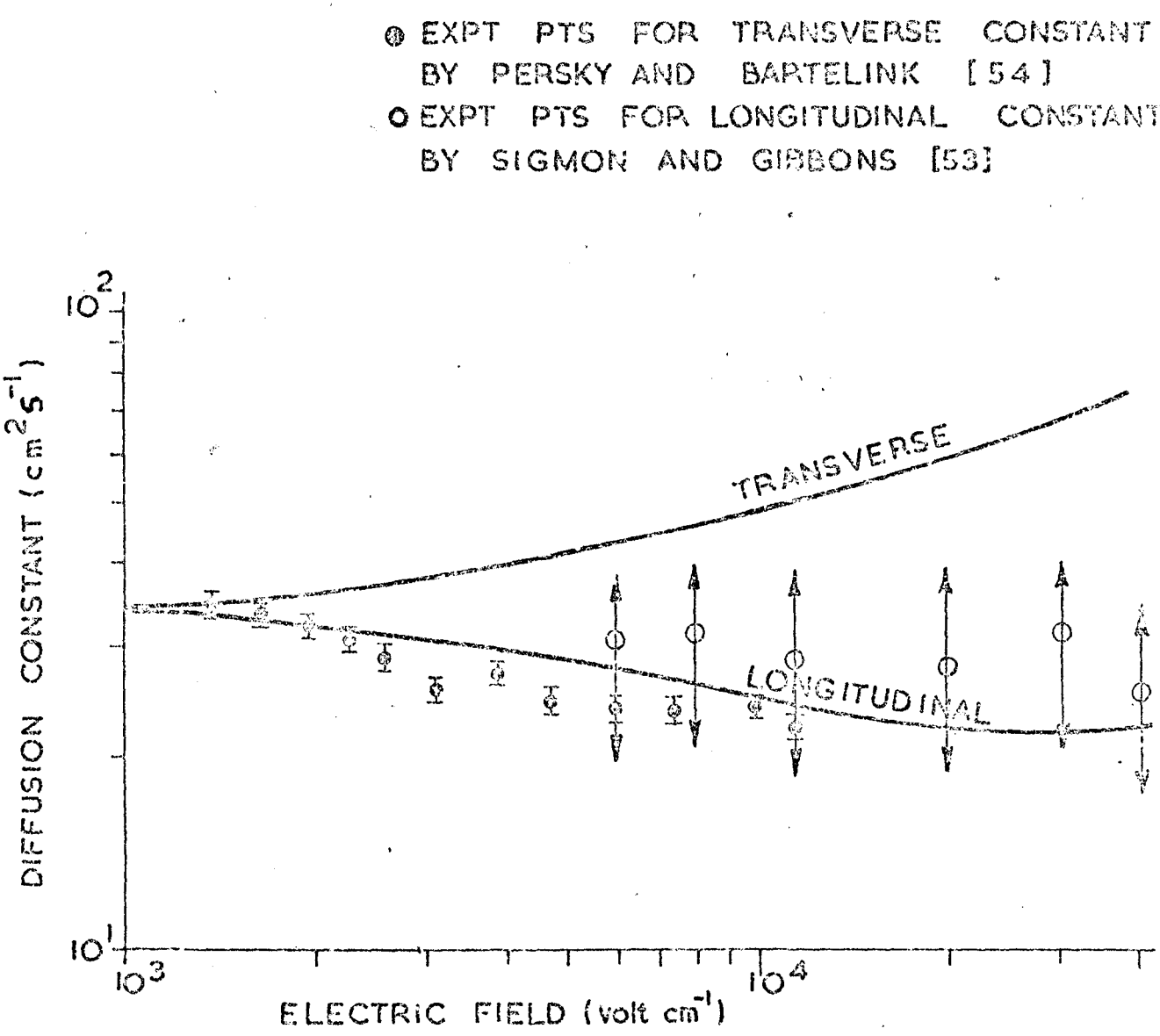
⊕ EXPT PTS FOR TRANSVERSE CONSTANT BY PERSKY AND BARTELINK [54]
O EXPT PTS FOR LONGITUDINAL CONSTANT BY SIGMON AND GIBBONS [53]
DIFFUSION CONSTANT ($cm^2 s^{-1}$)
10^2
10^1
TRANSVERSE
LONGITUDINAL
10^3
10^4
ELECTRIC FIELD (volt cm^{-1})

Diag. 3.6

Chapter 4 Gunn Domain Dynamics

§ 4.1 Introduction - the Gunn Effect

In 1963, Gunn [58] was first to observe microwave current oscillations in homogeneous samples of gallium arsenide and indium phosphide, when these were subjected to high electric fields. This effect, which is now named after its discoverer, was soon understood to be the result of the periodic recirculation of a narrow region of high field, the high field domain, through the samples [59. 60]. The high field domains are the resultant form of an electron instability that owes its origin to the existence of a negative slope in the velocity-field characteritic over a range of values of the electric field. In chapter 2 we have described in some detail for the case of gallium arsenide how this negative slope arises from the transfer of electrons from the central valley of low effective mass to the satellite valley of high effective mass. Even before the discovery of the Gunn Effect, Ridley and Watkins [61] and Hilsum [62] have independently put forward the idea that this mechanism would lead to a negative differential conductivity. The experiments of Hutson et al [63] later confirmed that intervalley transfer was indeed the relevant physical effect in producing the negative differential conductivity in the Gunn Effect.

The propagation properties of Gunn domains, i.e. their nucleation, the final shape and velocity, have been studied theoretically by many authors. The approach that is generally adopted is a phenomenological one in which the spatially- and time-dependent electric field and space-charge density are assumed to be governed by a set of differential equations referred to as the basic or constituitive equations, and no attempt is made to evaluate the time- and spatially-dependent electron distribution. (In chapter 2 we have given some idea of how

complicated this task is even when a homogeneous steady state is prevalent). By making various assumptions concerning the relaxation mechanisms that control the behaviour of the distribution function, the approximate interaction of the electrons with the spatially- and time-dependent electric field is obtained in terms of the basic equations. (In the 'diffusion' model [64] for instance, the electron distribution function is assumed to relax very much faster than the rate of change of the local instantaneous field, and the velocity of the electrons is consequently given by the steady state velocity field characteristic for a value of the field corresponding to the local instantaneous field. The basic equations then reduce essentially to Poisson's equation and the equation of continuity of total current.) In § 4.2 we shall give a brief description of the three formulations of Gunn domain dynamics that have been studied to date. They are the diffusion model [64], the energy transport model of McCumber and Chynoweth [65], and the intervalley model of Szekely and Tarnay [66].

Given a set of basic equations, an analysis in the small signal regime may be made to establish some criteria for instability [64, 65]. The role of the dynamic differential conductivity in the formation of an instability is immediately apparent from the small signal analysis. In general, the time dependence of a small space-charge disturbance to the steady state is found to be controlled by a differential dielectric relaxation time $\tau_D = \epsilon\epsilon_0/en_0(dv/dF)$ where ϵ is the dielectric constant, n_0 the doping density and $v = v(F)$ is the steady state velocity characteristic [64]. When $\tau_D < 0$, as is the case when the steady state electric field is biased into the region of negative differential conductivity, then the disturbance will grow with the characteristic time τ_D in the absence of diffusion or relaxation mechanisms which prevent the electron system from following the steady state velocity characteristic and modify the value of the characteristic time.

Finally, the instability criterion is expressed in terms of a critical value for the product $n_o l$, where l is the length of the sample, which must be greatly exceeded if domains are to nucleate. Theoretical estimates of the critical product ($\sim 5 \times 10^{11}$ cm^{-2} [64]) have been confirmed by experiment [67, 68]. To obtain the ultimate (large signal) form of the instability, the basic equations will generally need to be solved numerically. Kroemer [69] showed by a computor simulation method that it is necessary to include microscopic doping inhomogeneities for domains to nucleate. The fully formed domains are found to travel with constant shape and velocity in agreement with experiments.[59, 60]

The existing models have been successful in predicting the general features of domain propagation but the formulation can be criticised on several counts which we shall describe in detail in § 4.2. The three models we have cited have been formulated very much on an ad hoc basis and are not in all cases consistent with the Boltzmann equation. We wish to show that the moment balance equations we have described in chapter 1 may be used, after some modification, as basic equations for the Gunn Effect. The effects of diffusion, intervalley scattering and energy transport can then be studied systematically and consistently. In § 4.3 we shall describe the reformulation of the intervalley and energy transport models from the moment balance equations. These equations are solved by a simulation technique which we shall describe in §4.4. We are concerned primarily with the ultimate form of the domains and the discussion will be confined to gallium arsenide in which the transport processes are the best understood.

§ 4.2 Models for Gunn Domain Dynamics

The diffusion model which is the most successful formulation of Gunn domain dynamics to date has been analysed very fully by several authors [70, 71, 72, 73, 19]. The results are described in a review article by Butcher [64] so we shall therefore give only a brief account of the model here. In this formulation the relaxation mechanisms governing the behaviour of the distribution function are assumed to be sufficiently fast for the average electron velocity to follow the steady state velocity characteristic as the field varies. The spatial dependence of the electron density is allowed for by including a diffusion term with an average field-dependent diffusion coefficient in the current density. In this way, the properties of the instability are determined entirely by the steady state velocity characteristic and the field dependent diffusion coefficient. (Hence the diffusion model.) The basic equations consist then of Poisson's equation and the equation of conservation of electrons. It is convenient to rewrite the latter as the continuity equation for total current so we have:

$$\frac{\partial F}{\partial x} = \frac{e}{\epsilon \epsilon_o} (n - n_o) \qquad (4.1)$$

$$I(t) = e n v(F) - e \frac{\partial}{\partial x} [D(F)\, n] + \epsilon \epsilon_o \frac{\partial F}{\partial t} \qquad (4.2)$$

where the electron density n and the field F are functions of x and t, n_o is the doping density which is a constant, and the total current I is independent of x. We have adopted the convention that the electron carries a positive charge.

To calculate the ultimate form attained by an instability, one assumes a priori the existence of a uniformly propagating solution to equations (4.1) and (4.2) which depends on the single variable $y = x - v_D t$

To calculate the ultimate form attained by an instability, one assumes a priori the existence of a uniformly propagating solution to equations (4.1) and (4.2) which depends on the single variable $y = x - v_D t$ only, where v_D is the velocity of propagation of the domain. Moreover, the shape of the domain is to be such that the field F_R outside the domain is a constant so that the total current density is a constant given by $I = en_o v_R$, where $v_R = v(F_R)$. From (4.1) and (4.2) it is possible then to obtain a single ordinary differential equation in F and y:

$$\frac{d}{dy}\left[n D(F)\right] = n\left[v(F) - v_D\right] - n_o(v_R - v_D) \qquad (4.3)$$

where $$n = n_o + \frac{\epsilon \epsilon_o}{e} \frac{dF}{dy} \qquad (4.3a)$$

Equation (4.3) may be solved by numerical integration to obtain the domain profile. For a given F_R however, only a single value of v_D (to be determined by successive approximation) will yield a solution of the desired form, so equation (4.3) is essentially an eigenvalue equation. This method of solution of the basic equations is referred to as the invariant domain theory or calculation.

Certain simplifications in the analysis of (4.3) can be achieved if the diffusion term in (4.2) were written in a modified form. Firstly, the diffusion coefficient may be assumed to be a constant [71] and secondly, the field-dependent coefficient may be written to the left of the differentiation sign in (4.2) [72, 73]. In both cases one obtains the analytical result that $v_D = v_R$. Moreover, the peak domain field F_D is given respectively by the relations:

$$\int_{F_R}^{F_D} \left[v(F) - v_R\right] dF = 0 \qquad (4.4a)$$

$$\text{and} \int_{F_R}^{F_D} [v(F) - v_R] D^{-1}(F)\, dF = 0 \qquad (4.4b)$$

In general, without the modifications to the diffusion term we find that $v_D > v_R$ from the numerical solution of equation (4.3). The details of the calculation will be discussed in a later section. We note that in the diffusion model the only information required concerning the behaviour of the electron system can be expressed in terms of a velocity field characteristic v(F) and a field-dependent diffusion coefficient D(F). To carry out a calculation, experimental or theoretical data may be used, giving the model a great deal of flexibility.

The basic assumption concerning the rapidity of the relaxation rates in the diffusion model is not strictly valid. In particular the relative populations in the central and satellite valleys, and the average energy of the electrons will generally be unable to follow their respective steady state characteristics so the electron system as a whole will not follow the velocity characteristic as the field varies. To allow for these two effects two models have been proposed: the energy transport model of McCumber and Chynoweth [65] and the intervalley model of Szekely and Tarnay [66]. However, by attempting to keep the analysis simple, drastic assumptions have been made in both these models so the results are not expected to be very realistic. We shall give an account of these formulations merely for the purpose of illustrating the concepts of intervalley relaxation and energy transport.

In the intervalley model [66], the electron densities in the central and satellite valleys (labelled by the subscripts 1 and 2) are allowed to vary independently. The basic equations for F, n_1 and n_2 consist then of Poisson's equation (4.1) and the continuity equations for the two types of electrons. When diffusion is neglected in the current densities, the continuity equations in the frame moving with the domain velocity v_D take the form:

$$-\frac{d}{dy}\left[n_i(\mu_i F - v_D)\right] - \frac{n_i}{\tau_{ij}} + \frac{n_j}{\tau_{ji}} = 0 \qquad (4.5)$$

where i = 1, 2 . j = 2 when i = 1 etc., and $y = x - v_D t$. In (4.5), the mobilities μ_1 and μ_2 and the satellite-to-central valley relaxation time τ_{21} are assumed to be constants, while the central-to-satellite valley relaxation time τ_{12} is assumed to be a function of field given by the equation:

$$\tau_{12}(F) = \tau_{21}\frac{v(F) - \mu_2 F}{\mu_1 F - v(F)} \qquad (4.6)$$

where v(F) is the steady state velocity characteristic. Equation (4.6) is obtained by eliminating the steady state fractional population p_1^s and p_2^s from the expression $v(F) = (p_1^s \mu_1 + p_2^s \mu_2)F$ using the result $p_1^s/\tau_{12}(F) = p_2^s/\tau_{21}$ (and $p_1^s + p_2^s = 1$). A theoretical calculation for the steady state is necessary to determine p_1^s and p_2^s. Tarnay and Szekely have used the steady state determined by McCumber and Chynoweth [65] and assumed a value of $\tau_{21} = 2 \times 10^{-12}$ sec. (We shall show that the steady state calculation is in fact invalid.)

The intervalley model as described above is inadequate in many ways. In the hot electron regime the mobilities, especially that of the central valley, are hardly expected to be constants although τ_{21} does remain fairly constant since its value is largely controlled by the energy gap between the central and satellite valleys and is consequently insensitive to the electron distribution function in the satellite valley. The neglect of diffusion is a more serious approximation still , since the spatial variation of electron density is large in a domain. In view of these approximations we shall not discuss the results of the model in detail. The main feature to note is that the dynamic velocity characteristic followed by the electrons as a result of the finite intervalley relaxation times is indeed different from the steady state velocity character-

istic. In constrast to the diffusion model, the domain velocity v_D is smaller than the outside electron velocity v_R, and the shape of the domains are wider by comparison.

In the formulation of the basic equations by McCumber and Chynoweth [65], the electron distribution over the entire conduction band (i.e. the central and satellite valleys) is assumed to be thermalised to a single Maxwell-Boltzmann distribution at a temperature T which varies with position and time as the field varies. The fractional population in the satellite vallys p_2 is given by:

$$p_2(T) = \frac{\exp(-\Delta/k_BT)}{1 + \alpha \exp(-\Delta/k_BT)} \quad (\alpha + 1 + \frac{\Delta}{k_BT}) \qquad (4.7)$$

where α is the ratio of the density states in the satellite valleys to that in the central valley and Δ is the energy gap between the valleys. The average mobility μ amd the diffusion coefficient D can then be expressed as functions of T according to:

$$\mu(T) = p_1 \mu_1 + p_2 \mu_2 \qquad (4.8)$$

and

$$D(T) = \mu(T)\, k_BT/e \qquad (4.9)$$

where the mobilities μ_1 and μ_2 are again assumed to be constants. The basic equations consist then of equations (4.1) and (4.2), where in (4.2) v(F) and D(F) are replaced by $\mu(T)F$ and D(T) respectively, and an energy transport equation:

$$\frac{\partial E}{\partial t} = -\frac{\partial}{\partial x}(EJ) + eFJ - \frac{3}{2} k_B \frac{T - T_o}{\tau_T} \qquad (4.10)$$

where

$$E = \frac{3}{2} k_BT + \frac{\alpha \Delta \exp(-\Delta/k_Bt)}{1 + \alpha \exp(-\Delta/k_BT)}$$

and $J = \mu(T)F - n^{-1} \partial[D(T)n]/\partial x$ is the average electron velocity when diffusion is allowed for, T_o is the lattice temperature and τ_T is an energy relaxation time. Note that in these basic equations, the steady state velocity characteristic is contained implicitly in the numerical values assigned to μ_1, μ_2, Δ, α and τ_T. To obtain the

Steady state characterisitic, the spatial- and time- derivatives in (4.2) and (4.10) may be set to zero and the resultant equation solved for the T - F characteristic which will in turn yield the velocity-field characteristic from (4.8) and $v(F) = \mu(T)F$. McCumber and Chynoweth have carried out their calculations using the parameter values

$$\mu_1 = 5000 \text{ cm}^2 \text{ V}^{-1} \text{sec}^{-1}, \quad \mu_2 = 100 \text{ cm}^2 \text{ V}^{-1} \text{ sec}^{-1},$$

$$\Delta = 0.35\text{eV}, \qquad \alpha = 60$$

and $\tau_T = 2 \times 10^{-12}$ sec.

Hasty et al. [80] has carried out a similar study including a thermal conductivity term in (4.10).

The important feature in this formulation of the basic equations is that the average mobility and diffusion coefficient are more correctly regarded as functions of the electron temperature rather than field, and that the behaviour of the electron temperature is described by an energy transport equation. The assumption that the entire electron distribution thermalises to a single Maxwell-Boltzmann distribution is however a serious drawback of the model. It requires a very strong coupling between the electrons in the two types of valleys, when in reality, the coupling is weak and the two distribution functions are better approximated as two independent quantities. In fact, the steady state velocity characteristic obtained from the basic equations is in poor agreement with experiment. For this reason we shall not discuss further the results nor the other sources of criticism in the formulation such as the form of the energy transport equation (4.10) itself.

From the brief description of these three models for Gunn dynamics it is clear that the important effects that a successful model must account for are diffusion, intervalley scattering

and energy transport. These effects cannot be treated in isolation because they are comparable in magnitude, and are moreover mutually interacting. For instance, one cannot treat energy transport in a consistent fashion without having first established a framework in which the electron populations in the two types of valleys are allowed to vary independently, as in the intervalley model. In the next section we shall use the moment balance equations as a starting point in a reformulation of the basic equations. Starting from what is essentially the intervalley model, we include diffusion and variation of the mobility in the particle currents for each of the valleys. Energy transport equations can then be included for each of the two types of electrons.

§ 4.3. Basic Equations in the Moment Balance Formalism

We shall attempt firstly to reformulate the intervalley model without neglecting diffusion and the variation of mobility. The model will be referred to as the intervalley model for the sake of continuity although it now accounts for diffusion also. (Similarly in our formulation of the 'energy transport' model, diffusion and intervalley effects will be included.) We start with the moment balance equations (1.5) for $\varphi = 1$ and v_x, the component of $\underline{v}$ in the direction of the field:

$$\frac{\partial n_i}{\partial t} = -\frac{\partial}{\partial x}(n_i v_i) - \frac{n_i}{\tau_{ij}} + \frac{n_j}{\tau_{ji}} \tag{4.11}$$

$$\frac{\partial}{\partial t}(n_i v_i) = -\frac{\partial}{\partial x}\left[n_i(k T_i/m_i + v_i^2)\right] + n_i\left(\frac{eF}{m_i} - \frac{v_i}{\tau_{pi}}\right) \tag{4.12}$$

where we have written $\langle v_x^2 \rangle_i = k_B T_i/m_i + v_i^2$

$G_{ii}(1) = -G_{ji}(1) = -\tau_{ij}^{-1}$, $G_{ii}(v_x) = -v_i/\tau_{pi}$ and $G_{ij}(v_x) = 0$.

The relaxation times τ_{ij}, τ_{pi} are functionals of the electron distribution function f_i. Since the time and spatial variation of the distribution function will be assumed to be adequately represented by the variations of the moments contained in equations (4.11) and (4.12) in accordance with the general philosophy of the moment balance method (c.f. chapter 1), we may therefore express the relaxation times as functions of n_i, v_i and T_i in general. We shall ignore energy transport for the time being and try instead to form a close set of basic equations from (4.11) and (4.12) for i = 1 and 2, and Poisson's equation.

The moments of the distribution functions involved in these equations are n_i, v_i and T_i for i = 1 and 2, so including the field there are seven variables and only five equations. It is therefore necessary that we make some a priori assumption regarding the relxation mechanisms in order to remove two of the variables. Since we are not concerned with energy transport, the most consistent (or rather least inconsistent) assumption that we can make under the circumstances is that the characteristic time for energy relaxation is much shorter than the intervalley relaxation times and the characteristic time representing the rate of change of the field. We can then put $T_i = T_i(F)$, the steady state characteristic for the electron temperature. The relaxation times τ_{ij} and τ_{pi} are then functions of the field also since their values are more sensitive to T_i than v_i, and should be independent of n_i.

The assumption that we have made implies that some kind of 'quasi-equilibrium' is achieved between the local instantaneous field and the distribution functions of the two valleys taken separately i.e. the normalised distribution function in each valley is the same as that for a homogeneous steady state for a value of the electric field equal to the local instantaneous field. This

situation can be achieved (1) when the coupling between the valleys is weak, which is automatically implied when we say that the energy relaxation times are much shorter than the intervalley relaxation times and (2) when the characteristic time representing the rate of change of the local instantaneous field is long compared to the energy relaxation time. Condition (1) we have assumed a priori and we shall not, and in fact cannot, fully justify. The intervalley relaxation times are $\sim 10^{-12}$ sec and energy relaxation times (if they can be defined) are only slightly shorter. Condition (2) may be tested however, if for the sake of argument, we assume that the energy relaxation time is say, as short as the momentum relaxation time which (from the mobility) is of the order $\sim 5 \times 10^{-14}$ sec for $F > 3$kV/cm. The requirement then that the field changes slowly compared to the momentum relaxation time is equivalent to the inequality

$$\frac{\partial F}{\partial x}\,\frac{\lambda}{F} \ll 1$$

where λ is the mean free patch of the electrons given by $\lambda = \tau_{p_1} v_1 = e\tau_{p_1}^2 F/m_1$. Using Poisson's equation this can be written as:

$$n_o\left(1 - \frac{n_1+n_2}{n_o}\right) \ll 1.5 \times 10^{23}\ m^{-3} \qquad (4.13)$$

For 1Ω cm material where $n_o \sim 10^{21}\ m^{-3}$, the 'quasi-equilibrium' approximation is therefore good in the depletion layer of domains where $(n_1 + n_2)/n_o \lesssim 10^{-2}$ and at small and moderately large accumulation layers where $(n_1 + n_2)/n_o \lesssim 10$ [64].

Equation (4.12) as it stands can be simplified further because the momentum relaxation times are short in comparison with the intervalley relaxation times, and the time scale involved in the change of the electric field, subject to the conditions imposed in the previous paragraph. From (4.12) we have

$$j_i = n_i v_i = n_i \mu_i F - \tau_{pi}\left[\frac{\partial}{\partial x} n_i (k_B T_i + v_i^2) + \frac{\partial n_i v_i}{\partial t}\right] \qquad (4.12a)$$

where the mobility μ_i is given by $\tau_{pi}(F)e/m_i$ and using (4.11) the terms in the square brackets may be expanded to give

$$\frac{n_i v_i}{\tau_{ji}}\left(\frac{n_j}{n_i} - \frac{n_j}{n_i}\bigg|_F\right) + \frac{\partial}{\partial x}\left(\frac{n_i k_B T_i}{m_i}\right) + n_i\left(v_i \frac{\partial v_i}{\partial x} + \frac{\partial v_i}{\partial t}\right)$$

where $(n_j/n_i)|_F = \tau_{ji}(F)/\tau_{ij}(F)$ is the ratio n_j/n_i for a steady homogeneous field F. Since τ_{pi} is small $v_i \sim v_i(F) = \mu_i(F)F$ and v_i may be replaced by $v_i(F)$ in the square brackets. Equation (4.12a) then gives, after some rearrangement:

$$j_i = n_i \mu_i F - \left[n_i \mu_i F \frac{\tau_{pi}}{\tau_{ji}}\left(\frac{n_j}{n_i} - \frac{n_j}{n_i} F\right) + \frac{\mu_i}{e} \frac{\partial n_i k_B T_i}{\partial x} + \frac{\tau_{pi}}{\tau_{Di}} \frac{\varepsilon\varepsilon_o}{e}\left(v_i \frac{\partial F}{\partial x} + \frac{\partial F}{\partial t}\right)\right] \qquad (4.14)$$

where

$$\tau_{Di} = \left[\frac{n_i e}{\varepsilon\varepsilon_o} \frac{dv_i}{dF}\right]^{-1}$$

is the dielectric relaxation time for the electrons in valley i, and is a measure of the characteristic time associated with $\partial/\partial t$ and $v_i \partial/\partial x$. Thus for small momentum relaxation times, the electron current j_i is a function of n_i and F which is to be expected. The terms in the square brackets of (4.14) can be interpreted as corrections to the electron current(given for a homogeneous situation) arising respectively from the finite intervalley relaxation time and the sonsequent departure from equilibrium of the population ratio, the inhomogeneity of electron density (diffusion) and the spatial- and time-dependence of the electric field. Note that the diffusion term which has been derived from the Boltzmann equation is neither of the form $D_i \partial n_i/\partial x$ nor $\partial(n_i D_i)/\partial x$, as assumed in previous theories.

The equations of continuity of electron density for the two valleys (4.11) in which the current is given by (4.15) and Poisson's equation (4.1) form then the basic equations in our formulation of the intervalley model. The data required by the equations are the steady state values of μ_1, μ_2, τ_{12}, τ_{21}, T_1 and T_2 as expressed as functions of the electric field. It is a good approximation to treat τ_{21} as a constant (see 4.2) and write $\tau_{12}(F)$ as $\tau_{21} \times (n_1/n_2)_F$. The steady state velocity characteristic is then contained in the data for μ_1, μ_2 and $(n_1/n_2)_F$. The solution of the basic equations is given in the next section. It is found that the electron currents are adequately described (to within 5%) by

$$j_i = n_i \mu_i F - \frac{\mu_i}{e} \frac{\partial n_i k_B T}{\partial x} \qquad (4.14a)$$

when $\tau_{21} = 1 \times 10^{-12}$ sec and $n_o = 8 \times 10^{14}$ cm^{-1} (which ensure that τ_{pi} is never greater than a few per cent of τ_{ij} or τ_{Di}. We shall use this shortened form of the current density for the energy transport model.

To include energy transport, we take the moment balance equation for $\varphi = E(= m_i v^2/2)$ for each of the valleys:

$$\frac{\partial}{\partial t} n_i\left(\frac{3}{2} k_B T + \frac{m_i v_i^2}{2}\right) = -\frac{\partial}{\partial x} j_i\left(\frac{5}{2} k_B T - \frac{m_i v_i^2}{2}\right) + e j_i F - n_i W_i = n_j U_j \qquad (4.15)$$

where we have written $\langle v_y^2 \rangle = \langle v_z^2 \rangle = k_B T_i/m_i) = \langle (v_x - v_i)^2 \rangle_i)$, $\langle (v_x - v_i)^3 \rangle = 0$, $G_{ii}(E) = -W_i$, and $G_{ij}(E) = U_j$. The assumptions we have made regarding the moments are exactly correct for a displaced Maxwellian but should be a good approximation for the general case.

Putting the third order to zero implies that there is no electron thermal conductivity [75]. We neglect this effect because the coefficient cannot be estimated with any certainty and would involve a third order moment in any case. These approximations enable one to avoid introducing new variables into the equations when the energy transport equations are included. The energy loss due to scattering processes originating in valley i, W_i, and the energy gain due to scattering processes originating from valley j, U_j, are respectively functions of T_i and T_j and cannot in general be expressed in the form involving a constant relaxation time (except for U_2 which is $\sim \{\Delta + 3/2\ k\ T_2\} \tau_{21}^{-1}$). Since $m_i v_i^2/2$ is typically a few per cent of $k_\beta T_i$, it may be omitted from (4.15) The energy transport equation derived from the Boltzmann equation differs therefore from that of McCumber and Chynoweth (4.10) in many respects. These differences arise primarily from the decoupling of the two types of electrons. If (4.15) for the two valleys were added together, then using the continuity

equations (4.11), the resultant equation may be reduced to (4.10), except for the form of the lattice energy loss term. The basic equations consist then of the two energy transport equations (4.15), the two continuity equations (4.11) and Poisson's equation for the variables F, n_1, n_2, T_1 and T_2. In these equations, the relaxation times τ_{ij} and the mobilities μ_i are to be expressed as functions T_i. (We have used the abbreviated equations (4.14a) for the electron currents.)

The data required by the energy transport model are the values of μ_i, τ_{ij}, W_i and U_i expressed as functions of T_i for i = 1 and 2. In § 2.6 we have described how these functions can be derived from the Monte Carlo solution of the steady state Boltzmann equation. The justification of this procedure can be stated in two ways. In the first one assumes that the distribution function can be characterised very closely by its average energy and that the mobility, the relaxation times and energy loss rates are insensitive to the exact shape of the distribution. We have pointed out in § 2.6 the inadequacy of this supposition for the central valley where an energy threshold exists for intervalley scattering i.e. the mobility etc. must depend on factors such as the number of electrons with energy above and below the threshold, the average energy of these two groups of carriers etc. - information which cannot be derived from knowledge of the average energy of the entire distribution alone. To avoid this difficulty we can however state the problem in another way. The values of the mobilities, relaxation times and energy loss rates we have chosen satisfy the steady state equations, i.e. at a temperature T, provided the shape of the distribution function is identical to the steady state distribution of the same temperature, then the values of the mobilities etc. are exactly correct. In the time- and spatially-dependent situtation, the distribution function will not have the same shape as the steady state distribution so that given

the average energy (or T) we really do not know what the relaxation times etc. ought to be. The problem then is to decide if it is a good approximation to assume that the shape of the distribution function is close to that of the steady state. Since one is not prepared to evaluate the non-equilibrium distribution, such questions will have to remain unanswered although it must be of some consequence that in a situation where spatial inhomogeneities and time-dependences are small, then the basic equations will give the correct asymptotic behaviour of the electron system. We shall therefore proceed to the solution of the basic equations without further justification for the approximations made. Note that the information required by the basic equations we have described, such as rates of energy loss to the lattice, are not always measurable experimentally so one has to rely completely on theoretical estimates.

§ 4.4. Gunn Domain Simulation

The basic equations derived in the previous section for the intervalley and energy transport models cannot be conveniently solved using the invariant domain method. If the partial differential equations were reduced to ordinary differential equations by the transformation $y = x - v_D t$, a large number of boundary conditions (for the values of each variable and its first derivative, at least, at large distances from the domain) are required. Since these cannot be chosen accurately in general, the integration of the equations becomes unreliable when the number of variables increases. Moreover, the nature of an eigenvalue problem requires many trial integrations while the value of v_D is being ascertained by successive approximations. As the equations become more complex, the amount of effort required is increased, until the simulation method of solution, itself a large computational project, becomes a viable alternative. The advantages of the simulation method over the invariant

domain calculation are that it does not assume a priori the existence of a uniformly propagating domain, and that all stages of the simulation, from nucleation to uniform propagation (if the latter is achieved) are of physical relevance, unlike the wasteful trial integrations in the eigenvalue problem.

In the mathematical simulation of the propagation of Gunn Domains, a sample of gallium arsenide of length l is divided into equal elements of width Δx. We shall write $X_i^m(t)$ to denote the average value of the variable X_i, where X_i for i = 1...3(5), are the spatially and time-dependent variables contained in the basic equations, [F, n_1 and $v_2(T_1$ and $T_2)$] in the m^{th} element of the sample, at the instant of time t. If Δx is sufficiently small, then the average values of the derivatives of $X_i(t)$ w.r.t. x in the m^{th} element may be expressed approximately in terms of the $X_i^{m'}(t)$'s using finite differences in the central difference scheme. It is convenient then to rewrite the basic equations in the form:

$$\frac{\partial X_i^m}{\partial t} \simeq K_i^m(X_1^1 .. X_1^{m'} ..; X_2^1 .. X_2^{m'} ..; \text{etc}) = K_i^m(t) \quad (4.16)$$

i.e. the rate of change of $X_i^m(t)$ w.r.t. is a function $K_i^m(t)$ of the spatial distributions $X_j^{m'}(t)$ of all the variables X_j at time t. This can be done easily enough for $X_i = n_1$, n_2, T_1 and T_2, but to obtain the time derivative of F, it is necessary to replace Poisson's equation by the total current continuity equation which may be written as:

$$\epsilon\epsilon_0 \frac{\partial F}{\partial t} = - e(j_1 + j_2) + I(t) \quad (4.17)$$

That equation (4.17) is equivalent to Poisson's equation (4.1) can be shown by differentiating (4.17) w.r.t. x and using the continuity equations (4.11) subsequently. The time-dependent total current I(t) is determined by external conditions e.g. if a constant voltage (V) is applied across

the sample, then integrating (4.17) over the length of the sample gives:

$$I(t) = e \int (j_1 + j_2)\, dx \,/l \qquad (4.18)$$

The integration in (4.18) may be replaced by a summation over m so the right-hand side of (4.17) is a function of the $X_i^m(t)$'s only.

Having obtained the basic equations in the form (4.16) one can then simulate the time-dependent behaviour of the variables $X_i(x_1 t)$ at the various points $m\Delta x$ along the sample. If at some time t, the spatial distributions X_i^m's are known, then at a time $t + \Delta t$, we have:

$$X_i^m(t + \Delta t) \simeq X_i^m(t) + \Delta t\ K_i^m(t) \qquad (4.19)$$

The finite difference equations (4.16) and (4.19) are valid if $(X_i^{m+1} - X_i^{m-1}/X_i^m) \ll 1$ and $K_i^m(t)\ \Delta t \ll X_i^m(t)$ i.e. these inequalities are satisfied if $\Delta x \ll$ the size of the domain and $\Delta t \ll$ the smallest relevant relaxation time viz. the intervalley relaxation time or the time scale for energy relaxation. The values of Δx and Δt can then be chosen subject to one further condition: $\Delta x/\Delta t \gg v_1, v_2$ (4.20) which arises from the fact that it is only meaningful to speak of the average value of a variable X_i in an element of width Δx, if in the time Δt, an electron does not travel through a large fraction of the length Δx. In practice, for a domain of length 10μm, and intervalley relaxation time $\sim 1 \times 10^{-12}$ sec, and $v_1 < 2 \times 10^5$ m sec^{-1}, we have used $\Delta x = 0.1\mu m$ and $\Delta t = 2 \times 10^{-14}$ sec. To test that Δx and Δt are sufficiently small, typical simulations may be repeated, halving the step-sizes, to ensure that no noticeable changes in the results occur.

To initiate the nucleation of a domain, it is necessary to introduce a doping inhomogeneity into the sample [64]. This can be done by the re-introduction of Poisson's equation in place of the continuity equation for n_2 i.e.

$$n_2 = (n_0 - n_1) - (\epsilon\epsilon_0/e)\, \partial F/\partial X \qquad (4.1a)$$

where $n_o = n_o(X)$ is a function of x. To obtain the maximum efficiency for nucleation $n_o(x)$ is chosen to be a notch $\sim 1\mu$ wide with a minimum of ~ 0.9 the average value of n_o, situated a few microns away from the anode (in the convention where the electronic charge is positive).

When a domain has travelled across the entire sample, it will not necessarily have attained its maximum growth, if the samples are short ($<100\mu m$). Since we are primarily concerned with the shape and velocity of the full-grown domain, using the value of the outside field as a parameter, we have introduced into the computer programme several departures from 'real' simulation. Firstly, the ends of the samples are joined up so we can study the domain behaviour for periods exceeding the transit time, and secondly, the notch may be removed after the domain has moved away from it, so the field outside the domain can achieve a constant value everywhere. The simulation in this sense is purely mathematical and is to be regarded simply as a method of solving the basic equations.

In the comparison of the various models, small domains are of a particular interest since if any departure of the domain velocity v_D from the outside velocity v_R is to occur, then it is most apparent for small domains. To obtain small domains, starting from nucleation, one must have as short a sample as possible and the average electric field must be biased close to, and exceeding, the threshold field when the slope of the velocity characteristic becomes negative. This procedure is not always satisfactory because the sample length cannot be reduced to values much shorter than $\sim 12\mu m$. A more efficient way to obtain small domains is to decrease the voltage across the sample when a fully grown domain has developed. After a period corresponding to about ten times the differential dielectric relaxation time t_D (evaluated at the maximum negative slope), the domain will readjust to the new voltage and propagate uniformly.

§ 4.5. Results and Discussion

We have carried out simulations for the intervalley and energy transport models as well as the diffusion model where the results can be tested against those of the invariant domain calculations. Throughout the velocity characteristic and other relevant data were taken directly or derived from the Monte Carlo steady state calculation of Broadman, Fawcett and Swain [4]. We have restricted the calculations to a doping density n_o of 8.1×10^{20} m^{-3} which corresponds roughly to 1 Ω cm material. This value of n_o corresponds roughly to the upper limit allowed by equation (4.13) which ensures that the momentum relaxation times are short compared to the rate of change of the electric field. Since the rate of change of the electric field and hence also the time required for nucleation are approximately proportional to n_o, it has proved uneconomical in terms of computer time to carry out simulations at lower doping densities. Moreover, it is when the field is changing most rapidly that one expects the effects of the various relaxation mechanisms to be most apparent so we have used the quoted value for n_o.

The results of the simulation agree well with those of the invariant domain calculation for the diffusion model in the few test cases we have made. The values of the domain potential, velocity and peak field provide a direct basis for comparison and the overall shape of the domains from the two calculations are compared graphically. In the former cases agreement to within 0.2% is achieved. This indicates that the invariant domain hypothesis is valid, at least for the diffusion model, and that the numerical accuracy of the simulation calculation is good, although one should expect a deterioration as the basic equivalent becomes more complex.

In the intervalley model, the value of the intervalley relaxation time τ_{21} may be varied as a parameter in the input data. While the generally held value of τ_{21} is 2×10^{-12} sec

[21, 66, 74], using the data of the steady state Monte Carlo calculation of Broadman et al. [4], one obtains an estimate that is nearer to 5×10^{-13} sec because the revised value of the intervalley deformation potential field D_{12} (see table II, chapter 2) is approximately half that used in the earlier calculations ($\tau_{21}^{-1} \propto D_{12}^{2}$). We have used values of 2×10^{-12}, 1×10^{-12} and 5×10^{-13} in our calculations. In all cases, the domains were found to propagate uniformly (in terms of the domain potential, velocity and peak field) to within 0.2% for $\tau_{21} = 2 \times 10^{-12}$ sec, and 0.8% for $\tau_{21} = 5 \times 10^{-13}$ sec.

We show in diagram 4.1, curves B, the shape of the domains for $\tau_{21} = 2 \times 10^{-12}$. The values of the outside field are indicated in the diagram. We see that the domains are more symmetrical than those obtained for the diffusion (curves A) and enegy transport (curves C) models. We shall compare the results of the various models in detail a little later. By decreasing the intervalley relaxation times the domains become narrower and less symmetrical, as illustrated by diagram 4.2(a) where the domain profiles of two domains with approximately the same outside field for $\tau_{21} = 2 \times 10^{-12}$ sec and 5×10^{-13} sec are shown. This confirms previous results indicating that finite intervalley relaxation times produce a similar effect as diffusion [21, 66]. In diagrams 4.2(b) and 4.2(c) we show respectively the fractional population in the satellite valley (dashed lines) plotted as a function of the domain field for the two cases shown in diag. 4.2(a). The two parts of the dashed curve correspond to the two branches of the domain field where the field respectively rises and falls. The qualitative behaviour of the curves is very much to be expected. Taking a given point in the sample, during the time when the field is rising, n_2/n is less than the value predicted by the steady state characteristic (full line) and when the field is falling the reverse situation occurs. The area enclosed by the two parts of the curve measures the effect of the intervalley relaxation time, and is smaller for the lower value of τ_{21}. Note also that for

$\tau_{21} = 2 \times 10^{-12}$ sec, even during the period when the field is momentarily stationary (near the peak field) the dynamic and steady state curves do not coalesce.

The domain potentials and velocities are plotted against the value of the outside field in diagrams (4.4) and (4.5) respectively. For a given outside field the domain potentials for the three values of τ_{21} are very similar and we show the results for $\tau_{21} = 2 \times 10^{-12}$ sec. It is worthy of note that as τ_{21} is decreased the potential curves (not shown) are shifted very slightly to the left-hand side so there appears to be no tendency for the results of the intervalley model to approach those of the diffusion model. If the curves for the two models should coincide at all for the limit $\tau_{21} \to 0$, it is thus unclear how small τ_{21} needs to be. Physically, one does not expect τ_{21} to be smaller than the lowest value used in the calculation. The domain velocities for the intervalley model are found to be lower than the outside velocity. For a given outside field, the domain velocity is lowest for the largest value of τ_{21}. Again, there appears to be a qualitative difference between the intervalley and diffusion models.

Results for the energy transport model are shown as points rather than continuous curves because only a few points have been obtained. The increase in the number of variables in the basic equations causes the computer time to increase to barely tolerable limits, (a full run from nucleation takes 150 mins on an ICT 4130 computer as opposed to 80 mins for the intervalley model) so only a few selected points are calculated. Again, uniformly propagating domains, to about 0.5% are obtained.

The effect of energy transport is shown in diagram 3.4(a) where the electron energy (or temperature) of the central valley is plotted against the domain field. In the branch where the field is rising, the dynamic curve (dashed lines) behaves very much as one would expect, i.e. the electron temperature is lower than the steady state characteristic (full curve) since energy relaxation takes a finite time. In the branch where the field is falling, an 'unexpected' behaviour is observed where the electron energy rises initially as the field falls and then decreases rapidly

to a value below the steady state characteristic. This behaviour can be attributed to the large density gradients in the accumulation layer, which coincides with this region of decreasing field in the domain. Ahead of the point of maximum accumulation the density gradient drives a diffusion current that increases the value of j_1 and hence the input of energy from the field to the electron system, and establishes furthermore a gradient in the energy flux ($\frac{5}{2} j_1 k_\beta T_1$) that tends to produce heating in that region. At the trailing edge, the reverse occurs and rapid cooling takes place. These energy balance conditions must ultimately account for the reduction in the width of the accumulation layer going from the intervalley model to the energy transport model. We see in diagram 3.4(b) how the dynamic behaviour of the fractional populations reflects closely that of the central valley mean energy. Thus energy balance appear to enhance the average mobility difference between electrons in the leading and trailing edges of the accumulation layer, leading to a reduced layer width.

For a given outside field the domain potential (domain size) given by the energy transport model is very close to that given by the intervalley model (diag. 4.4) although the domain shape (curves C in diag. 4.1) are very different . The resemblance of the domain shapes between the energy transport and diffusion models (curves A in diag. 4.1) is a little misleading in that for a given outside field, the domain sizes given by the two models are very different (see domain potential curves diag. 4.4). The domain velocities are found to be equal to the outside velocity (to within the 0.5% uncertainty in the former) in this model. This corresponds to complete depletion since from the total current continuity, we have

$$
\begin{aligned}
I(t) &= e(j_1 + j_2) + (\epsilon\epsilon_o)^{-1}\frac{\partial F}{\partial t} \\
&= e(j_1 + j_2) - ev_D(n_1 + n_2 - n_o) \\
&= e n_o v_R \qquad \text{outside domain} \\
&= e n_o v_D \qquad \text{at minimum depletion for nearly complete depletion.}
\end{aligned}
$$

(In going from line 1 to 2 we have substituted $\partial/\partial t$ by $-v_D \partial/\partial x$ for an invariant domain, and used Poisson's equation for $\partial F/\partial x$.)
In the energy transport model, the extent of depletion is of the order of 99.9% for the smallest domains obtained, while for domains of comparable size, the intervalley and diffusion models give maximum depletion of ~ 95%.

Comparison between the three models shows that as far as domain sizes (potentials) are concerned, the intervalley and energy transport models give very similar values for a given outside field. Diag. 4.4 appears to indicate that the difference between the diffusion model and the other two models is large, but under experimental conditions, this difference is more difficult to detect. For a given voltage V and sample length l we have

$$V = \varphi + F_R l$$

from the definition of the domain potential so that φ may be determined from the intersection of the domain potential curve and a 'load' line that intersects the voltage axis at V and the field axis at V/l in diag. 4.4 for V = 35 volts and l = 100 μm giving V/l = 3.5 kVcm^{-1} (= threshold field for instability) the domain potentials given by the various models does not in fact differ greatly (see diagram 4.4).

Extrapolating the experimental results of Kuru et al. [77] to 1Ω cm material shows that the domain potential curve is nearly vertical at ~ 1.3 kV cm^{-1} which is close to the value given by the diffusion model. (The results for the diffusion model given in diagram 4.4 is not the same as that given by Butcher et al. [19] because the steady state velocity characteristic v(F) and the diffusion coefficient D(F) used are not the same, the latter being the values calculated for displaced Maxwellian distribution functions. Previous comparisons between theory and experiments were based on the results of [19]).

The comparison with experiment is however inconclusive since the velocity characteristics of real samples at high doping densities are not equal to the theoretical curve calculated for low impurity. Allowing for the lower values of v_R in impure samples, if one plots φ against v_R, the experimental results can be 'made' to give better agreement with the intervalley and energy relaxation models than the diffusion model. This is very much a bootstrap procedure and we shall not try to give it justification.

It is also difficult to test the models from measurements of the domain velocity. Experimental observations are made on domains with potentials of at least 40 volts where the values of v_D predicted by all the models are close to the outside velocity v_R.

Gunn, [78], has found that domain shapes are very nearly symmetrical with accumulation layer widths that are nearly ten times wider that those given by the diffusion model, but in agreement with the intervalley model.

The evidence we have presented from both the theoretical and experimental points of view are inconclusive. Theoretically, the diffusion model has been shown to be invalid and the intervalley and energy transport models ought to give successively better approximations to reality. We have pointed out the gross approximations involved in the energy transport model which may well explain its inadequacy though under the circumstances it was the best one can do. Increasing the number of transport equations would in principle give a better account of the variation of the electron distribution under inhomogenous and time-dependent situations. One would however run up against the problem of computing time. The transport equations as they stand may on the other hand be quite adequate, if only one could account for the change in the velocity characteristic etc. with doping density in real samples. This is an area that is yet unexplored. Bott and Hilsum [79] have investigated the change in the velocity characteristic with sample resistivity on a purely

empirical basis. One would need really a detailed analysis giving the effect of impurity scattering on all the relevant moments of the distribution function.

Thus on the theoretical side, two lines of further investigation may be pursued. As for experiments, as always, further measurements are required. Results of domain measurments should be accompanied with the low field properties (giving doping density and mobility) of the samples in order that comparison with theory may be made unambiguously. Further, in taking measurements, a priori assumptions concerning domain shapes should be avoided as much as possible (e.g. the domain potentials of Kuru et al. [77] were derived from indirect measurements on the basis that the accumulation layers are much narrower than the depletion layers.)

CAPTION TO DIAGRAMS

4.1 Domain profile in GaAs derived from the diffusion model (A), the intervalley model (B) and the energy transport model (C) for a doping density of 8×10^{16} cm^{-3} which corresponds to 1 Ω cm material. The outside fields are indicated by figures and the direction of propagation is from left to right. The curves (B) are obtained for an intervalley relaxation time $\tau_{21} = 2 \times 10^{-12}$ sec.

4.2 (a) Domain profiles for $\tau_{21} = 2 \times 10^{-12}$ sec (full line) and 5×10^{-13} sec (dashed line) from the intervalley model. The outside field for the domains are respectively 1.26 and 1.25 kV/cm and the domain potentials φ, 6.02 and 5.88 volts.

4.2 (b) and (c) The typical fractional population in the satellite valleys in a domain given by the intervalley model plotted as a function of the local instantaneous field (dashed lines). The arrows indicate the direction of the change of the field and the solid line is the steady state characteristic. The domains in 4.2 (b) and 4.2 (c) correspond to thos displayed in 4.2 (a).

4.3 (a) The typical dynamic electron temperature in the central valley given by the energy transport model is plotted as a function of the local instantaneous field (dashed lines). The arrows indicate the direction of change of the field and the full line is the steady state characteristic.

4.3 (b) The dynamic fractional population in the satellite valleys corresponding to the domain in 4.3 (a) is plotted as a function of the local instantaneous field. Note that the curve closely reflects the behaviour of the temperature in the central valley in the previous diagram.

4.4 Domain potentials given by the diffusion, intervalley and energy transport models are plotted as a function of the field outside the domain.

4.5 Domain velocities given by the diffusion, intervalley and energy transport models are plotted as a function of the outside field. The full line is the outside field velocity.

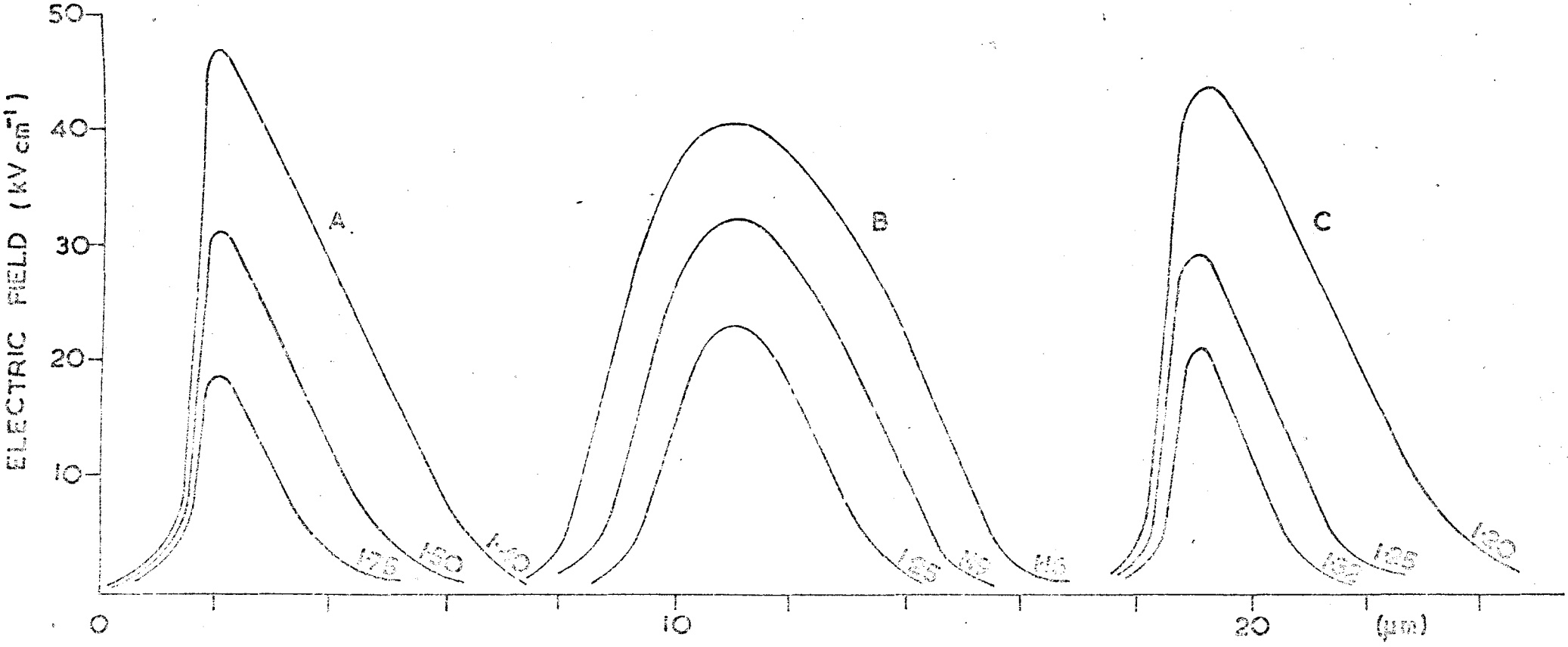
ELECTRIC FIELD (kV cm⁻¹)
50
40
30
20
10
0
10
20
(μm)
A
B
C
175
150
125
175
150
125
150
125

Diag. 4.1

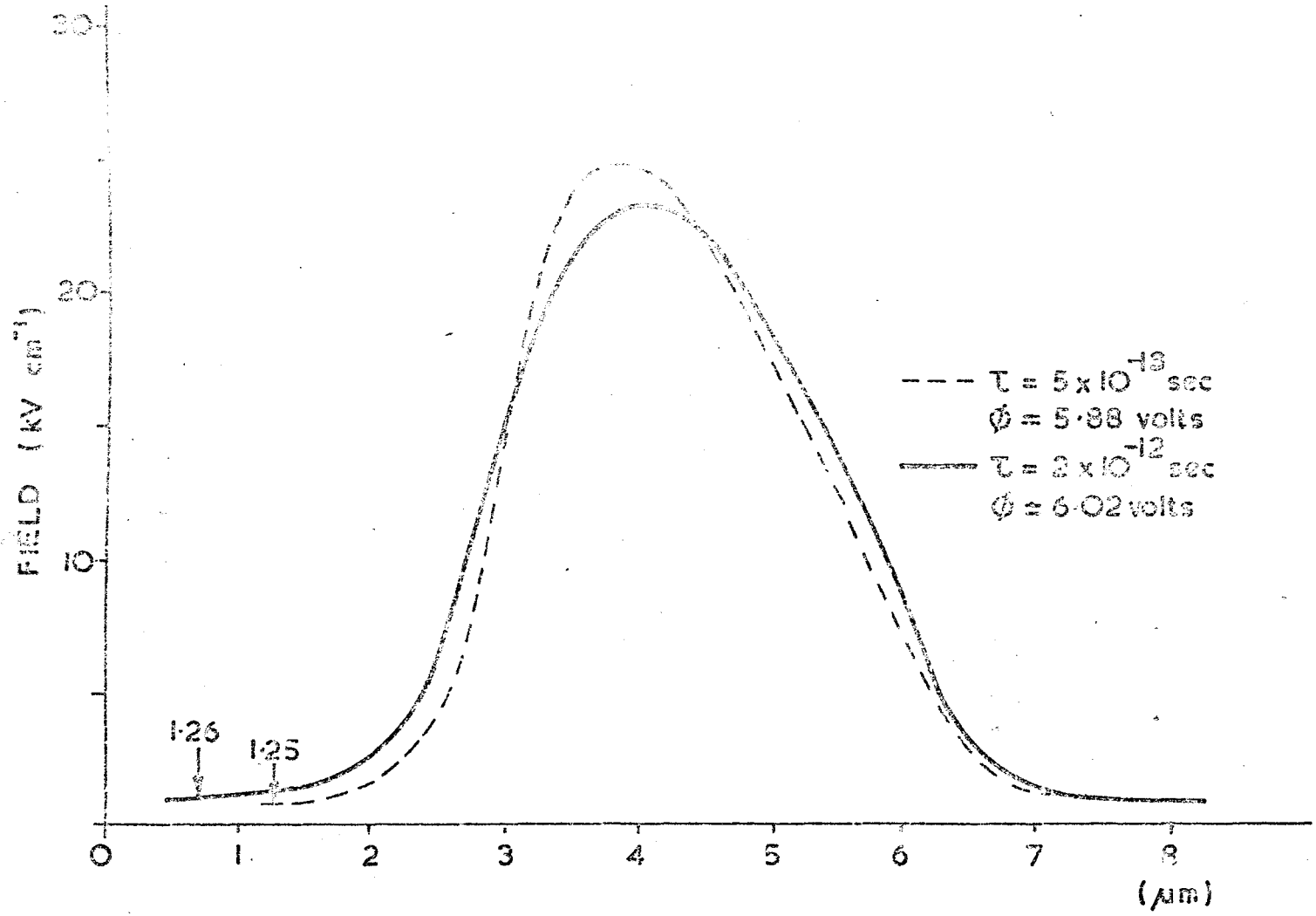
FIELD (kV cm⁻¹)
30
20
10
0
1
2
3
4
5
6
7
8
(μm)
1·26
1·25
τ = 5 x 10⁻¹³ sec
ϕ = 5·38 volts
τ = 2 x 10⁻¹² sec
ϕ = 6·02 volts

Diag. 4.2.(a).

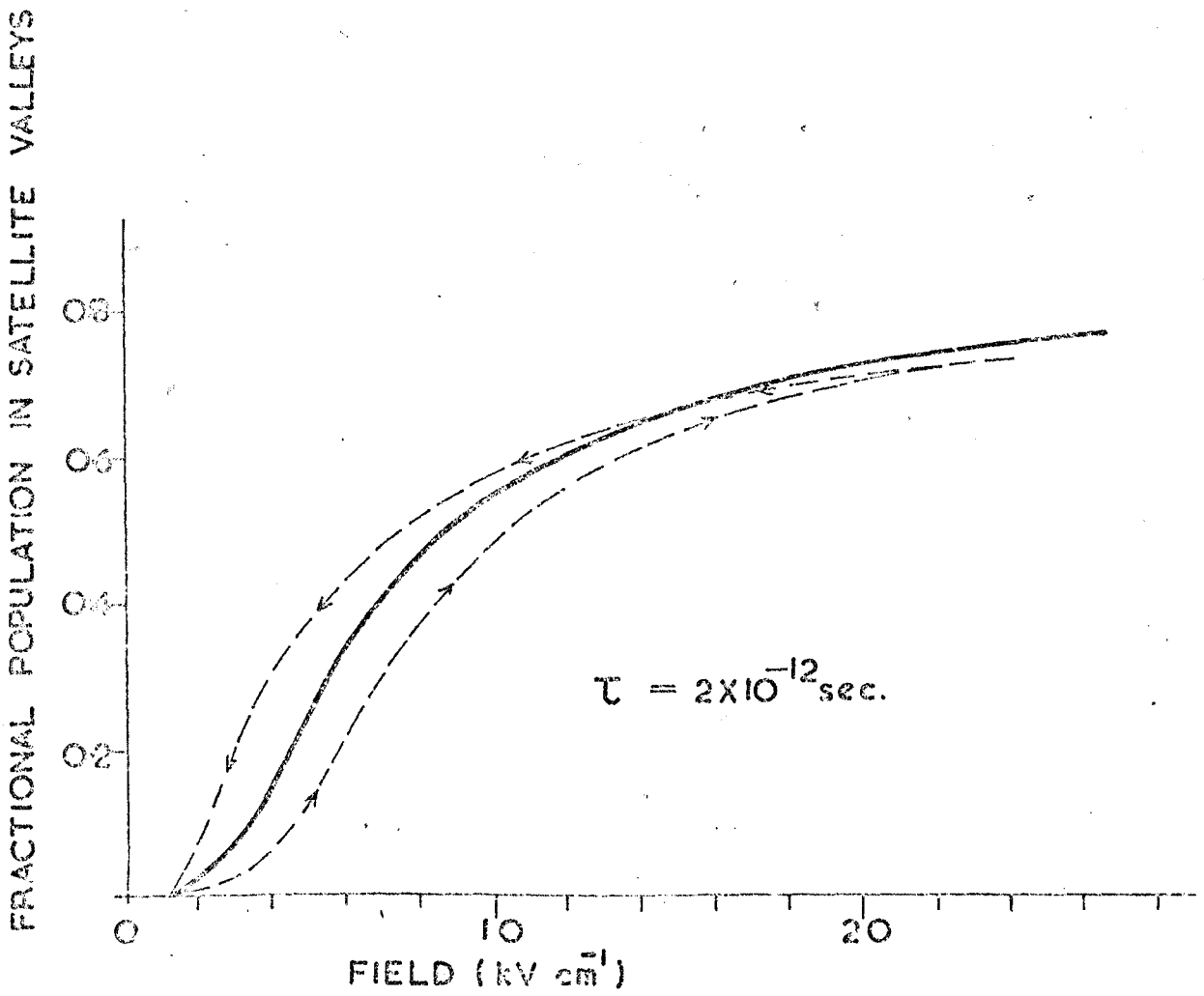
FRACTIONAL POPULATION IN SATELLITE VALLEYS
0·8
0·6
0·4
0·2
0
10
20
FIELD (kV cm⁻¹)
τ = 2X10⁻¹² sec.

Diag. 4.2(b)

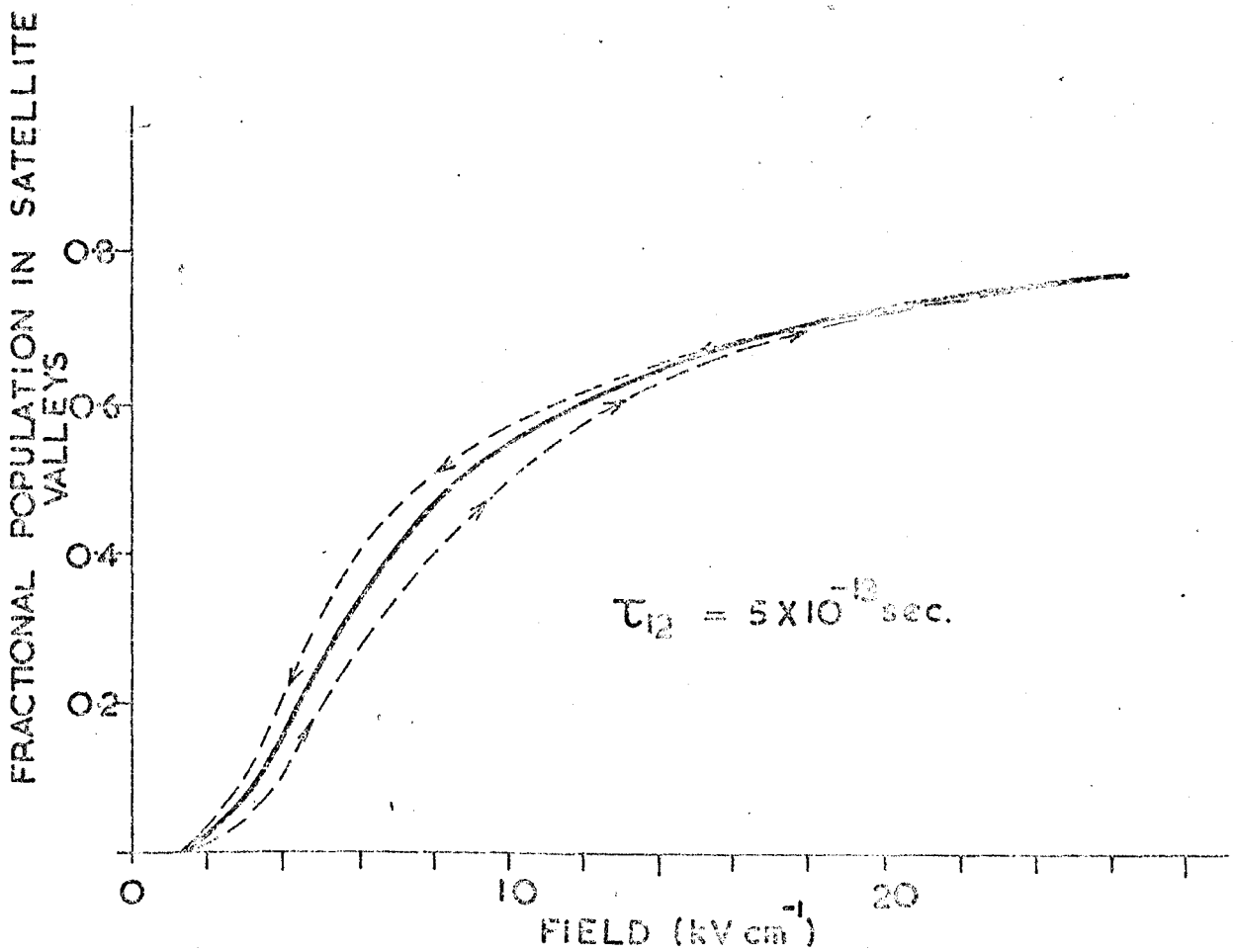
FRACTIONAL POPULATION IN SATELLITE VALLEYS
0·8
0·6
0·4
0·2
0
10
20
FIELD (kV cm⁻¹)
$\tau_{12} = 5 \times 10^{-12}$ sec.

Diag. 4.2 (c)

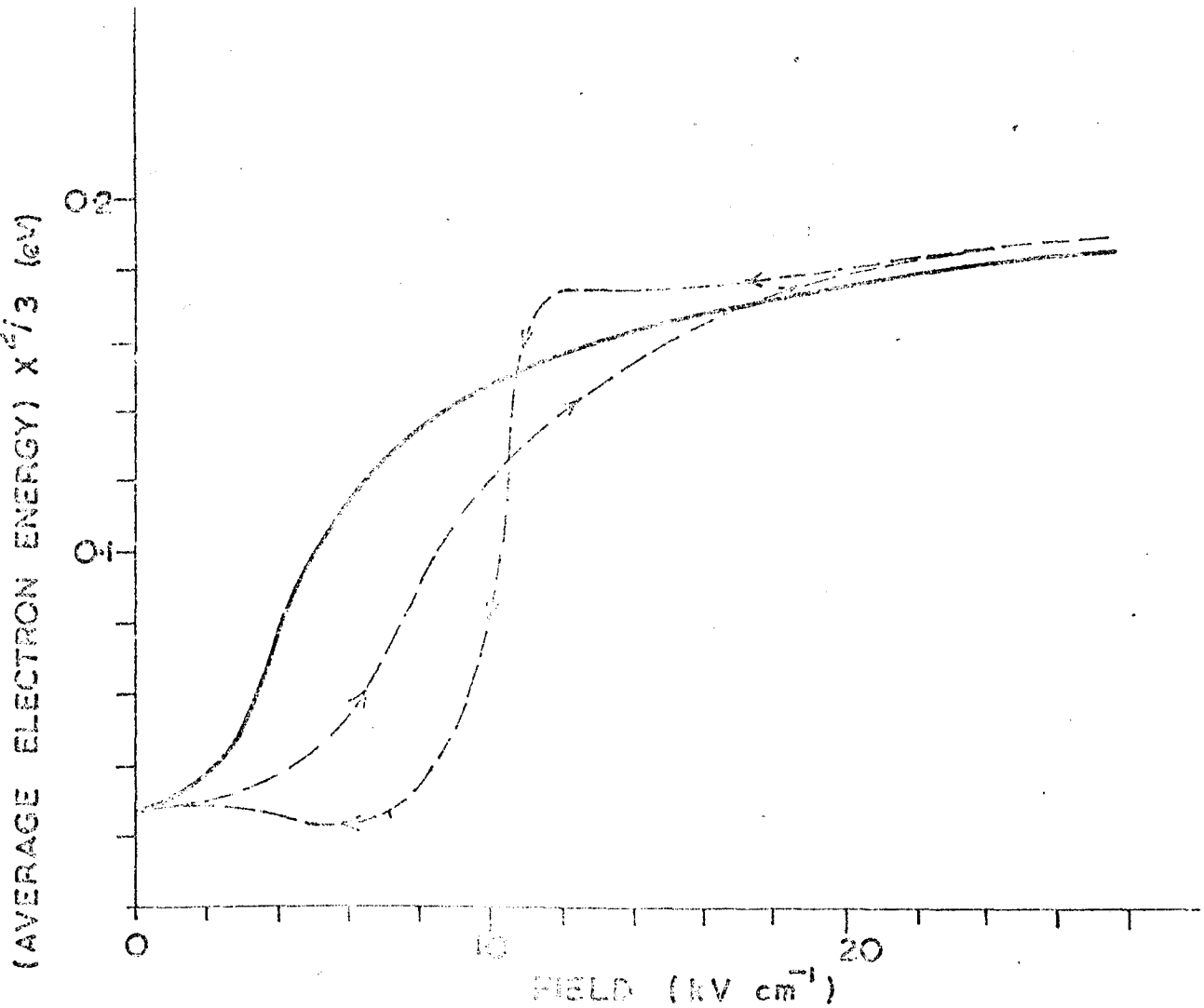

Diag. 4.3(a)

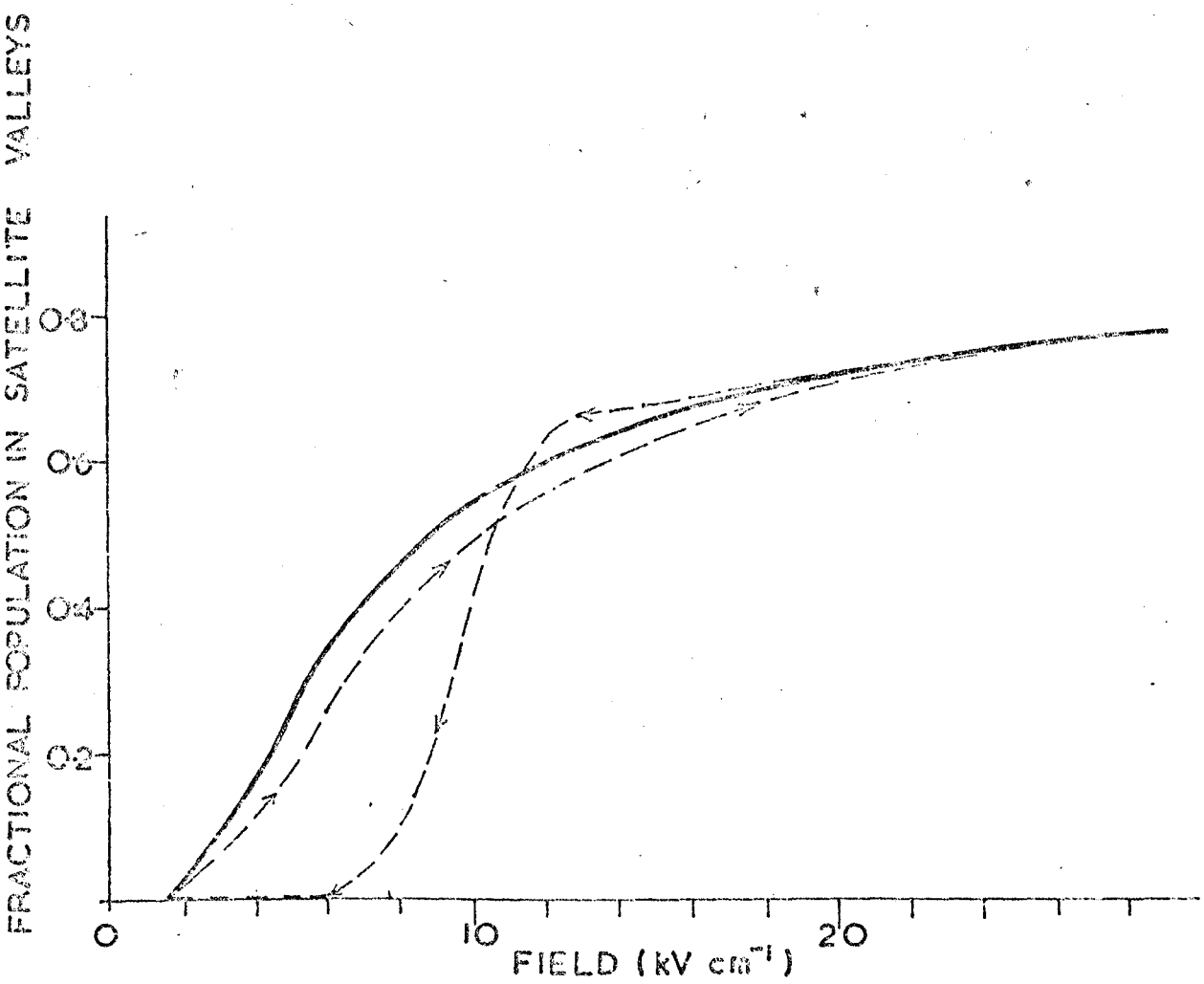
FRACTIONAL POPULATION IN SATELLITE VALLEYS
0·8
0·6
0·4
0·2
0
10
20
FIELD (kV cm⁻¹)

Diag. 4.3 (b)

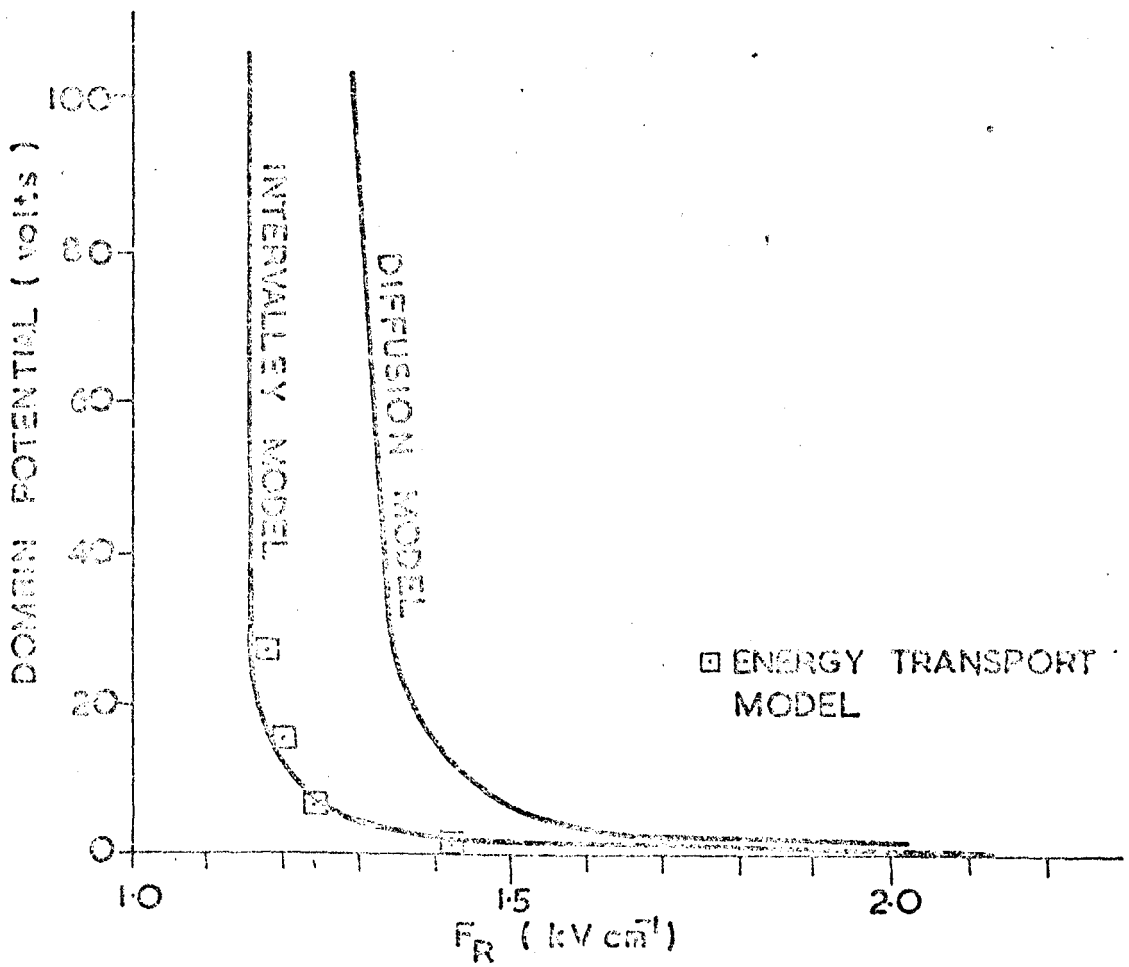
DOMAIN POTENTIAL (volts)
100
80
60
40
20
0
1·0
1·5
2·0
F_R (kV cm^{-1})
INTERVALLEY MODEL
DIFFUSION MODEL
ENERGY TRANSPORT MODEL

Diag. 4.4

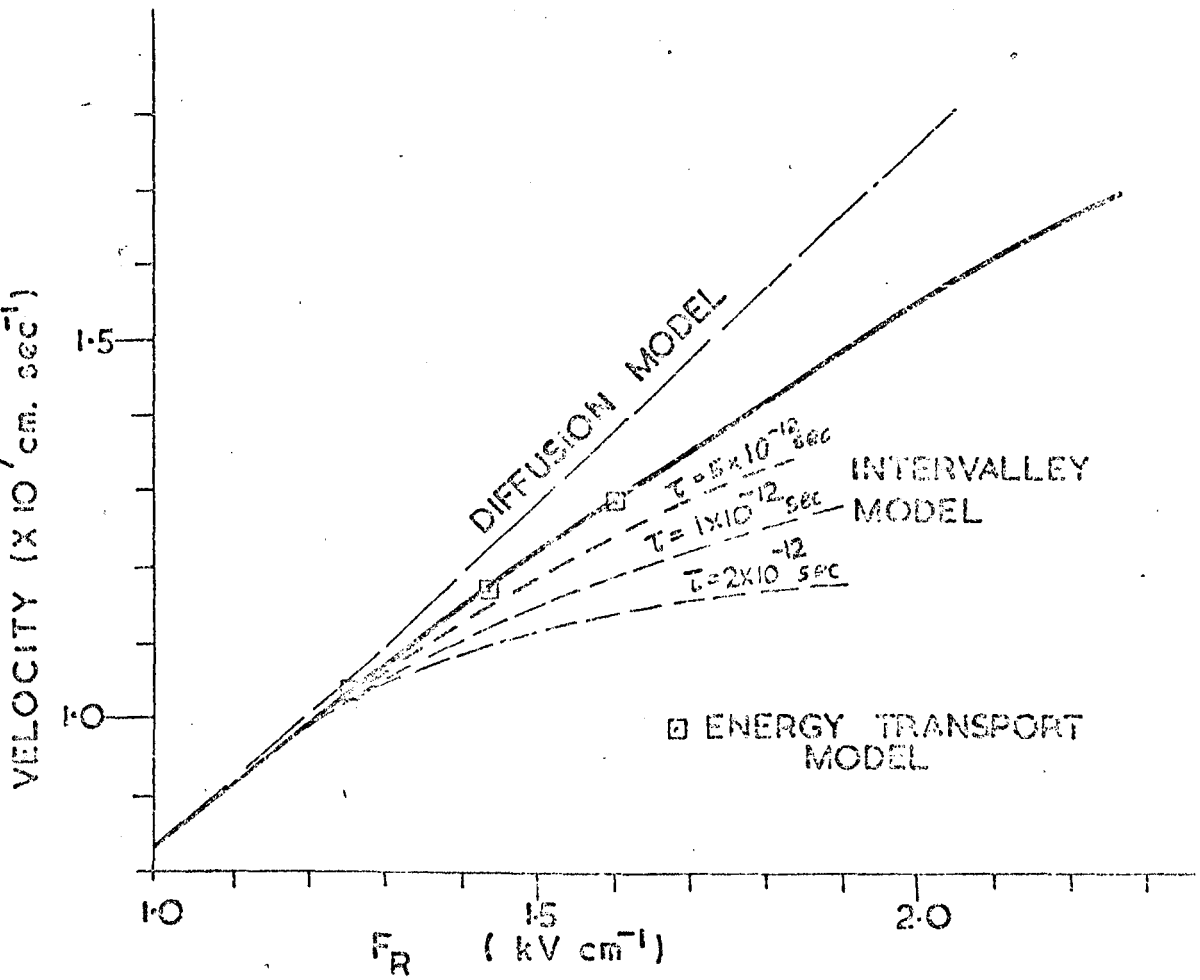
VELOCITY (X 10^7 cm. sec^-1)
1·5
1·0
DIFFUSION MODEL
τ = 5×10^-13 sec
τ = 1×10^-12 sec
τ = 2×10^-12 sec
INTERVALLEY MODEL
ENERGY TRANSPORT MODEL
1·0
1·5
2·0
F_R (kV cm^-1)

Diag. 4.5

Conclusion

In this thesis we have attempted to formulate closed sets of transport equations that are applicable to mildly and strongly inhomogeneous and time-dependent situations, starting from the Boltzmann equation. We have adopted the moment balance method, which is a well-tried approximate method for solving the steady-state, homogeneous Boltzmann equation, and extended the formalism to produce a theory for electronic diffusion in semiconductors, and basic equations for the Gunn Effect. These applications are respectively in the small and large signal regimes, and follow a phenomenological, macroscopic approach in which only the gross features of the electron distribution function, the low order moments, are regarded as being important in determining the response of the electron system to spatially- and time-dependent electric fields and density gradients.

The success of the formalism hinges largely on one's ability to find a parameterised distribution function that will closely approximate the real distribution function. While a better fit can usually be obtained by increasing the number of parameters in the distribution (or independent moments in the balance equations), the corresponding increase in the number of moment balance equations required renders it impractical to consider moments very much beyond those corresponding to the components of momentum and energy. In all cases we have restricted the calculations to include moments of the first and second order only. This was found to be satisfactory in the case of diffusion in silicon but not for gallium arsenide, the reason being that a threshold energy exists in the latter for intervalley scattering which causes the distribution function to change abruptly at this energy.

Given the number of parameters to be included, the choice of suitable parameterised distribution functions is governed chiefly by the requirement that the parameters must be related in a simple way to the moments of distribution. We have found displaced Maxwellians (or variants of the same) to be the most convenient forms when moments upt to second order are considered. In appendix I we have outlined a possible extension of this same basic distribution to include higher order moments through Hermite polynomials. Other lines of attack are possible and may form the bases of further research. For instance information theory may prove to be a powerful method since one is dealing precisely with the problem of deciding the least biased form of a distribution function when only a small number of its moments are specified. To make use of the steady state characteristics calculated by the Monte Carlo method we have devised a simple parameterisation in terms of electron energy.

The theory of diffusion is the first 'analytical' formulation of a very basic problem in electron transport in semi-conductors. While the macroscopic approach may not in all cases give good quantitative predictions, it provides nevertheless a useful frame-work in which microscopic events can be understood. The Einstein relations which we have established for diffusion in single, isotropic valleys are a case in point. These relations are also approximately valid for a more complex system such as silicon, when the electric field is orientated in the $<111>$ -direction, and when the constant energy surfaces are transformed to spheres in $\underline{k}^*$-space. The theory as it stands may be used to evaluate the diffusion coefficients for other orientations of the electric field. In the linear region, extension of the basic ideas to describe other transport phenomena is also possible. Thermal electric power in semi-conductors is the first to come to mind. Instead of density gradients, one may treat temperature gradients as the driving force that perturbs the electron system from its steady homogeneous state. The linear response of the system to these gradients may be obtained in a

fashion analogous to the theory of diffusion.

The basic equations obtained for the Gunn Effect from the moment balance equations have provided a systematic basis to study the dynamic processes involved in domain propagation. We have been able to give a consistent and unified account of the three important non-equilibrium processes of diffusion, intervalley scattering and energy transport, all of which have an important part to play. The effects of intervalley scattering have been known for some time but the results obtained with the inclusion of energy transport are new. The effect of energy balance in the accumulation layer is to render the layer more compact and cancels out the broadening from intervalley scattering. Further experimental work is necessary to confirm the results of the new calculations.

Appendix I - The moment generation rates $G_{ij}(\varphi)$ expressed as functions of the moments Ψ_j

The moment generation rate $G_{ij}(\varphi)$ is defined by the equation:

$$G_{ij}(\varphi) = n_j^{-1} \int \varphi(\underline{k}) \left[\frac{\partial f_i(\underline{k})}{\partial t}\right]_j^s d\underline{k} \tag{1.6}$$

where $\varphi(\underline{k})$ is some homogeneous function of the components of $\underline{k}$,

$$\left[\frac{\partial}{\partial t} f_i(\underline{k})\right]_i^s = \int\left[f_i(\underline{k}') \Lambda_{ii}(\underline{k}', \underline{k}) - f_i(\underline{k}) \{\Lambda_{ii}(\underline{k}, \underline{k}') + \sum_j B_{ij}(\underline{k}, \underline{k}')\}\right] d\underline{k}' \tag{1.2a}$$

$$\left[\frac{\partial}{\partial t} f_i(\underline{k})\right]_j^s = \int f_j(\underline{k}') B_{ji}(\underline{k}', \underline{k}) \, d\underline{k}' \tag{1.2b}$$

and $\Lambda_{ii}(\underline{k}, \underline{k}')$ is the intravalley transition rate in valley i, and $B_{ij}(\underline{k}, \underline{k}')$ the intervalley transition rate from valley i to valley j, for an initial state $\underline{k}$ and a final state $\underline{k}'$. We have omitted all time and space dependence for brevity.

The problem is to express $G_{ij}(\varphi)$ in terms of the moments Ψ_j of valley i where Ψ_j is defined by

$$\Psi_j = n_j^{-1} \int \psi(\underline{k}) f_j(\underline{k}) d\underline{k} \tag{1.4}$$

and $\psi(\underline{k})$ is a homogeneous function of $\underline{k}$. From (1.6) and (1.2) it is clear that $G_{ij}(\varphi)$ is a functional of the distribution function $f_j(\underline{k})$ so that if $f_j(\underline{k})$ is expressed as a function of Ψ_j, then $G_{ij}(\varphi)$ is automatically a function of Ψ_j. Since we are dealing with the moments and the distribution function of the same valley, we shall drop the subscript j for brevity. Moreover we shall choose the set $\psi_s^{pqr} = k_x^p k_y^q k_z^r$, where $(p + q + r) = s$ as the independent set of homogeneous moment functions of order s. The corresponding moment is denoted simply by Ψ_s^{pqr}. (All the integers are ≥ 0).

Because the moments are restricted to those

which are homogeneous, an arbitrary distribution function cannot in general be reduced to a function of these moments alone. However, if $f(\underline{k})$ can be written in the form $f_x(k_x)f_y(k_y)f_z(k_z)$ then we can proceed in principle at least, by expanding each of the $f_\alpha(k_\alpha)$ in the Hermite polynomials $H_l(k_\alpha)$, i.e.

$$f(\underline{k}) = \sum_{l=0}^{\infty}\sum_{m=0}^{\infty}\sum_{n=0}^{\infty} A_{lmn}\, l^{-(k_x^2+k_y^2+k_z^2)}\, H_l(k_x)H_m(k_y)H_n(k_z) \qquad (I.1)$$

taking as many terms as are necessary. (To effect a more rapid rate of convergence, we may rewrite (I.1) in terms of the variable $k_\alpha t_\alpha$ where t_α is some suitable parameter.) To determine the coefficients A_{lmn} we simply multiply both sides of (I.1) by $H_l(k_x)H_m(k_y)H_n(k_z)$ and integrate over all $\underline{k}$. The left-hand side will give the sum $\left(\sum_{p=}\sum_{q}\sum_{r}^{s\leq l+m+n} \psi_s^{pqr} B_{lms}^{pqr}\right)$ for all p, q and r subject to the condition $s \leq l+m+n$, and where B_{lms}^{pqr} are known constants. Thus it is possible to express $f(\underline{k})$ in terms of the homogeneous moments ψ_s^{pqr} in this case.

When $f(\underline{k})$ is a function of the form $f(\underline{k}) = g(k_\alpha)h(\sqrt{k_\beta^2 + k_\gamma^2})$, as when there is a strong magnetic field in the α - direction, then it is not possible to express $f(\underline{k})$ as a function of the homogeneous moments.

Appendix II Evaluation of the moment generation rates

§ II.1. Electron-Phonon interactions

The moment generation rates are defined by the equation:

$$G_{ij}(\varphi) = n_j^{-1} \int \varphi(\underline{k}) \left[\frac{\partial f_i(\underline{k})}{\partial t} \right]_j^S d\underline{k} \qquad (1.6)$$

We shall take firstly the case i = j when (1.6) may be expanded to give (using 1.2a):

$$G_{ii}(\varphi) = n_i^{-1} \int \left[\varphi(\underline{k}') - \varphi(\underline{k}) \right] \{ \left[f_i(\underline{k}') A_{ii}(\underline{k}', \underline{k}) - f_i(\underline{k}) A_{ii}(\underline{k}, \underline{k}') \right] - \sum_{j \neq i} B_{ij}(\underline{k}, \underline{k}') f_i(\underline{k}) \} \, d\underline{k} \, d\underline{k}'$$

$$= -n_i^{-1} \int \left[\varphi(\underline{k}') - \varphi(\underline{k}) \right] \{ 2A_{ii}(\underline{k}, \underline{k}') + \sum_{j \neq i} B_{ij}(\underline{k}, \underline{k}') \} f_i(\underline{k}) d\underline{k} \, d\underline{k}'$$

where we have used the microscopic reversibility principle $A_{ii}(\underline{k}', \underline{k}) = A_{ii}(\underline{k}, \underline{k}')$ and interchanged $\underline{k}'$ and $\underline{k}$ in part of the integral. The integration over $d\underline{k}'$ does not involve the distribution function and may therefore be carried out immediately. We have then in general:

$$G_{ii}(\varphi) = n_i^{-1} \int f_i(\underline{k}) \left[G_\varphi^{ii}(\underline{k})^s + F_\varphi^{ij}(\underline{k}) \right] d\underline{k} \qquad (II.1)$$

where $F_\varphi^{ii}(\underline{k}) = \int 2 \left[\varphi(\underline{k}') - \varphi(\underline{k}) \right] A_{ii}(\underline{k}, \underline{k}') \, d\underline{k}'$ (II.2)

and $F_\varphi^{ij}(\underline{k}) = \int \left[\varphi(\underline{k}') - \varphi(\underline{k}) \right] B_{ij}(\underline{k}, \underline{k}') \, d\underline{k}'$ (II.3)

Similarly, it can be shown that for $i \neq j$

$$G_{ij}(\varphi) = n_j^{-1} \int f_j(\underline{k}) F_\varphi^{ij}(\underline{k}) \, d\underline{k} \qquad (II.4)$$

When displaced Maxwellian distribution functions are assumed, the moment functions considered are $\varphi = 1$, k_α and E. It is possible in this case to obtain F_φ^{ij} and F_φ^{ii} for all the scattering mechanisms in analytical form. In the integration over $f(\underline{k})d\underline{k}$ it is convenient to use

polar coordinates. The angular integrations can be performed analytically for isotropic scattering leaving the integral over k (or energy $E = \hbar^2 k^2/2m_i$) for numerical integration. For anisotropic scattering, the integration over the polar angle θ must also be performed numerically.

When two-temperature displaced Maxwellians are assumed, an extra moment function $E_z = \hbar^2 k_z^2/2m_i$ is included. F_φ^{ij} and F_φ^{ii} for all φ and all scattering mechanisms can again be reduced to analytical form. The integration over $f(\underline{k})d\underline{k}$ is however always a double integral (for E and θ). We shall give the explicit form of $G_{ij}(\varphi)$ for the various isotropic scattering mechanisms and for a two-temperature displaced Maxwellian in the following sub-sections. In the formulae T_i and t_i are respectively the transverse temperature T_{ti} and the ratio T_{ti}/T_{ii}. To obtain the corresponding formulae for a displaced Maxwellian it is necessary simply to write $t_i = 1$ throughout. The formulae have also been written out for an isotropic valley of mass m_i. They are approriate therefore for ellipsoidal valleys if $\underline{k}$ and m_i are replaced respectively by $\underline{k}^*$ and m_o. Note that $G_{ii}(1)$ and $G_{ij}(\varphi)$ are zero for intravalley processes.

§ II.1.1. Polar optical phonon intravalley scattering

The scattering probability $A_{ii}(\underline{k}, \underline{k}')$ for this process is given in Table II of chapter 2. After considerable manipulation using (II.2) and (II.1) we have:

$$G^o_{ii}(\underline{k}) = -\underline{k}_i \Omega^o_{ii} \int_o^\infty \exp(-E/k_\beta T_i)\, \Phi_i(E) Q(E) E dE/(k_\beta T_i)^2 \qquad \text{(II.5)}$$

$$G^o_{ii}(E) = -\hbar w_o \Omega^o_{ii} \int_o^\infty \exp(-E/k_\beta T_i)\, \Phi_i(E)\, P_o(E)\, dE/k_\beta T_i \qquad \text{(II.6)}$$

$$G^o_{ii}(E_z) = -\hbar w_o \Omega^o_{ii} \int_o^\infty \exp(-E/k_\beta T) \left[\Phi_i \tfrac{3}{4}E) P_1(E) - \chi_i(E)\{P_o - 3P_1\}\right] dE/k_\beta T_i \qquad \text{(II.7)}$$

where $\Omega^o_{ii} = \dfrac{2e^2 w_o m_i}{\hbar}\left(\dfrac{1}{\epsilon_\infty} - \dfrac{1}{\epsilon_o}\right)\left(\dfrac{t_i}{2\pi m_i k_\beta T_i}\right)^{\frac{1}{2}} \exp\left(\dfrac{\hbar^2 k_i^2 t_i}{2m_i k_\beta T_i}\right)$.

has the dimensions of a frequency, then the dimensionless quantities Q, P_o and P_1 are defined by

$$Q(E) = E^{-1}\{(N_o+1)\left[E^{\frac{1}{2}}(E-\hbar w_o)^{\frac{1}{2}} + \tfrac{1}{2}\hbar w_o\, g(E-\hbar w_o)\right] + N_o\left[E^{\frac{1}{2}}(E+\hbar w_o)^{\frac{1}{2}} - \tfrac{1}{2}\hbar w_o\, g(E)\right]\}$$

$$g(E) = \log_e\left[\frac{(E+\hbar w_o)^{\frac{1}{2}} + E^{\frac{1}{2}}}{(E+\hbar w_o)^{\frac{1}{2}} - E^{\frac{1}{2}}}\right]$$

$$P_o(E) = (N_o + 1)\, g(E-\hbar w_o) - N_o g(E)$$

$$P_1(E) = \tfrac{1}{2}(N_o+1)\left[(\tfrac{1}{2} - E/\hbar w_o)(E-\hbar w_o)^{\frac{1}{2}}E^{-\frac{1}{2}} + \hbar w_o\, g(E-\hbar w_o)/4E\right] - \tfrac{1}{2}N_o\left[(\tfrac{1}{2} + E/\hbar w_o)(E+\hbar w_o)^{\frac{1}{2}}E^{-\frac{1}{2}} - \hbar w_o\, g(E)/4E\right]$$

The integrations over the polar angle $\Phi_1\Theta_1$ and χ_1 are defined by:

$$\Theta_1(E) = \int_{-1}^{1} x \exp\left[-a_1 x^2 + b_1 x\right] dx/b_1 \qquad \text{(II.8)}$$

$$\Phi_1(E) = \tfrac{1}{2}\int_{-1}^{1} \exp\left[-a_1 x^2 + b_1 x\right] dx \qquad \text{(II.9)}$$

$$\chi_1(E) = \tfrac{1}{2}\int_{-1}^{1} x^2 \exp\left[-a_1 x^2 + b_1 x\right] dx \qquad \text{(II.10)}$$

where $a_1 = E(t_1 - 1)/k_B T_1$

$$b_1 = 2t_1 (E\hbar^2 k_1^2/2m_1)^{\frac{1}{2}}/k_B T_1$$

N.B. for $t_1 = 1$, $a_1 = 0$

$$\Theta_1 = b_1^{-3}(x \cosh b_1 - \sinh b_1)$$

$$\Phi_1 = b_1^{-1} \sinh b_1$$

§ II. 1.2. Acoustic Intravalley phonon scattering (isotropic)

The moment generation rates for acoustic phonon intravalley scattering are evaluated from the expression for $A_{ii}(\underline{k}, \underline{k}')$ in Table II of chapter 2. The approximations made in obtaining the following formulae are given in § 2.5. In brief, we write the phonon occupancy number as $k_B T_o/\hbar s K$ and neglect s, the longitudinal sound velocity in comparison with a typical electron velocity. Then we find:

$$G^a_{ii}(\underline{k}) = -\underline{k}_i (k_B T_o/2m_i s^2)\, \Omega^a_{ii} \int_o^\infty \exp(-E/k_B T_i)\, \Phi_i(E)\, E^2\, dE/(k_B T_i)^3 \qquad \text{(II.11)}$$

$$G^a_{ii}(E) = -\Omega^a_{ii} \int_o^\infty \exp(-E/k_B t_i)\, \bar{\Phi}_i(E)\, E(E-2k_B T_o)\, dE/(k_B T_i)^2 \qquad \text{(II.12)}$$

$$G^a_{ii}(E_z) = -(k_B T_o/2m_i s^2)\Omega^a_{ii} \int_o^\infty \exp(-E/k_B T)\left[\chi_i(E) - \bar{\Phi}_i(E)/3\right] E^2\, dE/(k_B T_i)^2 \qquad \text{(II.13)}$$

where $\Omega^a_{ii} = \dfrac{8m_i^3 \Xi_a^2}{\pi \hbar^4 \rho}\left(\dfrac{k_B T_i t_i}{2\pi m_i}\right)^{\frac{1}{2}} \exp\left(-\dfrac{\hbar^2 k_i^2 t_i}{2m_i k_B T_i}\right)$

has the dimensions of a frequency.

§ II.1.3 Intervalley phonon scattering

The transition probability of intervalley scattering $B_{ij}(\underline{k}, \underline{k}')$ is given in Table II of chapter 2. Using (II.1), (II.3) and (II.4) we have:

$$G_{ii}(1) = -G_{ji}(1) = -\Omega^I_{ij} \int_o^\infty \bar{\Phi}_i(E)\, H_{ij}^{(11)}(E)\, dE/(k_B T_i)^2 \qquad \text{(II.14)}$$

$$G_{ii}(\underline{k}) = -\underline{k}_i\, \Omega^I_{ij} \int_o^\infty \Phi_i(E) H_{ij}^{(31)}(E)\, dE/(k_B T_i)^3 \qquad \text{(II.15)}$$

$$G_{ij}(\underline{k}) = 0 \qquad \text{(II.16)}$$

$$G_{ii}(E) = -\Omega^I_{ij} \int_o^\infty \bar{\Phi}_i(E)\, H_{ij}^{(31)}(E)\, dE/(k_B T_i)^2 \qquad \text{(II.17)}$$

$$G_{j\,i}(E) = +\Omega^{I}_{i\,j}\int_{o}^{\infty}\Phi_{i}(E)H^{(13)}_{i\,j}(E)\,dE/(k_{B}T_{i})^{2} \qquad \text{(II.18}$$

$$G_{i\,i}(E_{z}) = -\Omega^{I}_{i\,j}\int_{o}^{\infty}\chi_{i}(E)\,H_{i\,j}{}^{(31)}(E)\,dE/(k_{B}T_{i})^{2} \qquad \text{(II.19)}$$

$$G_{j\,i}(E_{z}) = +1/3\,G_{j\,i}(E) \qquad \text{(II.20)}$$

$$\text{where } \Omega^{I}_{i\,j} = \frac{2\,D^{2}_{i\,j}\,m^{2}_{j}}{\pi\hbar^{2}\rho\hbar\omega_{i\,j}}\left(\frac{k_{B}T_{i}t_{i}}{2\pi m_{j}}\right)^{\frac{1}{2}}\exp\left[-\frac{\hbar^{2}k^{2}_{i}t_{i}}{k_{B}T_{i}}\right]$$

which has the dimensions of a frequency and

$$H^{(m\,n)}_{i\,j}(E) = \exp(-E/k_{B}T_{i})\left[(N_{i\,j}+1)\{E^{m}(E+\Delta_{i\,j}-\hbar\omega_{i\,j})^{n}\}\right.$$

$$\left.+N_{i\,j}\{E^{m}(E+\Delta_{i\,j}+\hbar\omega_{i\,j})^{n}\}^{\frac{1}{2}}\right]$$

§ II.2 Anisotropic acoustic phonon intravalley scattering

The transition probability for anisotropic acoustic phonon scattering is given in § 3.3. We shall first evaluate the rates of loss of momentum and energy by an electron with wave-vector $\underline{k}^{*}$. The expressions correspond respectively to $F^{i\,i}_{k^{*}}(\underline{k}^{*})$ and $F^{i\,i}_{E}(E)$ in equations (II.1) and (II.2). For anisotropic scattering it is convenient to label the symmetry axis of the constant energy surfaces as the $\hat{z}$-axis. Thus we have:

$$\left.\frac{d\,\underline{k}^{*}}{dt}\right|_{\underline{k}^{*}} = -AE^{\frac{1}{2}}\left(\frac{k_{B}T_{o}}{2m_{o}m_{t}s_{1}}\right)^{2}\left[\hat{z}(\underline{k}^{*}.\hat{z})\,F_{1\,1}(\theta)+(\hat{z}\wedge\underline{k}^{*})\wedge\hat{z}\,F\,(\theta)\right] \qquad \text{(II.21)}$$

$$\left.\frac{dE}{dt}\right|_{\underline{k}^{*}} = -AE^{3/2}\left[\left(\frac{5+\lambda^{2}}{6}+\frac{\lambda^{2}-1}{2}\cos^{2}\theta\right)-\frac{k_{B}T_{o}}{E}\left(\frac{3+\lambda^{2}}{2}+\frac{\lambda^{2}-1}{2}\cos^{2}\theta\right)\right]$$

(II.22)

where $A = 2^{3/2} m_o^{5/2} m_t\, m_l^{\frac{1}{2}} \Xi_d^2 / \pi \hbar^4 \rho$,

$$\lambda^2 = r^2 (\Xi_u/\Xi_d + 1)^2 ,$$

$$r^2 = m_l / m_t ,$$

$$F_{\parallel}(\theta) = 1 + (\lambda^2 - r^2)(r^2 - 3)(r^2 - 1)^{-2} + \gamma r^2 (r^2 + 5)(r^2 - 1)^{-3}$$

$$+ 2\, g(\theta)\, (r^2 - 1)^{-4} \left[3(\lambda^2 - r^2)(r^2 - 1) - \gamma r^2 (5r^2 + 4) \right]$$

$$+ h(\theta)(r^2 - 1)^{-4} \left[2\sin^2\theta\, r^2 \{(\lambda^2 - r^2)(r^2 - 1) - \gamma(r^2 + 2)\} - \right.$$

$$\left. 4\cos^2\theta \{(\lambda^2 - r^2)(r^2 - 1) - r^2(2r^2 + 1)\} \right]$$

$$F_{\perp}(\theta) = 1 + (\lambda^2 - r^2)(r^2 + 1/3)(r^2 - 1)^{-2} - \gamma r^2 (11 r^2 + 1)(r^2 - 1)^{-3}/3$$

$$+ 4\, g(\theta)(r^2 - 1)^{-4} \left[\cos^2\theta \{(\lambda^2 - r^2)(r^2 - 1) - \gamma r^2 (2r^2 + 1)\} - \right.$$

$$\left. \sin^2\theta \{2(\lambda^2 - r^2)(r^2 - 1) - \gamma r^4 (r^2 + 5)\} \right]$$

$$+ 4\, h(\theta)(r^2 - 1)^{-4} \left[r^2 (\lambda^2 - r^2)(r^2 - 1) - \gamma r^4 (r^2 + 2) \right]$$

$$\gamma = \Xi_u^2 / \Xi_d^2 \, (s_l^2 / s_t^2 - 1)$$

$$g(\theta) = \left[(\cos^2\theta + r^2 \sin^2\theta)^{\frac{1}{2}} - 1 \right] / \sin^2\theta$$

$$h(\theta) = \log_e \left[\{\cos\theta + (\cos^2\theta + r^2 \sin^2\theta)^{\frac{1}{2}}\} / \, (\cos\theta + 1) \right] / \cos\theta$$

The expression (II.22) for the energy loss rate by an electron of wavevector $\underline{k}^*$ is more general than that given by Conwell [43] since the orientation of $\underline{k}^*$ is not restricted to the directions parallel and normal to the z-axis (i.e. $\theta = 0, \pi/2$). For the orientations where com-

parison is possible, (II.22) agrees with the result given in [43], except for the term containing $k_B T_o/E$ which is neglected in [43].

When the moment generation rates are evaluated according to (II.1) for a displaced Maxwellian in $\underline{k}^*$-space, we have:

$$G_{11}^{aa}(k_{x,y}) = -k^*_{x,y1}\,\Omega_{11}^{aa}(k_B T_o/2m_o m_t s_1^2)\int_o^\infty \exp(-E/k_B T_1)\Theta_1^{\perp}(E)E^2\,dE/(k_B T_1)^3 \qquad (II.23)$$

$$G_{11}^{aa}(k^*_z) = -k^*_{z1}\,\Omega_{11}^{aa}(k_B T_o/2m_o m_t s_1^2)\int_o^\infty \exp(-E/k_B T_1)\Theta_1^{II}(E)E^2\,dE/(k_B T_1)^3 \qquad (II.24)$$

$$G_{11}^{aa}(E) = -\Omega_{11}^{aa}\int_o^\infty \exp(-E/k_B T_1)\{\left[(2\lambda^2+1)\Phi_1(E)/3 - (\lambda^2-1)\Theta_1(E)/2\right]E - \left[(1+\lambda^2)\Phi_1(E) - (\lambda^2-1)\Theta_1(E)/2\right]k_B T_o\}\,E\,dE/(k_B T_1)^2 \qquad (II.25)$$

where $\Omega_{11}^{aa} = \dfrac{8m_o^3 m_t m_1^{\frac{1}{2}}}{\pi\hbar^4\rho}\,d^2\left(\dfrac{k_B T_1}{2\pi m_o}\right)^{\frac{1}{2}}\exp\left(-\dfrac{W_1}{k_B T_1}\right)$

$$W_1 = \sum_{\underline{\alpha}} \hbar^2 k_{\alpha 1}^2/2m_\alpha m_o$$

$$\Theta_1^{\perp}(E) = \int_{-1}^{1}\exp(\xi_1 E^{\frac{1}{2}}\cos\theta\cos\theta_1)\sin^2\theta F\left\{\frac{I_1(\xi_1 E^{\frac{1}{2}}\sin\theta\sin\theta_1)}{\xi_1 E^{\frac{1}{2}}\sin\theta\sin\theta_1}\right\}d(-\cos\theta)$$

$$\Theta_1^{II}(E) = \int_{-1}^{1}\exp(\xi_1 E^{\frac{1}{2}}\cos\theta\cos\theta_1)\cos^2\theta F(\theta)\left\{\frac{I_o(\xi_1 E^{\frac{1}{2}}\sin\theta\sin\theta_1)}{\xi_1 E^{\frac{1}{2}}\cos\theta\cos\theta_1}\right\}d(-\cos\theta)$$

$$\xi_1 = W_1^{\frac{1}{2}}/k_B T_1,\quad \cos\theta_1 = (\underline{k}^*_1\cdot\hat{\underline{z}})/\underline{k}^*_1\ ,$$

Θ_1 and Φ_1 are as defined in (II.8) and (II.9), and I_o and I_1 are Bessel functions.

§ II.3. Electron-Electron Scattering

The moment generation rate that is non-zero for electron-electron scattering that we are concerned with is $G_{11}^{ee}(E_z)$ which we shall evaluate for a two temperature displaced Maxwellian in $\underline{k}^*$-space. The interaction potential etc. are given in § 3.5 so we shall simply quote the result:

$$G_{11}^{ee}(E_z) = -\Omega_{11}^{ee}\int_0^{\infty} \exp(-E/2k_B T_1)\, \Phi_{11}(E)\, L(E)\, dE \qquad (II.26)$$

where $\Omega_{11}^{ee} = \dfrac{n c e^4 t_1^{\frac{1}{2}}}{16 m_o^{\frac{1}{2}} (\pi k_B T_1)\ (e e_o)^2}$

has the dimensions of frequency,

$$\Phi_{11}^{ee}(E) = \int_{-1}^{1} \exp\left[-E(t_1 - 1)x^2/k_B T_1\right](3x^2 - 1)/2\, dx \ ,$$

$$L(E) = (E\lambda/E + \tfrac{1}{2})\log_e\left[(E_\lambda + E)/E_\lambda\right] - 1 \ ,$$

and $$E_\lambda = \hbar^2 \lambda^2/2m_o .$$

(The symbols are defined in §3.5.) The property of electron-electron collisions which tend to reduce the electron distribution to a displaced Maxwellian is clearly illustrated by (II.26). It can be shown that $L(E) > 0$ and $\Phi_1^{ee}(E)$ has the same sign as $(t_1 - 1)$. Thus when $T_{\parallel 1} > T_{\perp 1}$ $(t_1 < 1)$ then $G_{11}^{ee}(E_z)$ is negative and vice versa, i.e. electron-electron collisions always tend to reduce the temperature anisotropy of the electrons. Note also that the average electron drift does not enter into (II.26).

Appendix III Interpretation of the field gradient coefficients $\underline{d}(\varphi_i)$

The field gradient coefficients $\underline{d}(\varphi_i)$ is defined by the equation

$$\delta\varphi_i = \underline{d}(\varphi_i).\delta\underline{F} \qquad (2.7b)$$

where $\delta\varphi_i$ is the perturbation of the moment φ_i caused by a small perturbation $\delta\underline{F}$ to the uniform applied field $\underline{F}$. The interpretation of the components of $\underline{d}(\varphi_i)$ in the direction of $\underline{F}$ (the z-direction) presents no difficulty since by definition:

$$d_z(\varphi_i) = \lim_{\delta F_z \to 0} \frac{\delta\varphi_i}{\delta F_z} = \frac{d}{dF}(\varphi_i) \qquad (III.1)$$

To obtain an expression for the transverse components, consider the case when $\delta\underline{F}$ is parallel to the x-axis. The resultant field $(\underline{F} + \delta\underline{F})$ is then equal in magnitude to $\underline{F}$ but is rotated through a small angle $\theta = \delta F_x/F$ about the y-axis. The moments v_{xi} and $\langle v_x v_z \rangle_i$ which were previously zero now take the values δv_{xi} and $\delta\langle v_x v_z \rangle_i$.

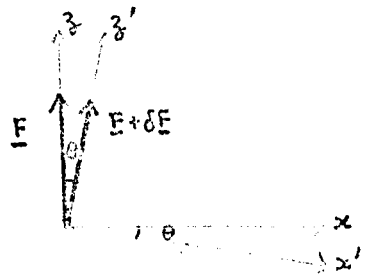

In a new coordinate system (s') obtained by rotating the old axes (s) through an angle θ about the y-axis, the perturbed field is parallel to the z'-axis. ince the perturbed field in s' has exactly the same value as the unperturbed field in s, and the system is isotropic, the values of the perturbed moments in s' must be identical to those of the unperturbed moments in s. To transform from s to s', we have, for small θ,

$$\begin{aligned} v_x &= v'_x + v'_z\,\theta \\ v_z &= v'_z - v'_x\,\theta \end{aligned} \qquad (III.2)$$

consequently,

$$\delta v_{xi} = \langle v'_x + v'_z\,\theta \rangle_i - \theta\, v_{zi}$$

and

$$\delta \langle v_x v_z \rangle_1 = \langle (v_x' + v_z' \theta)(v_z' - v_x' \theta) \rangle_1$$
$$= \theta (\langle v^2 \rangle_1 - \langle v_x^2 \rangle_1) + O(\theta^2)$$

$$d_x(v_{x1}) = v_{z1}/F \tag{III.3}$$

$$d_x(\langle v_x v_z \rangle_1) = \left[\frac{k_B}{m_1} (T_{z1} - T_{t1}) + v_{z1}^2 \right] / F \tag{III.4}$$

The assymetry of the results for the field arises from the fact that when $\delta \underline{F}$ is parallel to $\underline{F}$, the rate of energy gain by the electrons from the field $(e\underline{F}.\ \underline{v})$ is non-zero to first order in $\delta \underline{F}$. The effect of heating is most clearly illustrated in the case of the coefficients $d_x(v_{x1})$ and $d_z(v_{z1})$. In the absence of heating, the incremental increase in velocity, in the x-direction say, due to an increase of the field in the same direction is given by

$$\delta v_x = \frac{e\tau_p}{m} \delta F_x \tag{III.5}$$

where the isotropic momentum relaxation time τ_p can be obtained from the relation

$$v_z = \frac{e\tau_p}{m} F \tag{III.6}$$

so the result (III.3) is obtained. When $\delta \underline{F}$ is parallel to $\underline{F}$, the heating of the electrons causes the momentum relaxation time to change to that from (III.6) we have

$$\delta v = \frac{e\tau_p}{m} \delta F + \frac{eF}{m} \frac{d\tau_p}{dF} \delta F$$

leading thus to the relation

$$d_z(v_z) = \frac{dv_z}{dF}$$

references

[1] A. Hasegawa and J. Yamashita, J.Phys.Chem.Solids 23, 875 (1962).

[2] W. Kohn and J.M. Luttinger, Phys.Rev. 108, 590 (1957).

[3] M. Dresden, Rev.Mod.Phys. 33, 265 (1961).

[4] W. Fawcett, A.D. Boardman and S. Swain, J.Phys.Chem.Solids 31, 1963 (1970).

[5] W. Fawcett and H.D. Rees, Phys.Letters 28A, 731 (1969).

[6] H.D. Rees, J.Phys.Chem.Solids 30, 643 (1969).

[7] W. Fawcett and J.G. Ruch, Appl.Phys.Letters 15, 368 (1969).

[8] P.N. Butcher and W.Fawcett, Proc.Phys.Soc. 86, 1205 (1965).

[9] P.N. Butcher and W. Fawcett, Phys.Letters 21, 489 (1966).

[10] W. Heinle, Phys.Rev. 178, 1319 (1969).

[11] M. Costato and L. Reggiani, Phys.Stat.Sol. 42, 591 (1970).

[12] H. Hillbrand and D. Kranger, Phys.Stat.Sol. 42, K79 (1970).

[13] W. Fawcett, Proc.Int.Con.Phys.Semicond., (Cambridge, Mass., 1970) pp.51.

[14] G. Persky and D.J. Bartelink, IBM J.Res.Develop.13, 607(1969).

[15] D.J. Bartelink and G. Persky, Phys.Rev.B1 , 1614 (1970).

[16] P.N. Butcher and C.J. Hearn, Electron.Letters 4, 459 (1968).

[17] W. Fawcett and H.D. Rees, Phys.Letters 29A, 578 (1969).

[18] R.E. Peierls, 'Quantum theory of solids', pp.204 (Oxford University Press, 1954).

[19] P.N. Butcher, W. Fawcett and N.R. Ogg, Brit.J.Appl.Phys. 18, 755 (1967)

[20] W. Shockley, J.A. Copeland and R.P. James, 'Quantum Theory of Atoms, Molecules, and the Solid State'(Ed.Par-Olov Löwdin) pp.537 (Academic Press N.Y., 1966).

[21] T.Ohmi and S. Hasuo, Proc.Int.Con.Phys.Semicond.,(Cambridge, Mass., 1970)pp.60.

[22] H. Ehrenreich, J.Chem.Solids 2, 131 (1957).

[23] E.G.S. Paige, Progress in Semiconductors, 8, Eds A.F. Gibson and R.E. Burgess pp 1-244 (London:Heywood, 1964).

[24] H.G. Reik, Phonons and Phonon Interactions, Ed. T.A. Bak, pp 138-66 (New York: Benjamin, 1964).

[25] C. Hilsum, Proc.Int.Con.Phys.Semicond., (Paris 1964) p.1127.

[26] C. Hilsum, Progress in Semiconductors, 9, Eds.A.F. Gibson and p.137 (London, Heywood, 1965).

[27] J.L.T. Waugh and G. Dolling, Phys.Rev. 132, 2410 (1963).

[28] H. Ehrenreich, Phys.Rev. 120, 1951 (1960).

[29] E. Haga and K. Kimura, J. Phys. Soc. Japan 19, 658 (1964).

[30] J. L. Birman, M. Lax, and R. Loudon, Phys.Rev. 145, 620 (1966).

[31] J.G. Ruch and G.S. Kino, Phys. Rev. 174, 921 (1968).

[32] P.N. Butcher, 'The Gunn Effect', Report Prog.Phys. 30, part 1, 97 (1967).

[33] T. Kurasawa, J.Phys.Soc.Japan, Suppl 21 424 (1966).

[34] S.M. Sze, 'Physics of Semiconductor Devices', p 58, (Wiley-Interscience 1969

[35] F.J. Morin, T.H. Geballe and C. Herring, Phys.Rev. 105, 525 (1957).

[36] W.A. Harrison, Phys.Rev. 104,128 (1956).

[37] M. Lax and J.T. Hopfield, Phys.Rev. 124, 115 (1961).

[38] C. Herring and E. Vogt, Phys.Rev. 101, 944 (1956).

[39] A. Onton, Phys.Rev.Letters 22, 288 (1969).

[40] W.P. Dumke, Phys.Rev. 118, 938 (1960).

[41] N.O. Folland, Phys.Rev. B1, 1648 (1970).

[42] C. Herring, Bell Syst.Tech.J. 34, 237(1955).

[43] E.M. Conwell, High Field Transport in Semiconductors, Solid State Phys.Suppl. 9, 152, (Academic Press, 1967).

[44] R.A. Stradling and V.V. Zhukov, Proc.Phys.Soc 87, 263 (1966).

[45] K. Murase, K. Enjouji and E. Otsuka, J.Phys.Soc.Japan 29, 1248 (1970).

[46] H. Fritzsche, Phys.Rev. 120, 1120 (1960).

[47] J.E. Aubrey, W. Gubler, T. Henningsen and S.H. Koenig, Phys.Rev.130, 1667 (1963).

[48] G. Weinreich, T.M.Sander & H.G.White, Phys.Rev.114, 33 (1959).

[49] A.K. Walton, G.P.Williams and K.V.K. Reddy, Phys.Stat.Sol.(b) 47,K29, 1971.

[50] M. Costato and L. Reggiani, Lett.Nuovo.Cimento III,728 (1970).

[51] M. Cardona, W. Paul and H. Brooks, Helv.Phys.Acta 33, 329 (1960).

[52] D.Brust, Phys.Rev. 134A, 1337 (1964).

[53] T.W. Sigmon and J.F. Gibbons, Appl.Phys.Letters 15, 320 (1969).

[54] G.Persky and D.J. Bartelink, J.Appl.Phys. 42, 4414 (1971).

[55] M. Asche and O.G. Sarbei, Phys. Stat. Sol. 33, 9 (1969).

[56] M. Asche, B L. Boichenko, V.M. Bondar and O.G. Sarbei, Phys.Stat.Sol. (b)44, 173 (1971).

[57] C.J. Hearn, Proc.Phys.Soc. 86, 881 (1965).

[58] J.B. Gunn, Solid St. Commun., 1, 88 (1963).

[59] J.B. Gunn, Proc.Int.Conf.Phys.Semicond. (Paris 1964) p 199.

[60] J.S. Heeks, A.D. Woode, and C.P. Sandbank, Proc.I.E.R.E.-I.E.E. Symp. on Microwave Applications of Semiconductors, London 1965.

[61] B.K. Ridley and T.B. Watkins, Proc.Phys.Soc., 78, 293 (1961).

[62] C.Hilsum, Proc.Inst.Radio Engrs. (N.Y.), 50, 185 (1962).

[63] A.R. Hutson, A. Jayaraman, A.G. Chynoweth, A.S. Corriell and M.L. Feldman, Phys.Rev.Letters, 14, 639 (1965).

[64] P.N. Butcher, Report Prog.Phys. 30, Part 1, p 97 (1967).

[65] D.E. McCumber and A.G. Chynoweth, I.E.E.E. trans. ED-13, 4 (1944).

[66] V. Székely and K. Tarnay, Electron.Letters 4, 593 (1968).

[67] H.W. Thim and M.R. Barber, I.E.E.E. trans. ED-13, 110 (1966).

[68] G.F. Day, I.E.E.E. trans. ED-13, 88 (1966).

[69] H. Kroemer, " " " 27 (1966).

[70] J.A. Copeland, J.Appl.Phys. 36, 2-9 (1966).

[71] P.N. Butcher and W. Fawcett, Brit.J.Appl.Phys. 17, 1425 (1966).

[72] J.W. Allen, W. Shockley and G.L. Pearson, J. Appl.Phys. 37, 319 (1966).

[73] B.W. Knight and G.A. Peterson, Phys.Rev. 147, 617 (1966).

[74] E.M. Conwell and M.O. Vassell, I.E.E.E. trans. ED-13, 22 (1966).

[75] I.E. Hasty, R. Stratton and E.L. Jones, J.Appl.Phys. 39, 4623 (1968).

[76] R. Stratton, Phys.Rev. 126, 2002 (1962).

[77] I. Kuru, P.N. Robson and G.S. Kino, I.E.E.E. trans. ED-15, 21 (1968).

[78] J.B. Gunn, Proc.Int.Conf.Phys.Semicond., (Kyoto, 1966) p 505.

[79] I.B. Bott and C. Hilsum, I.E.E.E. trans. ED-14, 492 (1967).